

NOLTR 61-89

A631795

STATIC WIND TUNNEL TESTS OF THE  
M823 RESEARCH STORE WITH SPLIT-  
SKIRT STABILIZERS

CLEARINGHOUSE FOR FEDERAL SCIENTIFIC AND TECHNICAL INFORMATION			
Hardcopy	Microfiche		
\$ 11.60	\$ .75	121	PP 23
ARCHIVE COPY			

*Code 1*

# NOL

12 JANUARY 1966

UNITED STATES NAVAL ORDNANCE LABORATORY, WHITE OAK, MARYLAND

NOLTR 61-89

D D C  
RECEIVED  
MAY 6 1966  
RECEIVED

Distribution of this document is unlimited.

NOLTR 61-89

Aerodynamics Research Report 160

STATIC WIND TUNNEL TESTS OF THE M823  
RESEARCH STORE WITH SPLIT-SKIRT STABILIZERS

Prepared by:  
F. J. Regan  
M. E. Falsui  
J. E. Holmes

**ABSTRACT:** The M823 configuration is an instrumented free fall store used in bomb research programs. This report presents the results of static wind tunnel tests for the basic forebody with split-skirt tail stabilizers attached.

U. S. NAVAL ORDNANCE LABORATORY  
White Oak, Silver Spring, Maryland

NOLTR 61-89

12 January 1966

**STATIC WIND TUNNEL TESTS OF THE M823 RESEARCH STORE WITH  
SPLIT-SKIRT STABILIZERS**

The purpose of this investigation was to obtain static stability data on the M823 research store with split-skirt stabilizers.

The authors wish to acknowledge the assistance rendered by Mrs. V. L. Schermerhorn in data acquisition and Messrs. M. Hardy and A. Comproni in report preparation.

J. A. DARE  
Captain, USN  
Commander

*K. R. Enkenhus*  
K. R. ENKENHUS  
By direction

CONTENTS

	Page
Introduction .....	1
Symbols .....	2
Description of Bomb Configurations .....	2
Test Technique .....	3
Data Reduction .....	3
Discussion of Results .....	4
References .....	6

ILLUSTRATIONS

Figure	Title
1	Wind Tunnel Model of M823 Research Store with Split-Skirt Tail
2	M823 Free Fall Research Store
3	Sting Geometry
4	Definition of Roll Orientation
5-31	Normal Force Coefficient and Pitching Moment Coefficient Versus Angle of Attack for the 10 Degree Split-Skirt Stabilizer at Roll Angles of 0, 22.5 and 45.0 Degrees and Mach Numbers of 0.50, 0.60, 0.70, 0.80, 0.85, 0.90, 0.95, 1.50, and 1.75
32-55	Normal Force Coefficient and Pitching Moment Coefficient Versus Angle of Attack for the 15 Degree Split-Skirt Stabilizer at Roll Angles of 0, 22.5 and 45.0 Degrees and Mach Numbers of 0.50, 0.60, 0.70, 0.80, 0.85, 0.90, 1.50, and 1.75
56-82	Side Force Coefficient and Yawing Moment Coefficient Versus Angle of Attack for the 10 Degree Split-Skirt Stabilizer at Roll Angles of 0, 22.5 and 45.0 Degrees and Mach Numbers of 0.50, 0.60, 0.70, 0.80, 0.85, 0.90, 0.95, 1.50, and 1.75
83-106	Side Force Coefficient and Yawing Moment Coefficient Versus Angle of Attack for the 15 Degree Split-Skirt Stabilizer at Roll Angles of 0, 22.5 and 45.0 Degrees and Mach Numbers of 0.50, 0.60, 0.70, 0.80, 0.85, 0.90, 1.50, and 1.75

NOLTR 61-89

TABLES

Table	Title
1	Configurations
2	Tunnel Test Conditions

## INTRODUCTION

The Naval Ordnance Laboratory (NOL) has been engaged in a cooperative bomb research program with the British Royal Aircraft Establishment (RAE) and the Australian Weapons Research Establishment (WRE). This effort was undertaken, primarily, to ascertain the suitability of six-degree-of-freedom digital computer trajectory programs for predicting the flight path of free fall weapons. A study of this type became feasible when it was learned that the instrumented bomb research program of the WRE was being conducted. Subsequently, as a result of joint meetings among representatives of NOL, WRE and RAE, a mutual effort was agreed upon. NOL was to make the needed wind tunnel measurements and perform some of the trajectory computations. The United Kingdom Laboratories were to make available various instrumented bombs for the free fall portion of the study.

In addition to comparing the digital computer trajectory calculations with data obtained from the instrumented store program, it was decided to extend this effort to less conventional stabilizers. These stabilizers would include such devices as free-spinning cruciform tails, free-spinning monoplane tails and split-skirt tails. As its part in this effort, NOL will provide static and dynamic force and moment data on configurations formed by using the basic forebody with these various stabilizers attached to it.

A portion of the wind tunnel tests have been completed. Static force and moment measurements have been made for the fixed and free-spinning cruciform tails and for the free-spinning monoplane tails (see ref. (1)).

This report presents results of static wind tunnel measurements for the fixed split-skirt stabilizers (1.75 calibers in length and with skirt openings of 10 and 15 degrees). The advantage of this rather novel stabilizer lies in its ability to act as a variable (drag) retardation device. Drag data are not presented herein since previous examinations of both the stabilization and retardation properties of similar split skirts have been made.

## NOLTR 61-89

### SYMBOLS

A	reference area, $\pi d^2/4$
$C_m$	static pitching moment coefficient, $M_y/QAd$
$C_N$	normal force coefficient, $F_N/QA$
$C_n$	yawing moment coefficient, $M_z/QAd$
$C_y$	side force coefficient, $F_y/QA$
d	maximum body diameter
$F_N$	normal force (measured along z axis)
$F_y$	side force (measured along y axis)
$M_y$	pitching moment (measured about y axis)
$M_z$	yawing moment (measured about z axis)
Q	wind tunnel dynamic pressure
x, y, z	conventional body axes
$\alpha$	angle of attack
$\delta$	angle of skirt opening
$\theta$	roll angle

### DESCRIPTION OF BOMB CONFIGURATIONS

Table 1 lists the various configurations that are included in the test program. Each shape is designated symbolically by a letter. In this report static wind tunnel data are given for configurations C and E; these are fixed, split-skirt stabilizers with skirt openings of 10 and 15 degrees, respectively.

The wind tunnel model of the split-skirt configuration with the 15 degree skirt opening is illustrated in Figure 1. Since the forebody remains unchanged throughout the test program, only the skirt opening is changed (to 10 degrees) to form the second of the two split-skirt configurations tested.

The wind tunnel model used in this investigation is 0.1 scale. The model, with appropriate dimensions, is illustrated in Figure 2; and the base and sting geometry are shown in Figure 3.

In order to make measurements at the various roll angles desired, the tail was repositioned as follows. A retaining screw was released, the tail surfaces were rotated to the desired angle (in accordance with the definitions in Figure 4) and the assembly locked in place for the next test.

### TEST TECHNIQUE

The wind tunnel tests were carried out in the NOL Supersonic Tunnel No. 1. This facility is a blowdown wind tunnel with an open jet in the test section. Relevant tunnel flow conditions are given in Table 2.

Force and moment data were obtained using a five-component internal strain-gage balance. The sting mount was fixed into a rotating sector arm so that an angle of attack traverse could be made for the test. After tunnel flow had been established, the model-sting combination was pitched at a rate of four degrees per second providing the angle of attack desired. The strain-gage signals were sampled (at 80 samples per second) and recorded on magnetic tape. The strain-gage signals were also used as an input to an analog coefficient computer (see ref. (3)). The output from this computer was used to drive the pen on an X-Y plotter, so that the data are recorded on line graphically as coefficients versus angle of attack. The signals were also recorded on magnetic tape for data reduction by digital computation.

### DATA REDUCTION

As mentioned above, the strain-gage signal outputs were sampled and recorded on magnetic tape. The balance calibration and physical constants (such as dynamic pressure, reference lengths and areas, electrical gage center, moment reference center) were previously recorded on IBM cards. These cards were stored on magnetic tape in the computer. Using the calibration and data tapes as inputs, an IBM 7090 reduction program calculated the desired aerodynamic coefficients. This reduction procedure is described in reference (4). The output of the reduction program appeared

## NOLTR 61-89

as a printed record of the coefficients - versus angle of attack - and as a plot tape. This tape was then used as the input to an EAI high-speed plotter which produced a graphical presentation of the coefficients versus angle of attack for each test condition.

For the data presentation in this report, the maximum body diameter was used as the reference length, and the maximum cross-sectional area was the reference area. The moment reference center for this investigation was the body mid-point (see Fig. 2).

### DISCUSSION OF RESULTS

Table 1 lists all configurations in the free fall research program.

Figures 5 through 106 present the static data for configurations C and E. These data are the normal force coefficient,  $C_N$ , the pitching moment coefficient,  $C_m$ , the side force coefficient,  $C_y$ , and the yawing moment coefficient,  $C_n$ . The aerodynamic coefficients are plotted as functions of angle of attack with roll angle and Mach number as parameters. The rolling moment coefficient,  $C_l$ , was measured but found to be insignificant, hence it is not included in the data presentation. In order to evaluate results of these tests, the static characteristics of both configurations will be discussed briefly.

The normal force and pitching moment coefficients for the C configuration are given in Figures 5 through 31. After examining these figures, it became apparent that the center of pressure is near the body mid-point for all test Mach numbers and roll angles. At small angles of attack (less than 10 degrees), there is a slight decrease in the static pitching moment coefficient when the model is roll positioned from 0 through 45.0 degrees. Generally, however, the configuration appears to be rather insensitive to roll angle (see for example Figs. 14, 15 and 16). It is interesting to note that a sudden increase in the static pitching moment coefficient slope occurs at an angle of attack of about 26 degrees, at 0 and 45.0 degrees of roll angle. However, for a roll angle

of 22.5 degrees there is only a gradual change in static pitching moment coefficient.

The normal force and pitching moment coefficients for the E configuration are given in Figures 32 to 55. These data indicate the same trends as noted above for the C configuration. The E configuration is somewhat more sensitive to roll angle than the C configuration (compare Figs. 41, 42 and 43 with Figs. 14, 15 and 16). These Figures also illustrate the sudden increase in static pitching moment coefficient at approximately  $\alpha = 26$  degrees, for roll angles of 0 and 45.0 degrees; and, the gradual change in this coefficient with angle of attack for a roll angle of 22.5 degrees.

The side force and yawing moment coefficients for the C configuration are given in Figures 56 to 82; and for the E configuration in Figures 83 to 106. Both stabilizers indicate an increase in side force and yawing moment coefficients above 22 degrees angle of attack, for a roll angle of 0 degrees (see for example Figs. 62 and 89). At a roll angle of 45.0 degrees, the C configuration has a steadily increasing yawing moment coefficient, for angles of attack as low as 4 degrees (see for example Figs. 61, 64 and 76). At a roll angle of 45.0 degrees the E configuration has a nearly constant yawing moment coefficient, until large angles of attack are reached - above 24 degrees - (see for example Figs. 88, 91 and 100). As expected, both configurations have their maximum side force and yawing moment coefficients at a roll angle of 22.5 degrees.

REFERENCES

- (1) Regan, F. J., Falusi, M. E., Holmes, J. E., "Static Wind Tunnel Tests of the M823 Research Store with Fixed and Free Spinning Tails," NOLTR 65-14, (unpublished)
- (2) Regan, F. J., "The Aerodynamic Characteristics of an Ogive Cylinder with Split-Skirt Stabilizer at Subsonic, Transonic and Supersonic Speeds," NOLTR 63-86, Oct 1965
- (3) Willis, J. W., "Analog Computer for the Evaluation of Aerodynamic Coefficients," NOLTR 64-74, Aug 1964
- (4) Shantz, I., Gilbert, B., White, C., "NOL Wind Tunnel Internal Strain-Gage Balance System," NAVORD 2972, Sep 1953

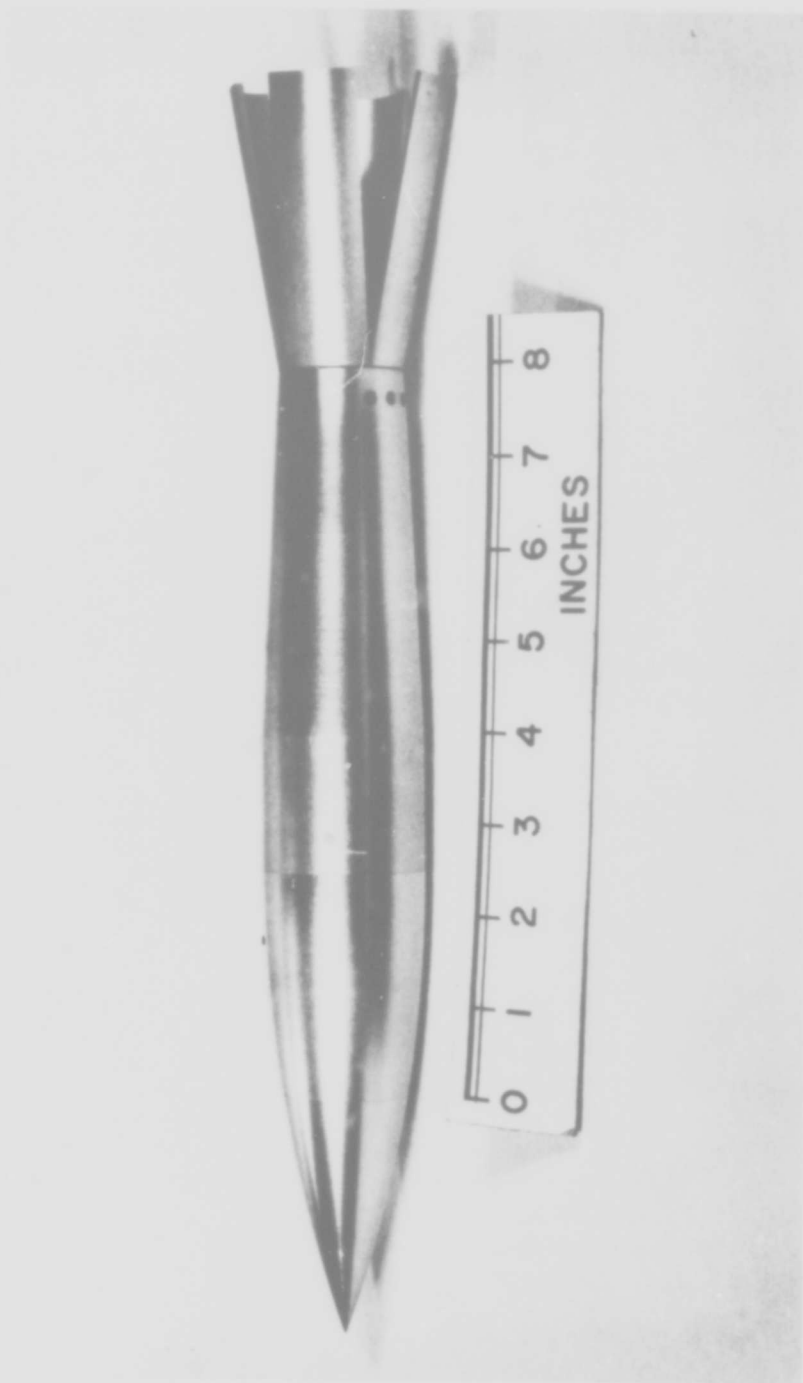
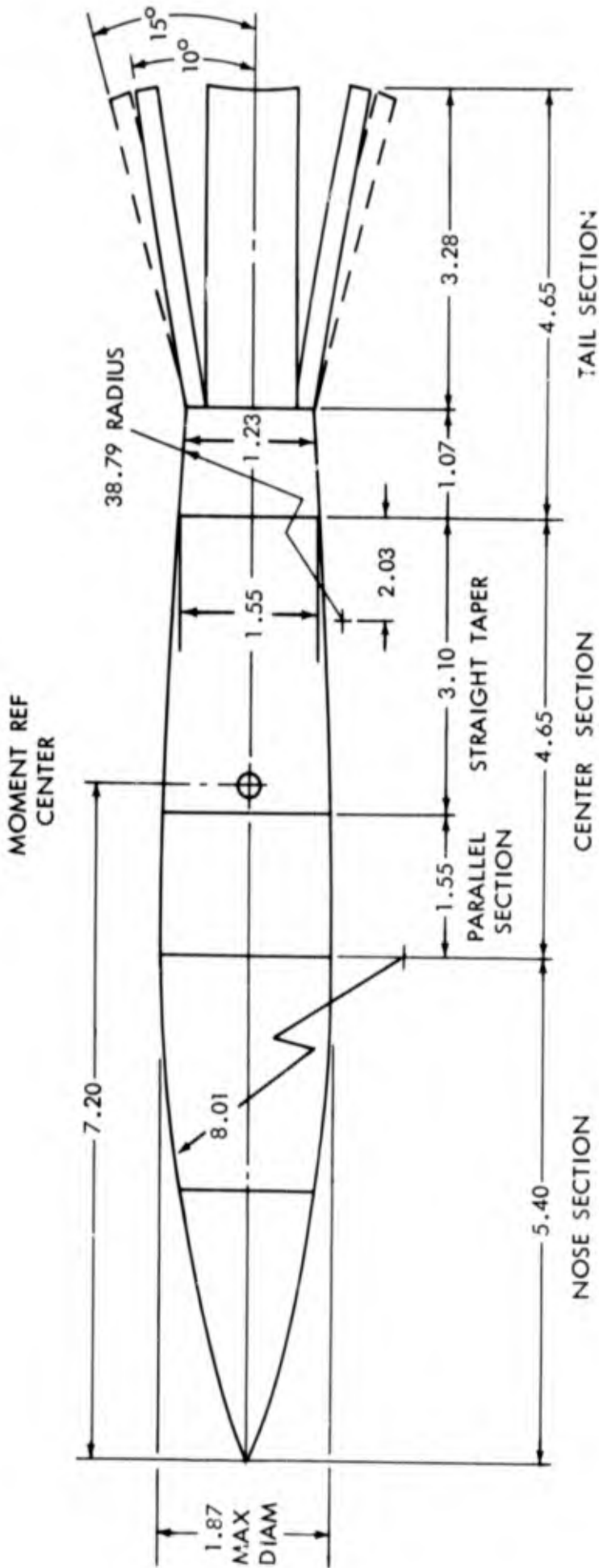


FIG. 1 WIND TUNNEL MODEL OF M823 RESEARCH STORE WITH SPLIT-SKIRT TAIL



ALL DIMENSIONS IN INCHES

FIG. 2 M823 FREE FALL RESEARCH STORE

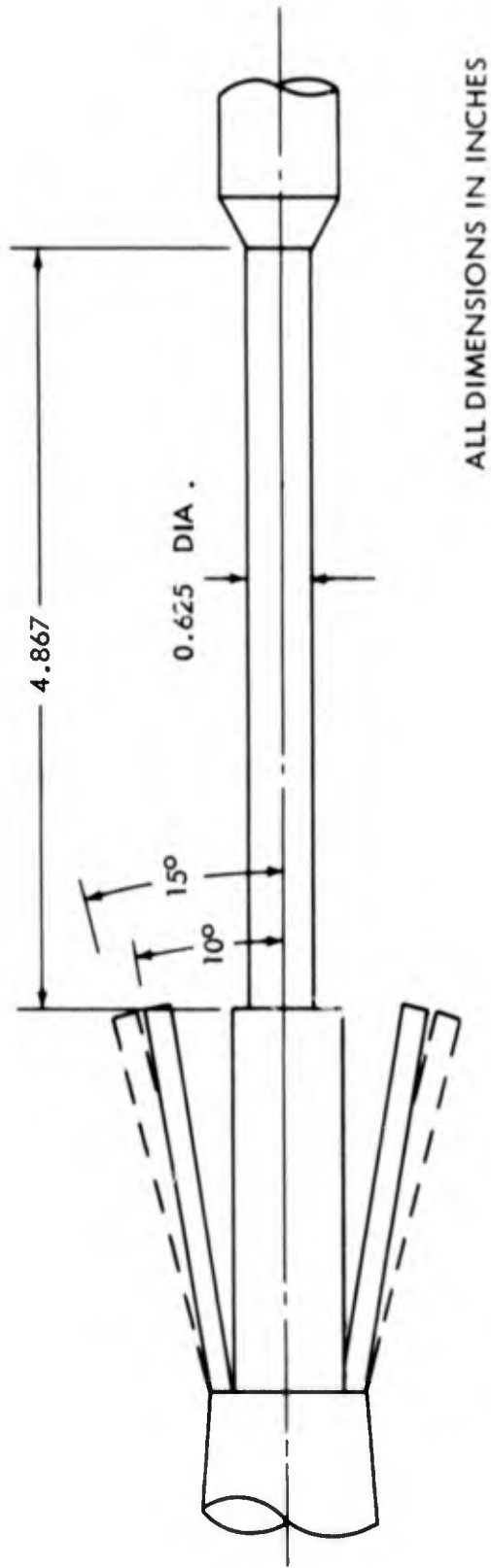
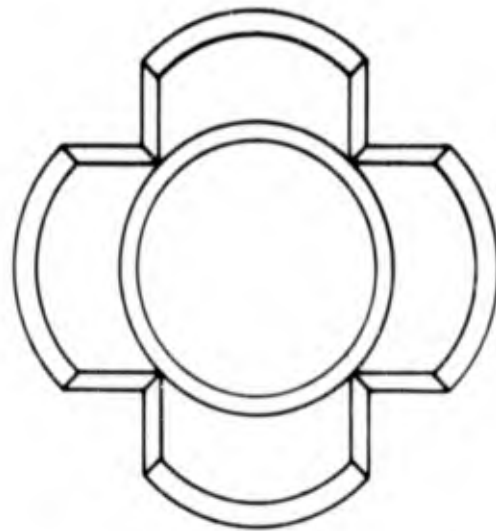
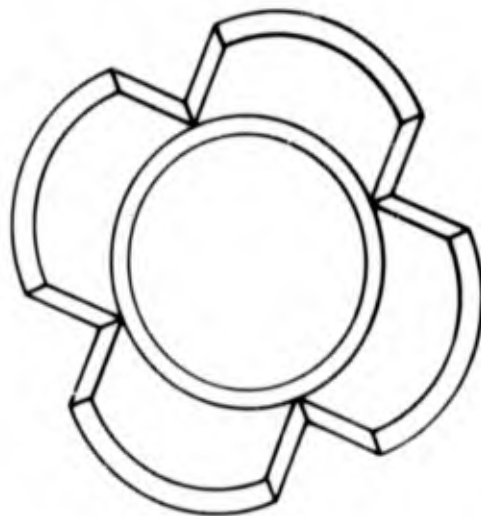


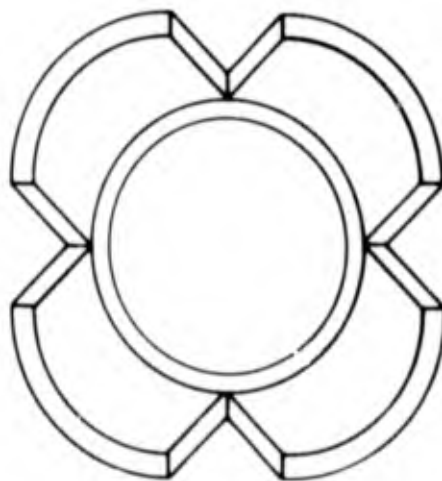
FIG.3 STING GEOMETRY



$\phi = 0^\circ$



$\phi = 22.5^\circ$



$\phi = 45^\circ$

FIG.4 DEFINITION OF ROLL ORIENTATION

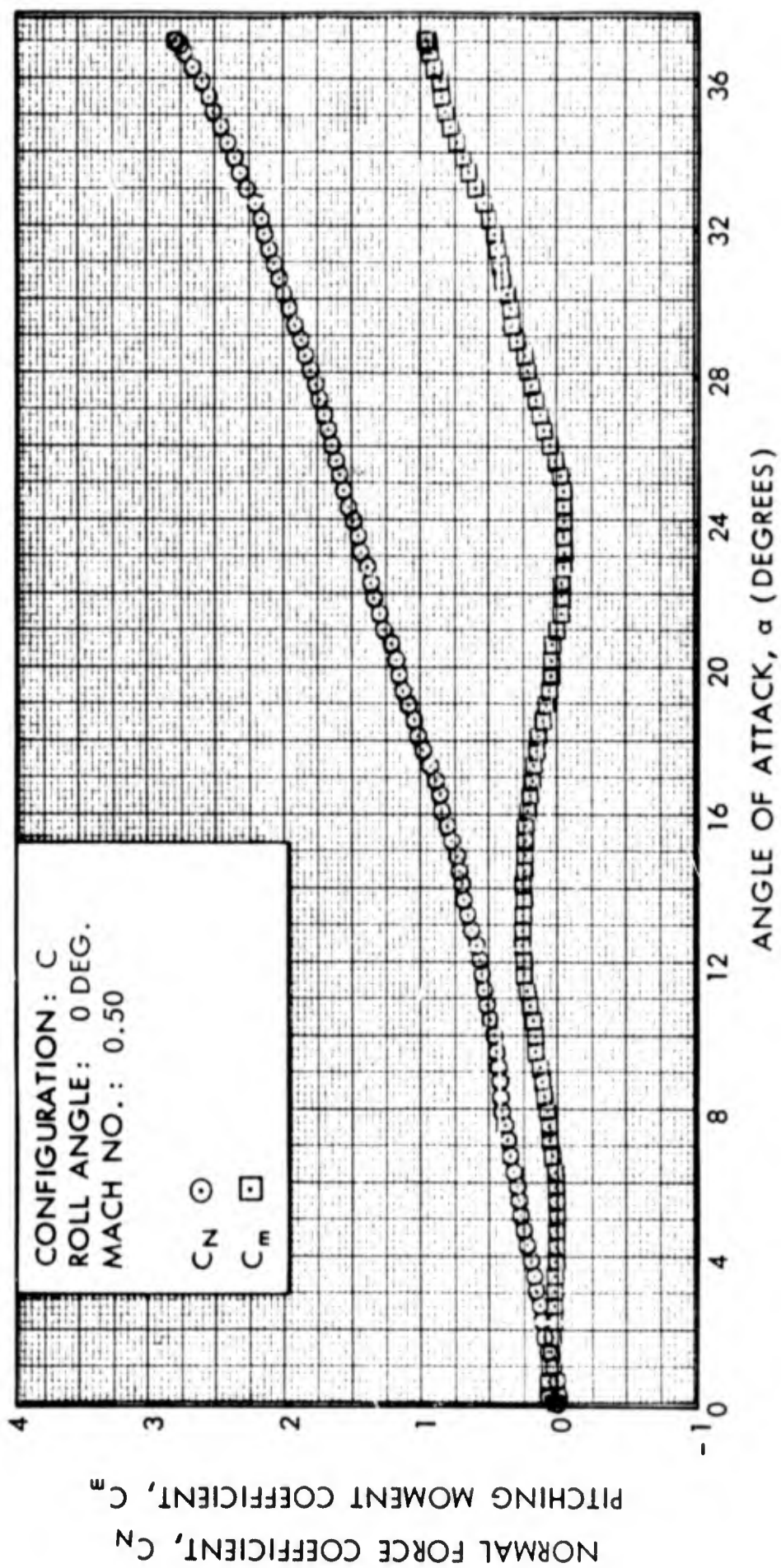


FIG. 5 NORMAL FORCE COEFFICIENT AND PITCHING MOMENT COEFFICIENT VERSUS ANGLE OF ATTACK

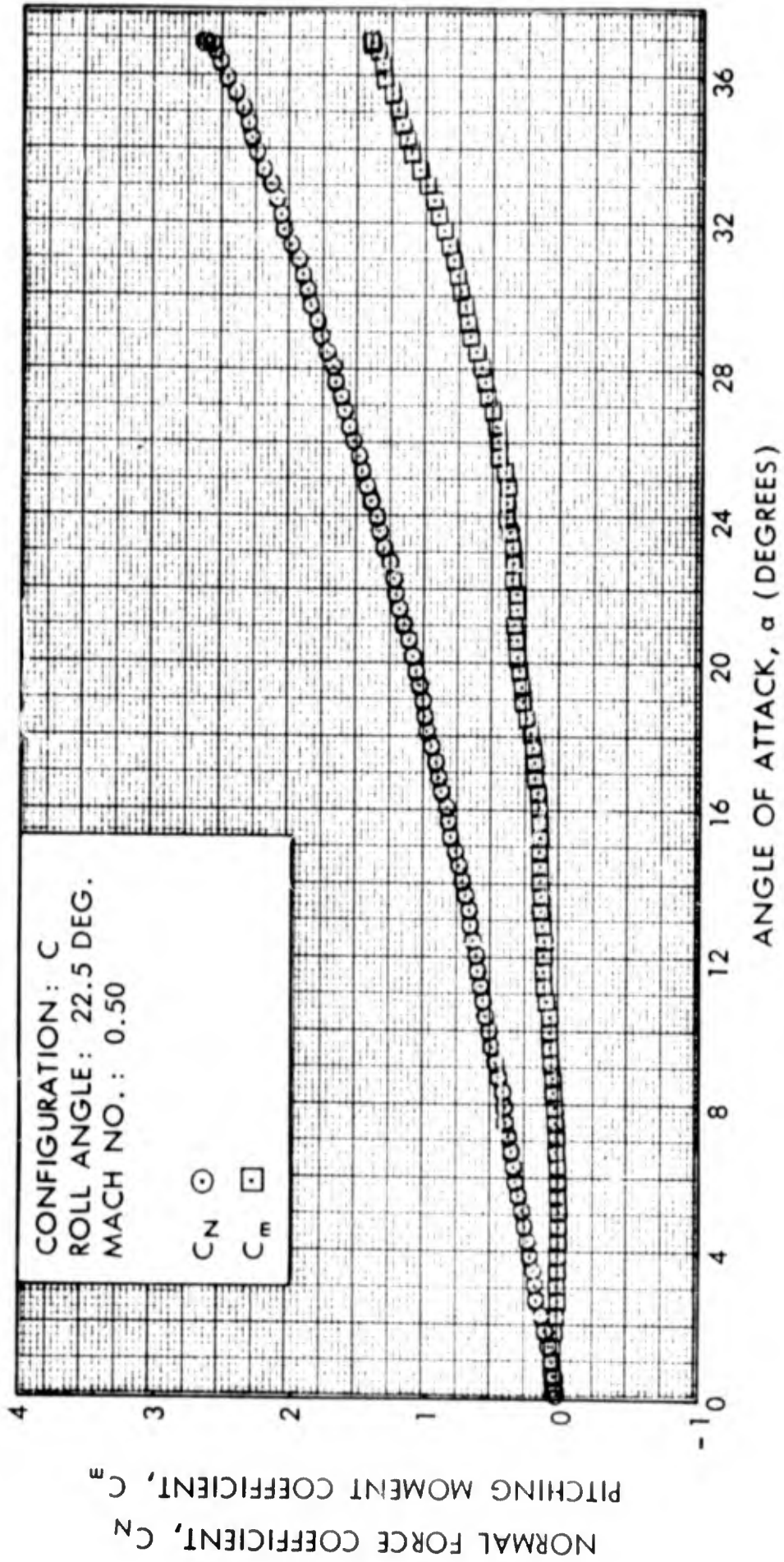


FIG. 6 NORMAL FORCE COEFFICIENT AND PITCHING MOMENT COEFFICIENT VERSUS ANGLE OF ATTACK

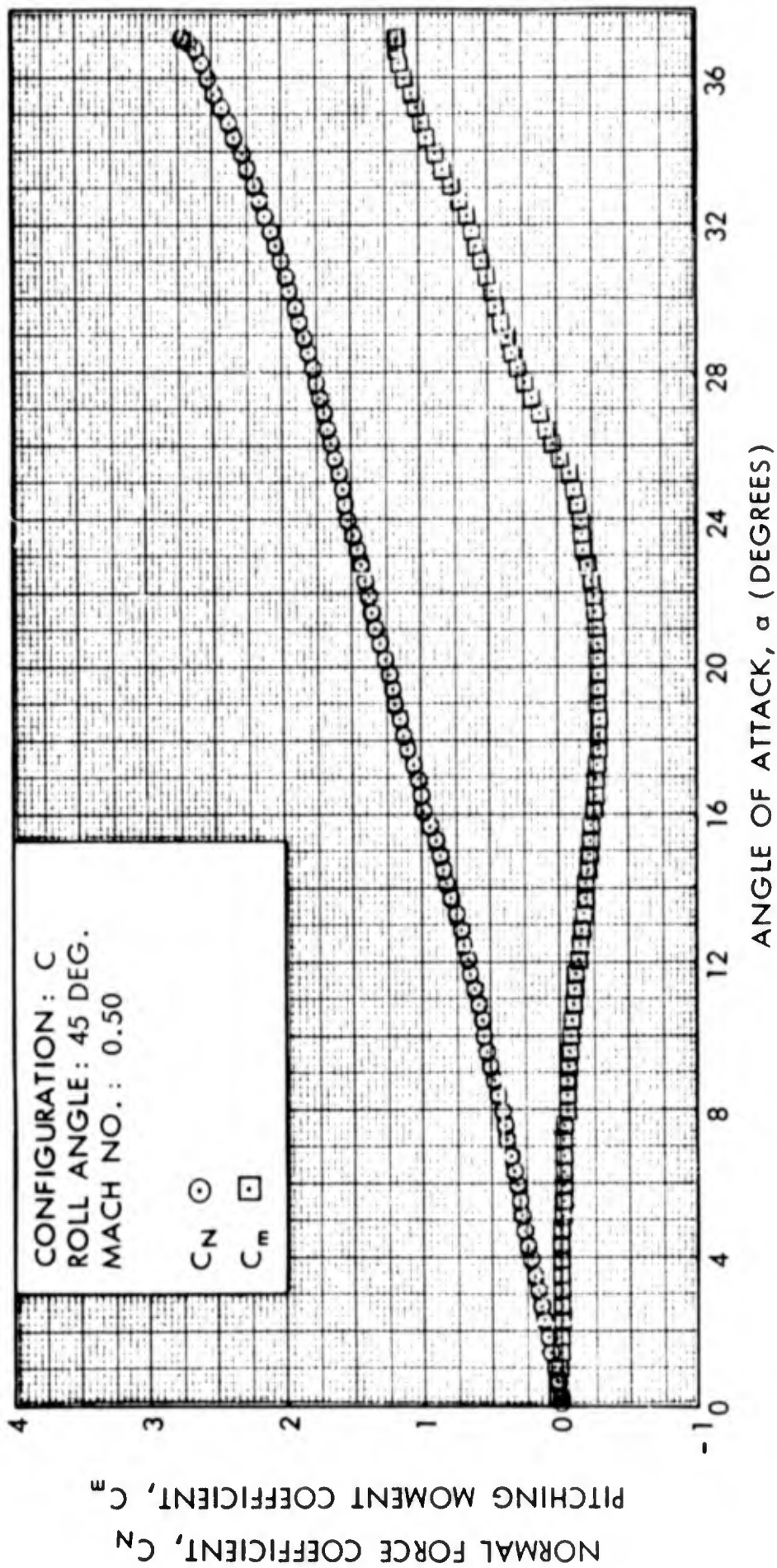


FIG. 7 NORMAL FORCE COEFFICIENT AND PITCHING MOMENT COEFFICIENT VERSUS ANGLE OF ATTACK

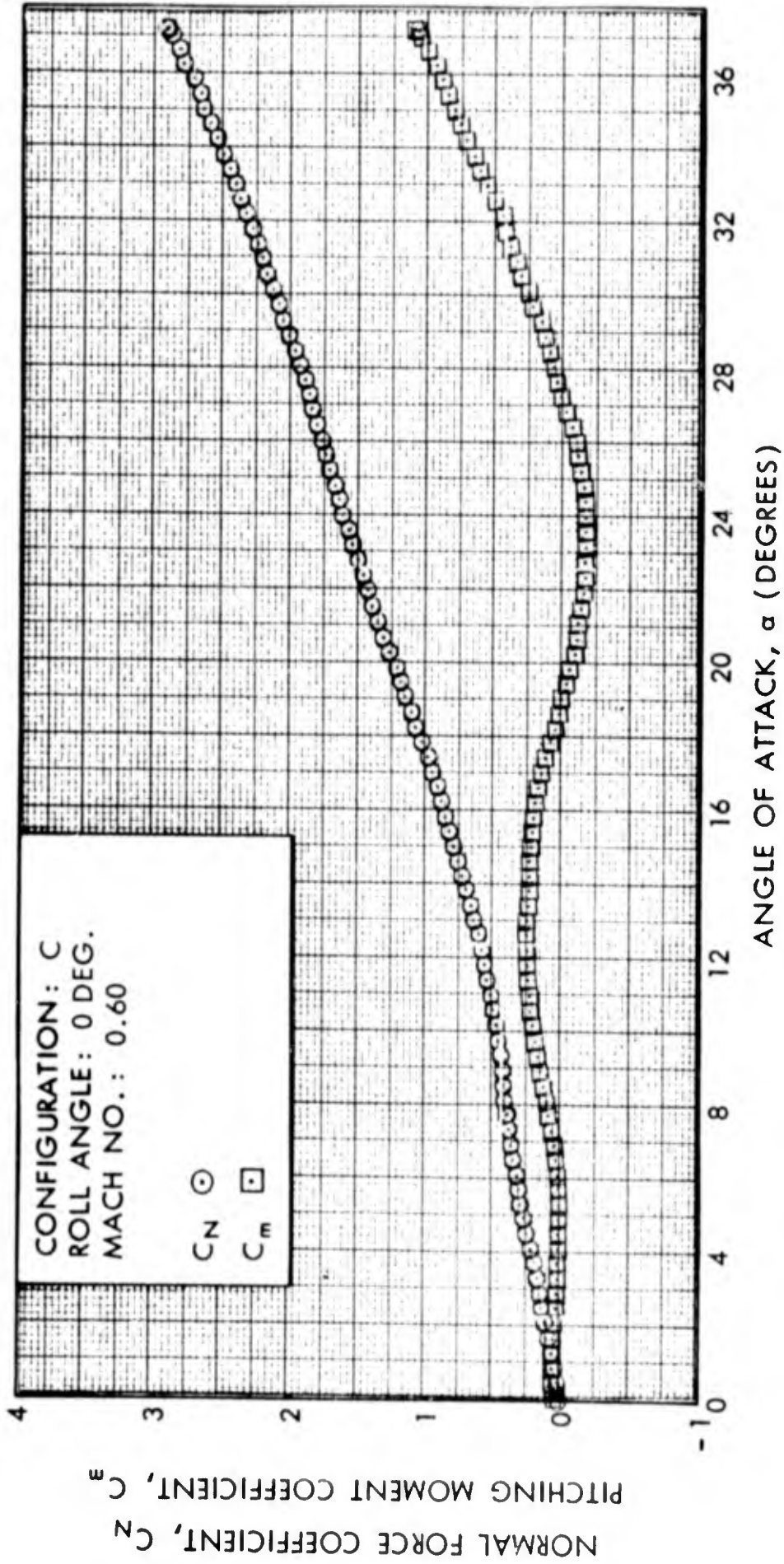


FIG. 8 NORMAL FORCE COEFFICIENT AND PITCHING MOMENT COEFFICIENT VERSUS ANGLE OF ATTACK

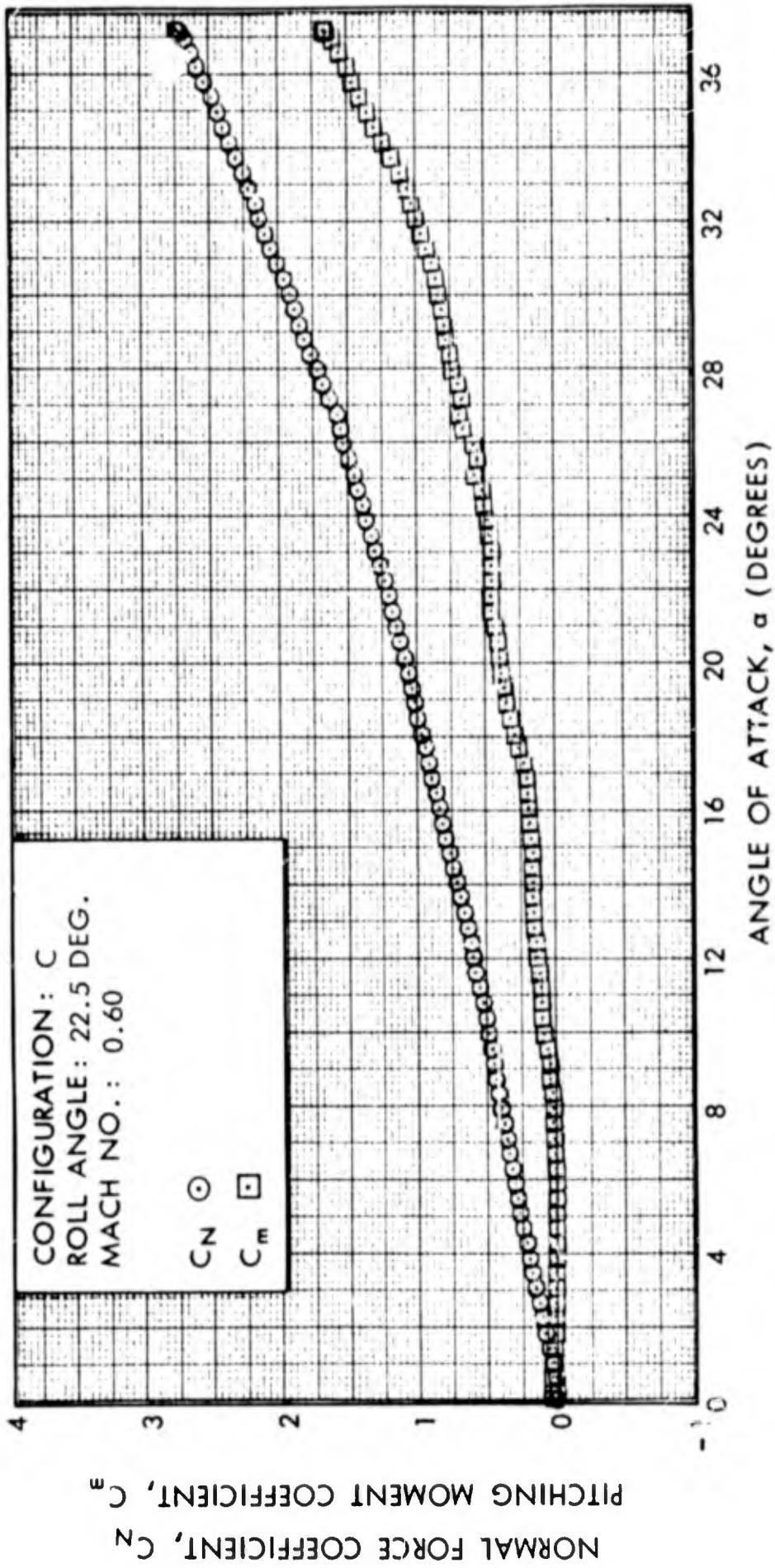


FIG. 9 NORMAL FORCE COEFFICIENT AND PITCHING  
MOMENT COEFFICIENT VERSUS ANGLE OF ATTACK

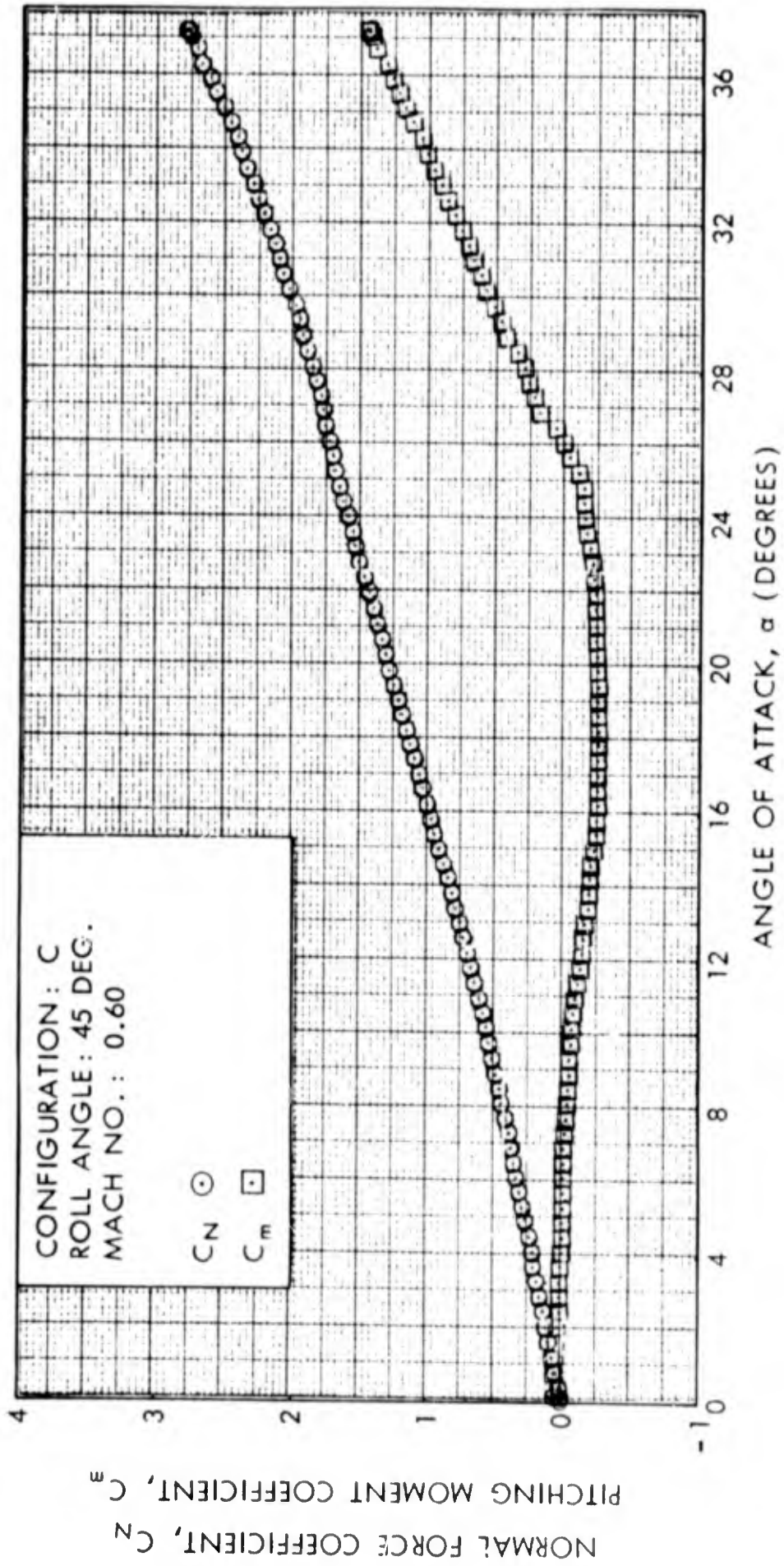


FIG. 10 NORMAL FORCE COEFFICIENT AND PITCHING  
MOMENT COEFFICIENT VERSUS ANGLE OF ATTACK

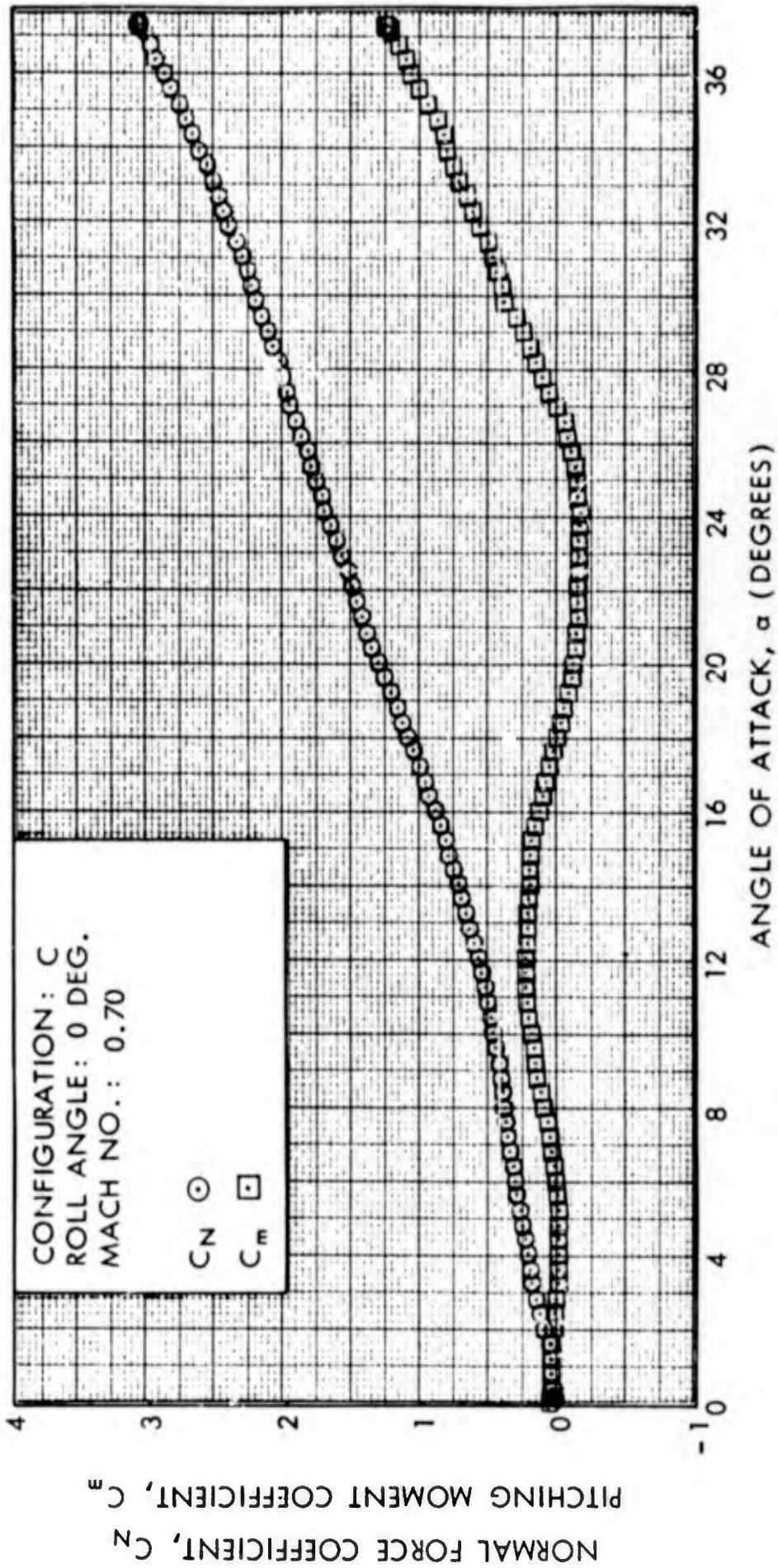


FIG. 11 NORMAL FORCE COEFFICIENT AND PITCHING MOMENT COEFFICIENT VERSUS ANGLE OF ATTACK

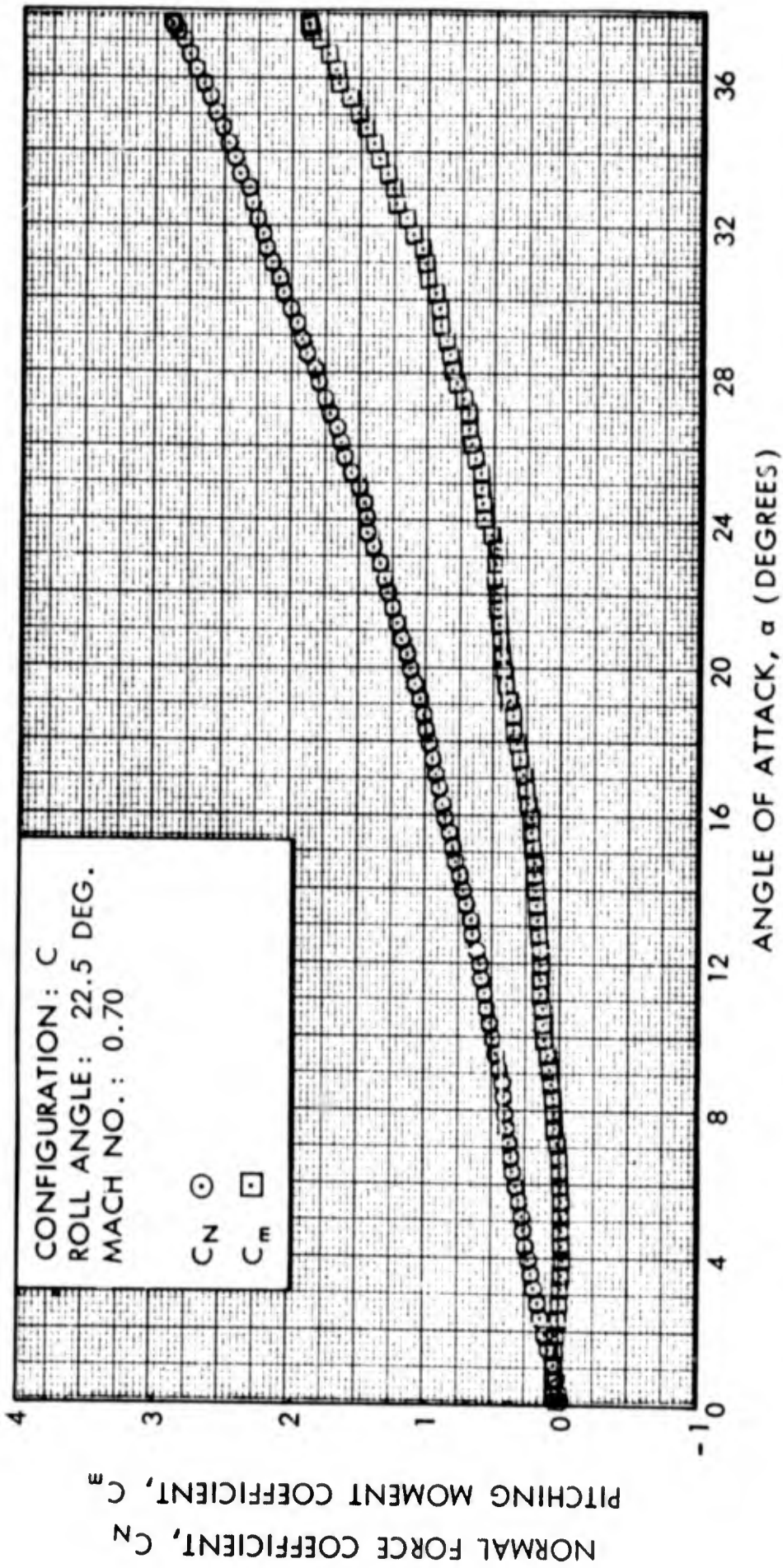


FIG. 12 NORMAL FORCE COEFFICIENT AND PITCHING MOMENT COEFFICIENT VERSUS ANGLE OF ATTACK

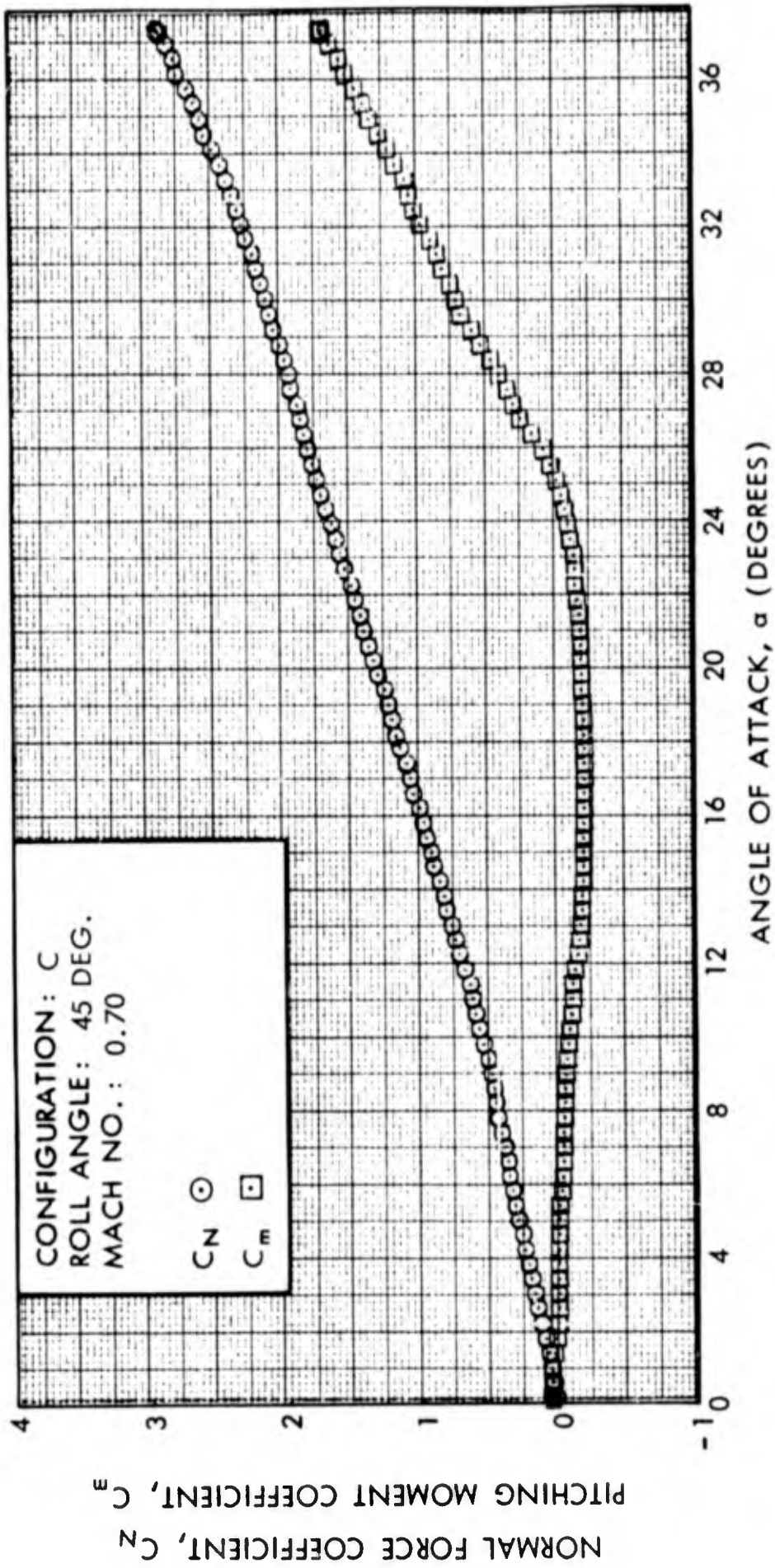


FIG. 13 NORMAL FORCE COEFFICIENT AND PITCHING MOMENT COEFFICIENT VERSUS ANGLE OF ATTACK

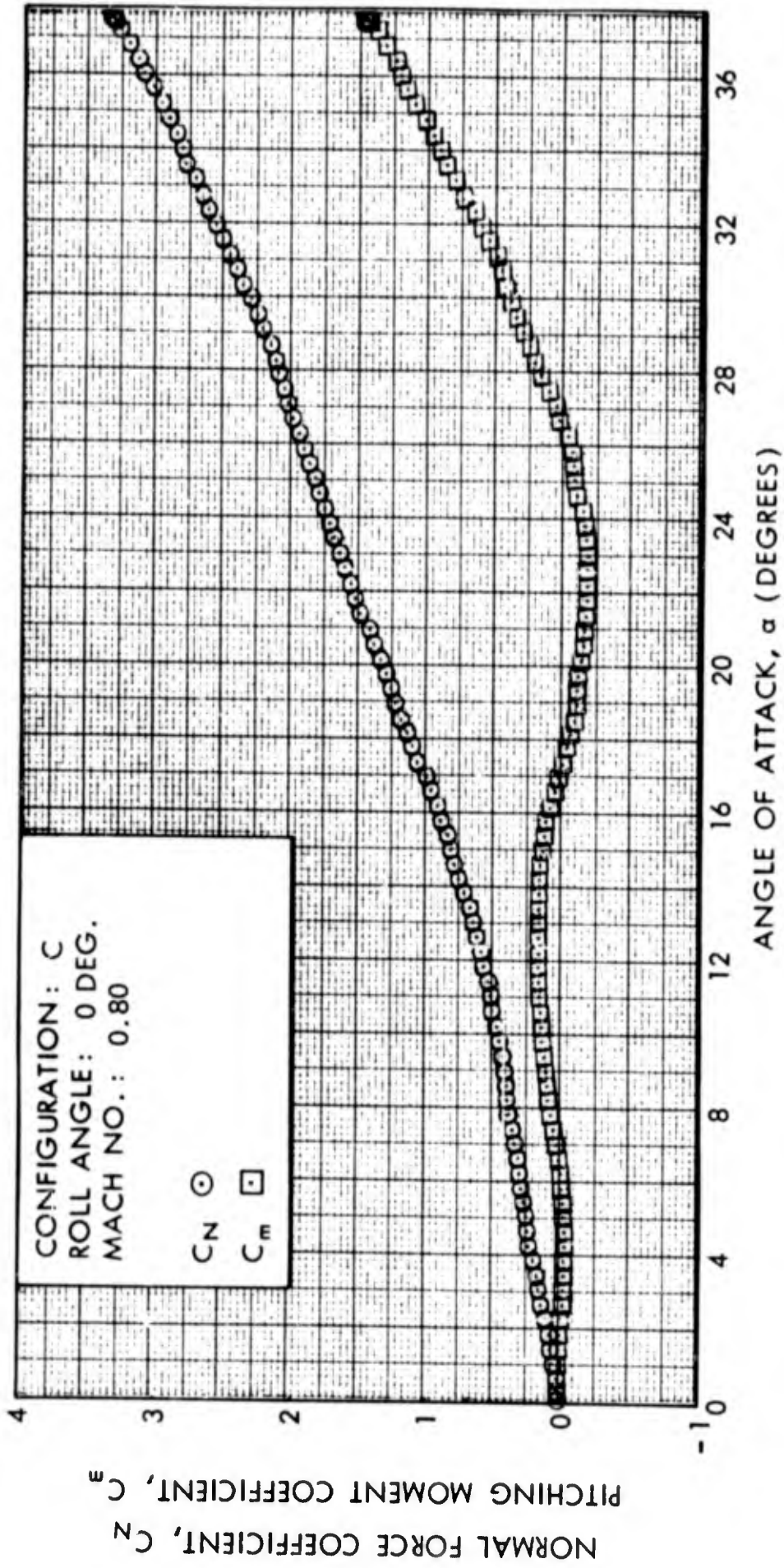


FIG. 14 NORMAL FORCE COEFFICIENT AND PITCHING MOMENT COEFFICIENT VERSUS ANGLE OF ATTACK

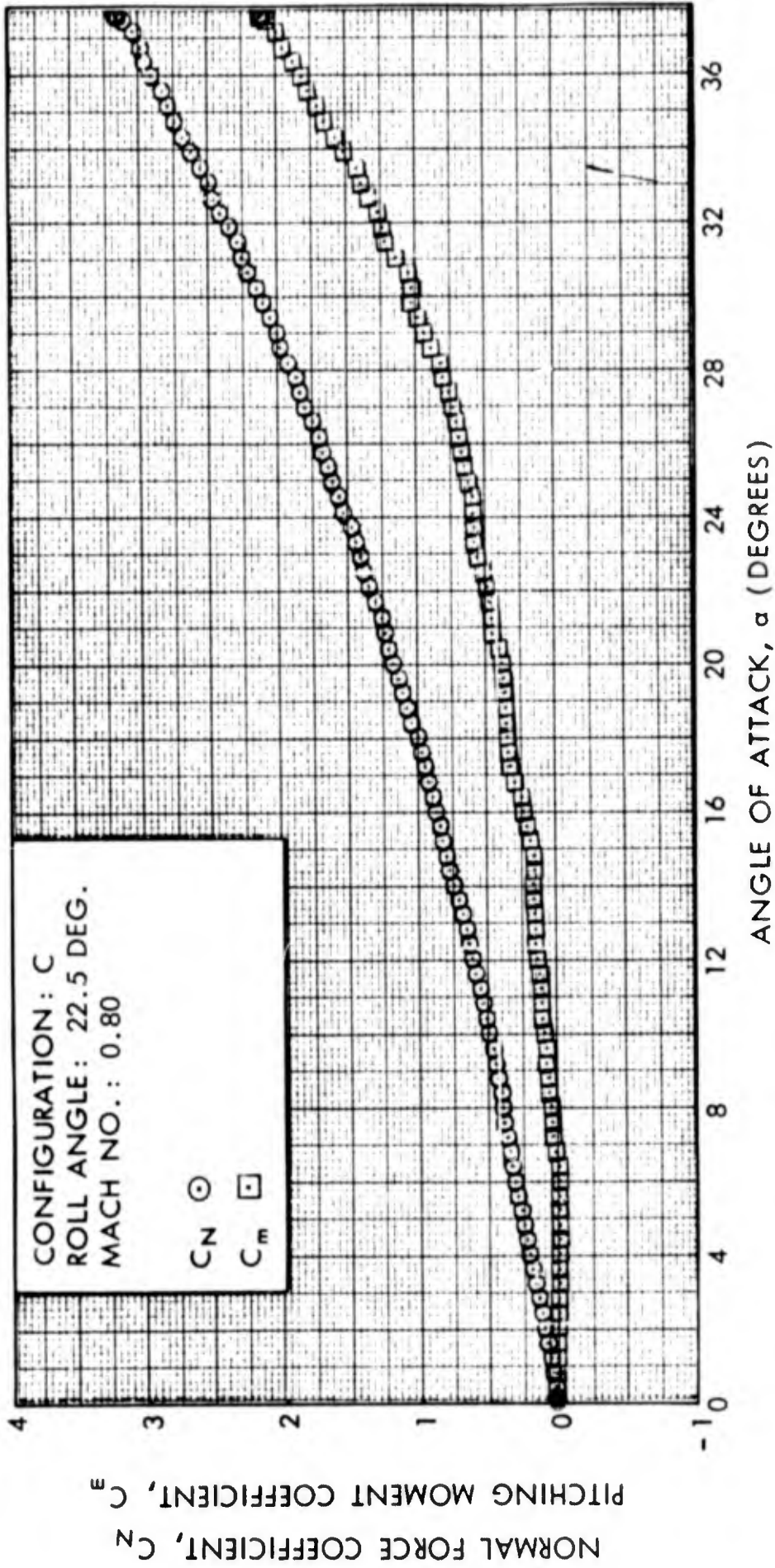


FIG. 15 NORMAL FORCE COEFFICIENT AND PITCHING MOMENT COEFFICIENT VERSUS ANGLE OF ATTACK

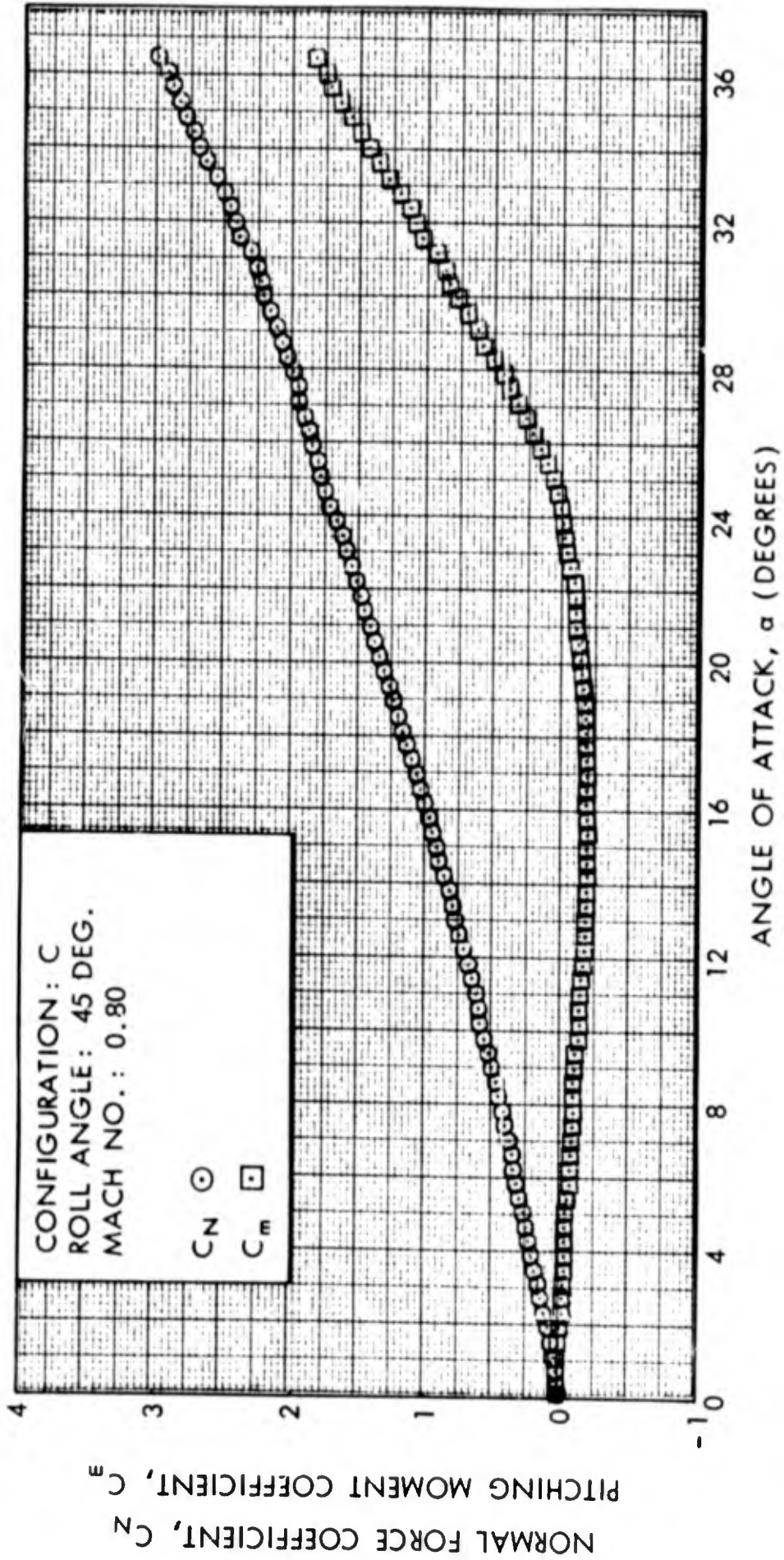


FIG. 16 NORMAL FORCE COEFFICIENT AND PITCHING MOMENT COEFFICIENT VERSUS ANGLE OF ATTACK

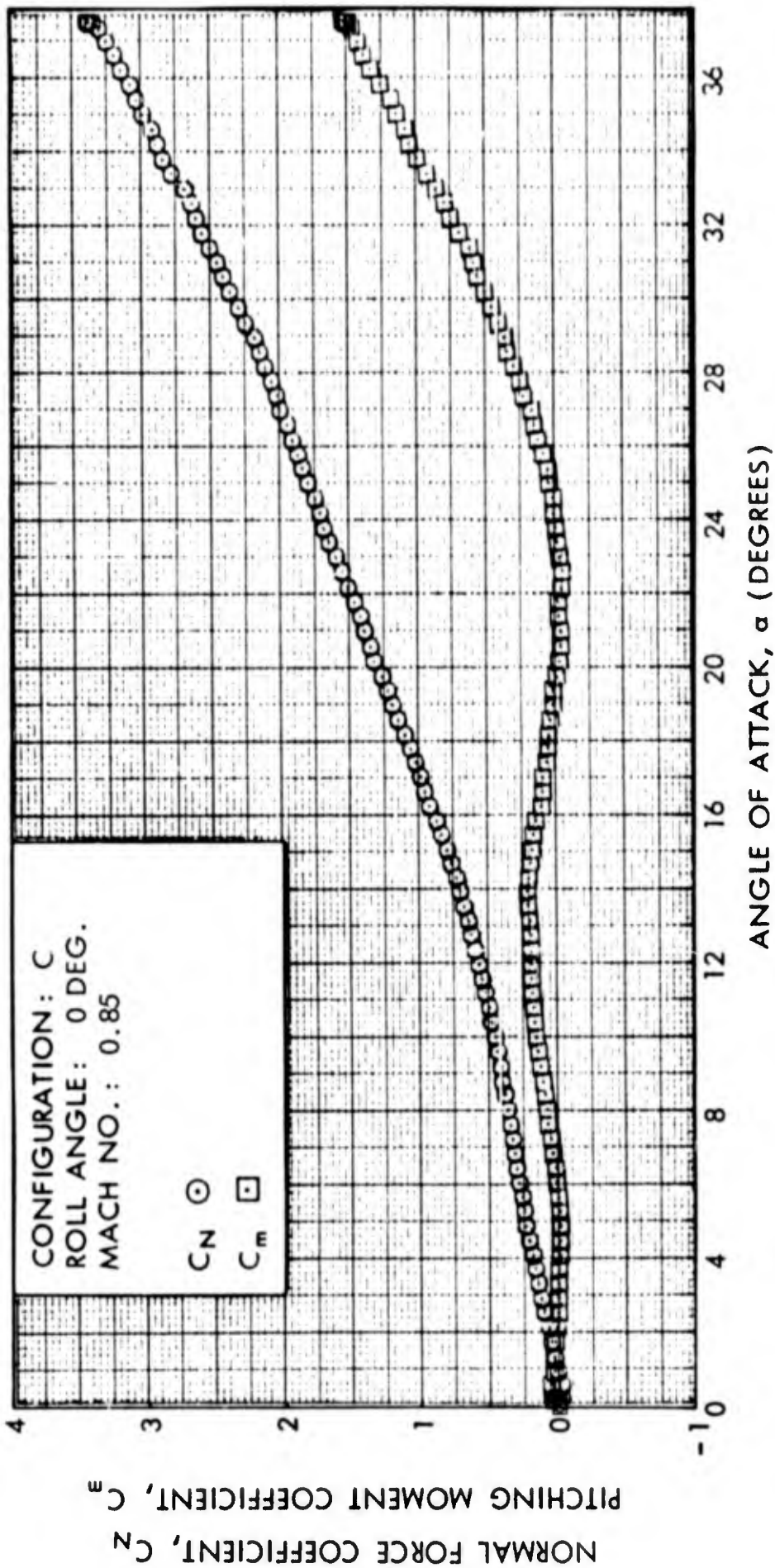


FIG. 17 NORMAL FORCE COEFFICIENT AND PITCHING MOMENT COEFFICIENT VERSUS ANGLE OF ATTACK

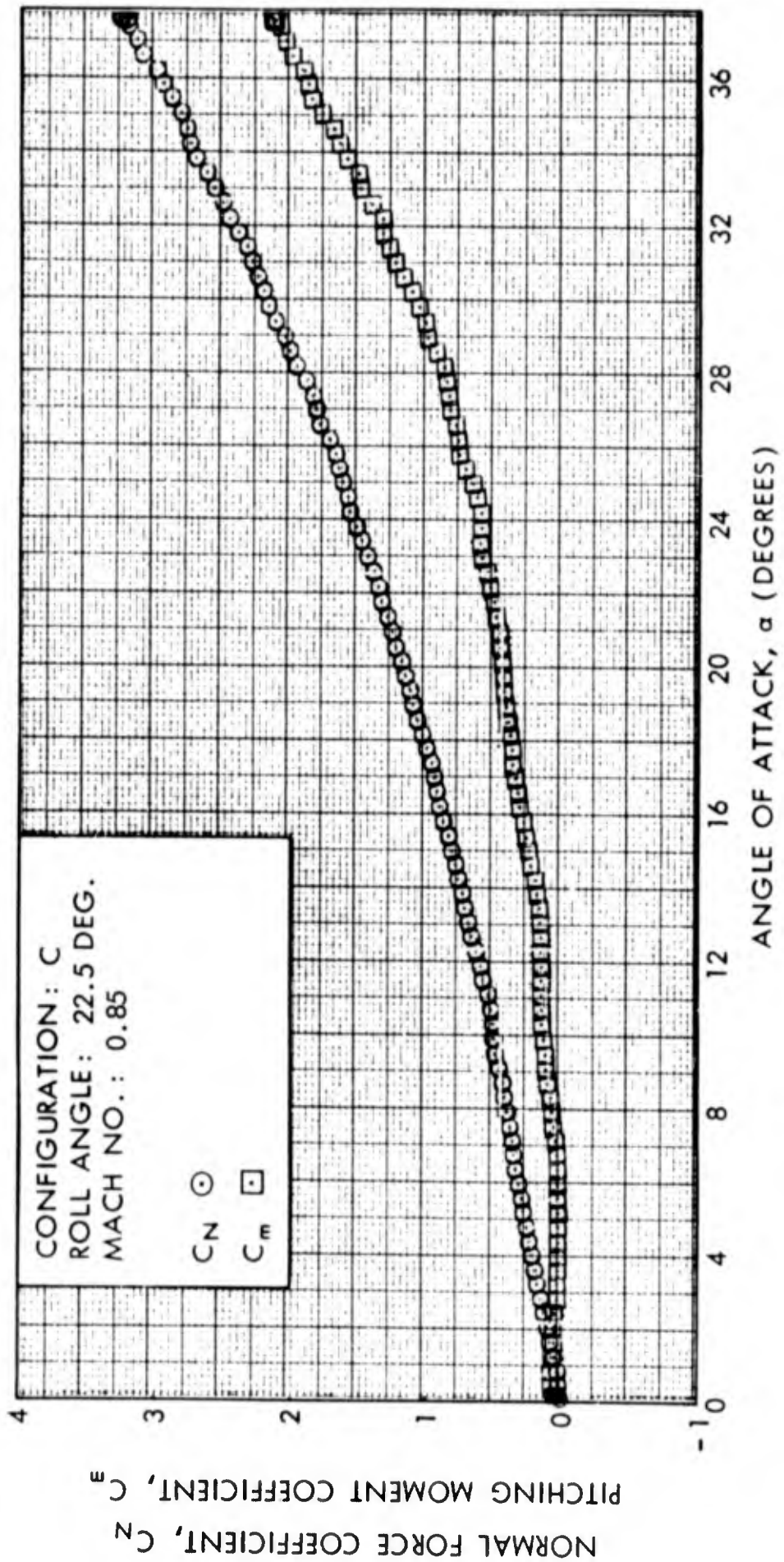


FIG. 18 NORMAL FORCE COEFFICIENT AND PITCHING MOMENT COEFFICIENT VERSUS ANGLE OF ATTACK

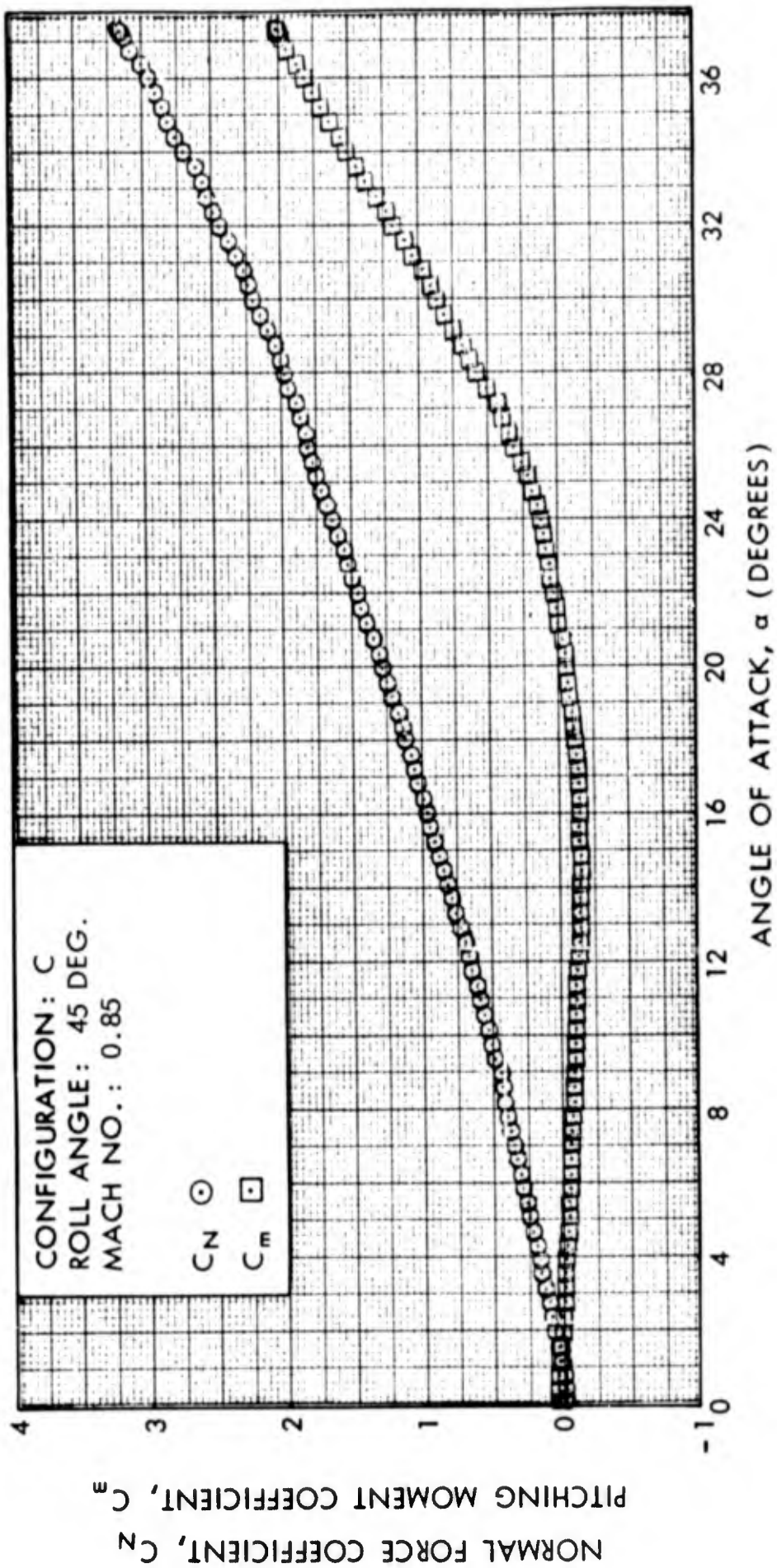


FIG. 19 NORMAL FORCE COEFFICIENT AND PITCHING MOMENT COEFFICIENT VERSUS ANGLE OF ATTACK

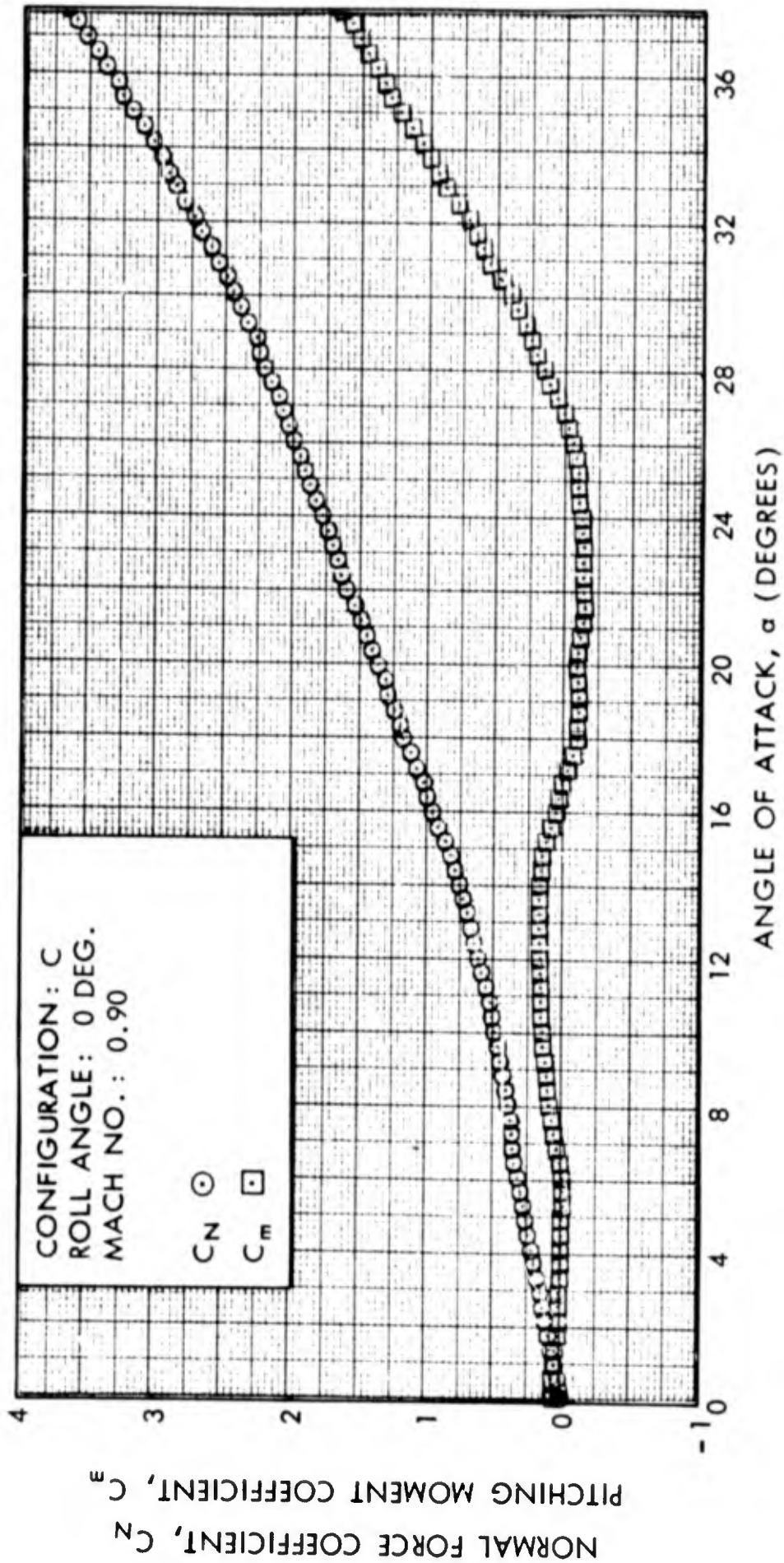


FIG. 20 NORMAL FORCE COEFFICIENT AND PITCHING MOMENT COEFFICIENT VERSUS ANGLE OF ATTACK

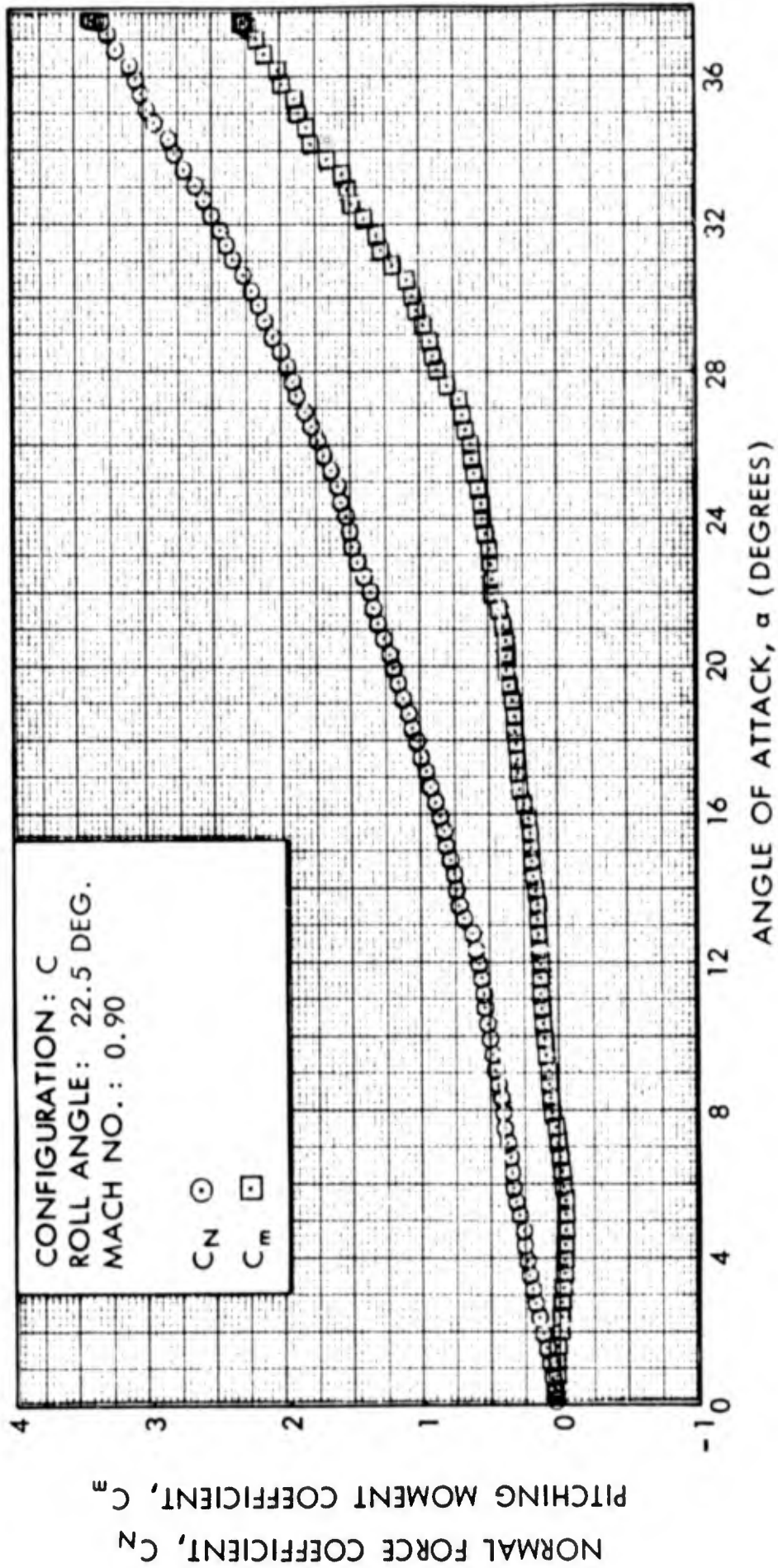


FIG. 21 NORMAL FORCE COEFFICIENT AND PITCHING MOMENT COEFFICIENT VERSUS ANGLE OF ATTACK

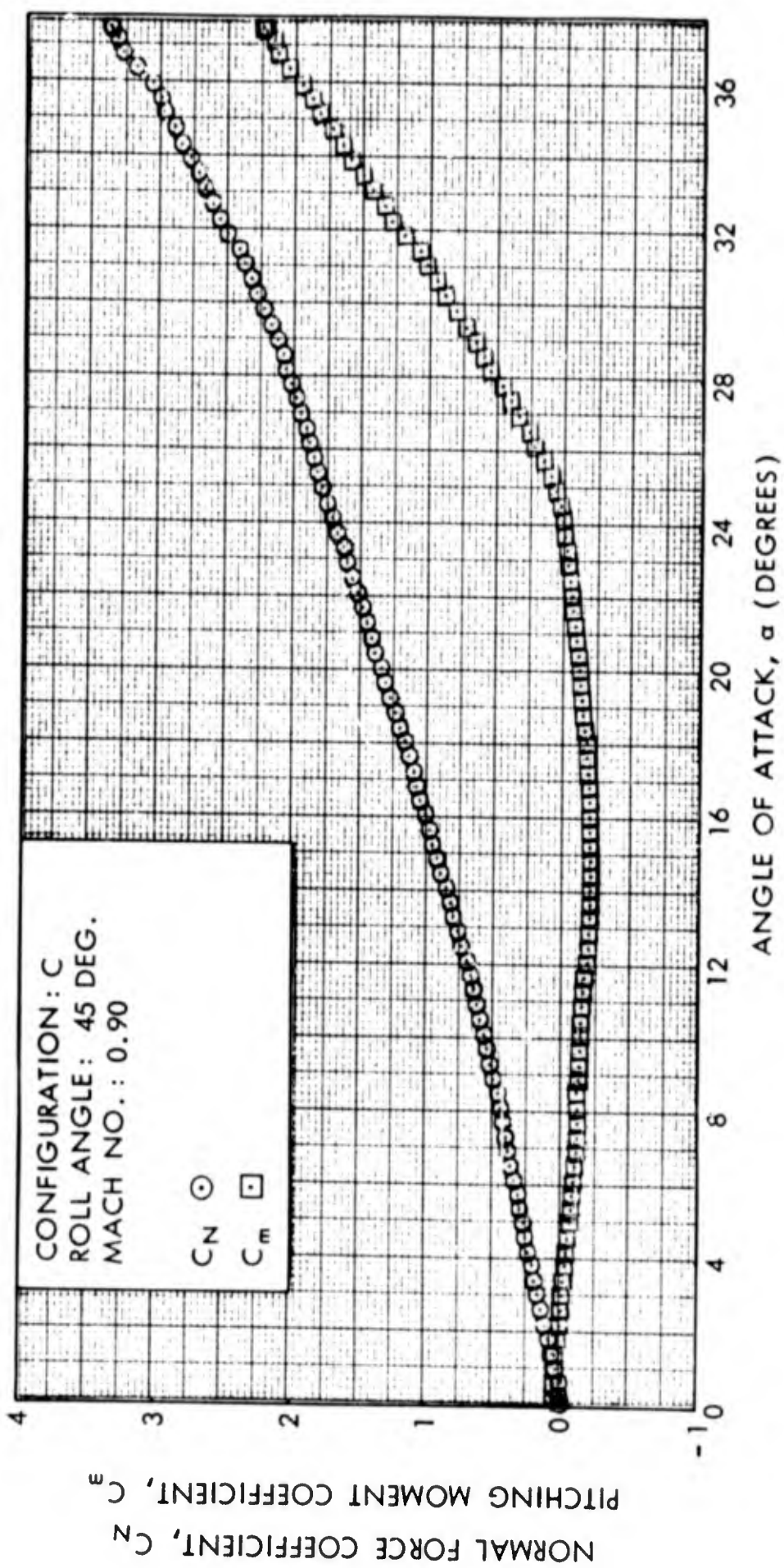


FIG. 22 NORMAL FORCE COEFFICIENT AND PITCHING MOMENT COEFFICIENT VERSUS ANGLE OF ATTACK

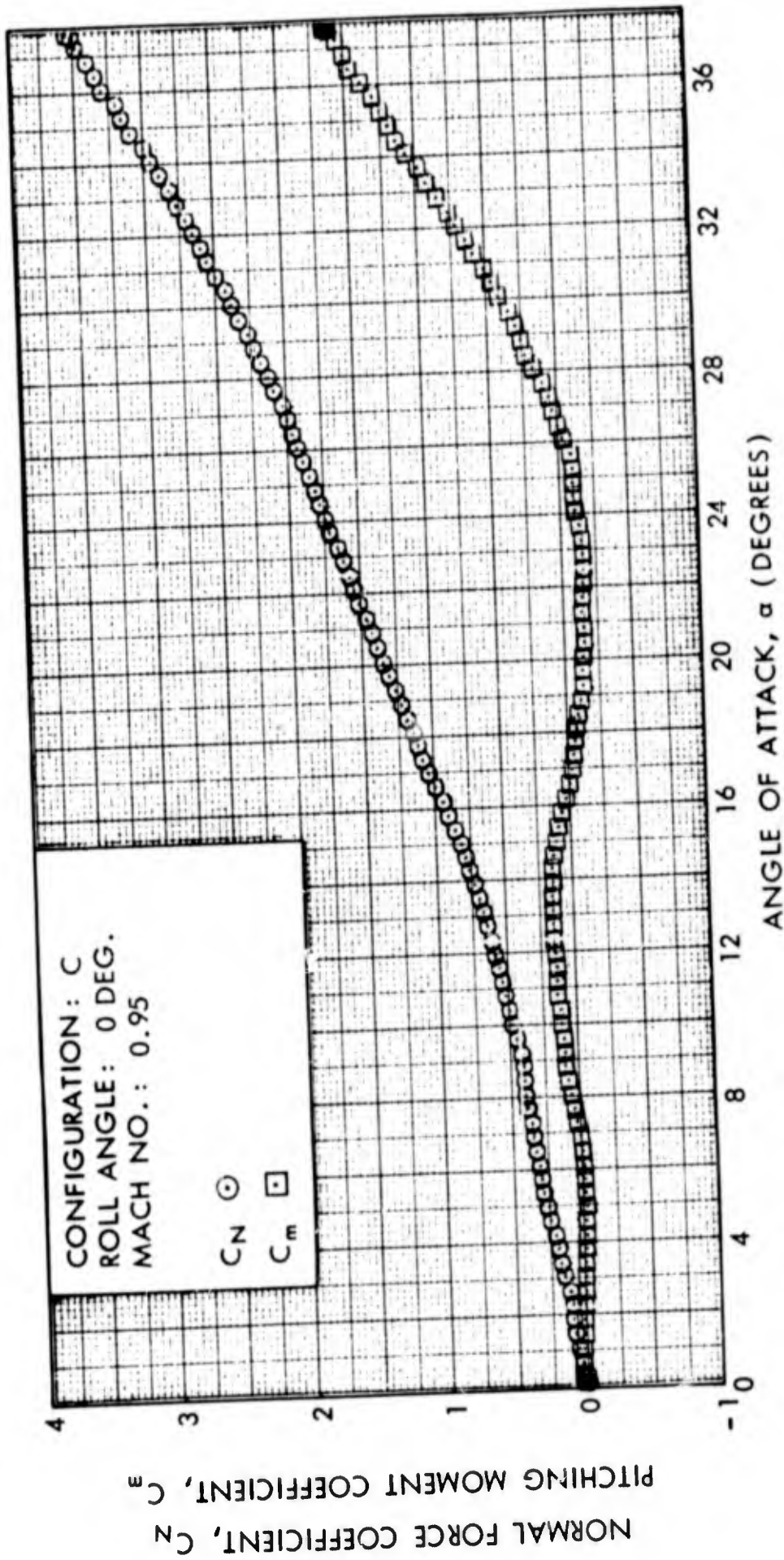


FIG. 23 NORMAL FORCE COEFFICIENT AND PITCHING MOMENT COEFFICIENT VERSUS ANGLE OF ATTACK.

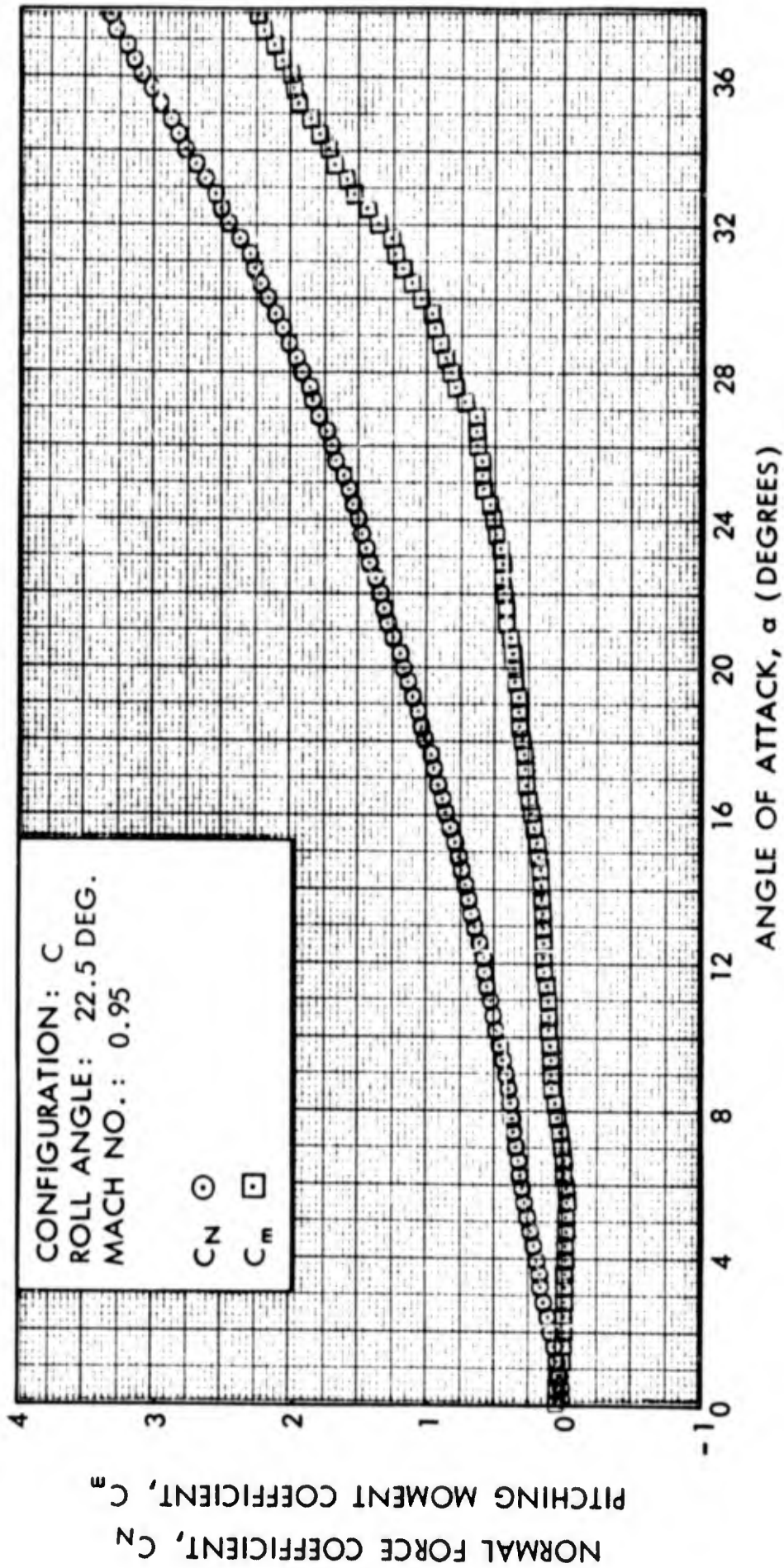


FIG. 24 NORMAL FORCE COEFFICIENT AND PITCHING MOMENT COEFFICIENT VERSUS ANGLE OF ATTACK

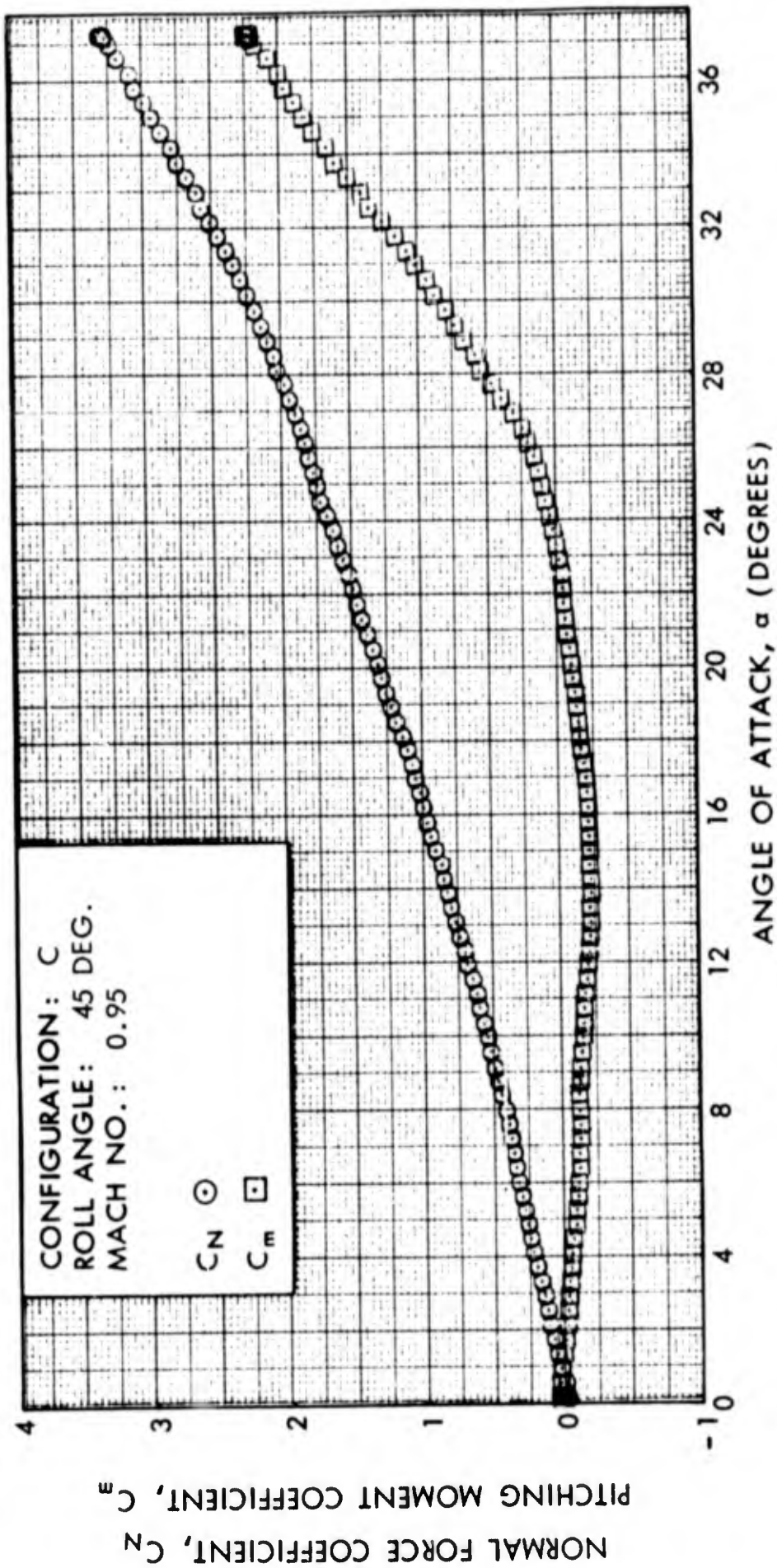


FIG. 25 NORMAL FORCE COEFFICIENT AND PITCHING MOMENT COEFFICIENT VERSUS ANGLE OF ATTACK

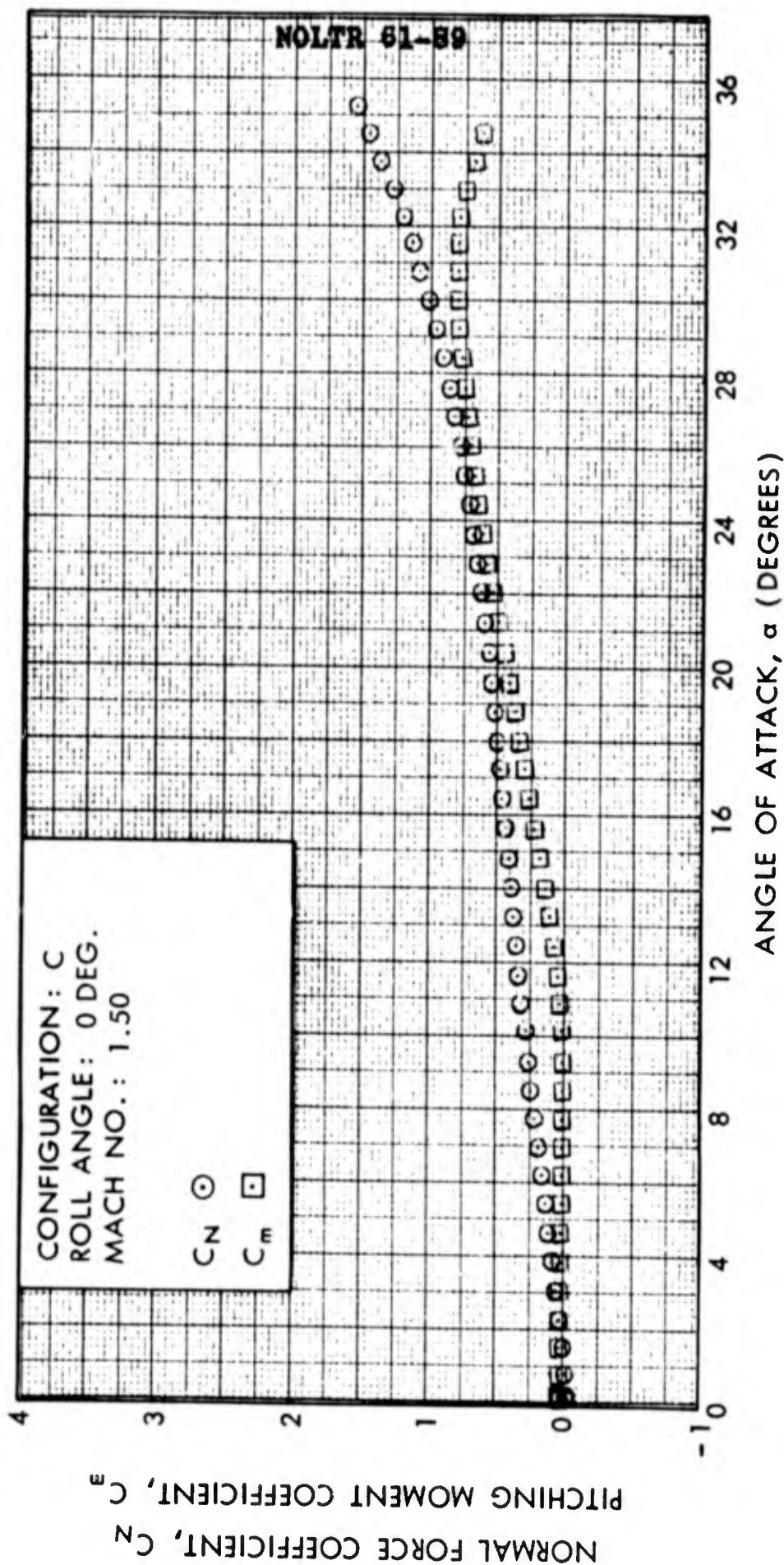


FIG. 26 NORMAL FORCE COEFFICIENT AND PITCHING MOMENT COEFFICIENT VERSUS ANGLE OF ATTACK

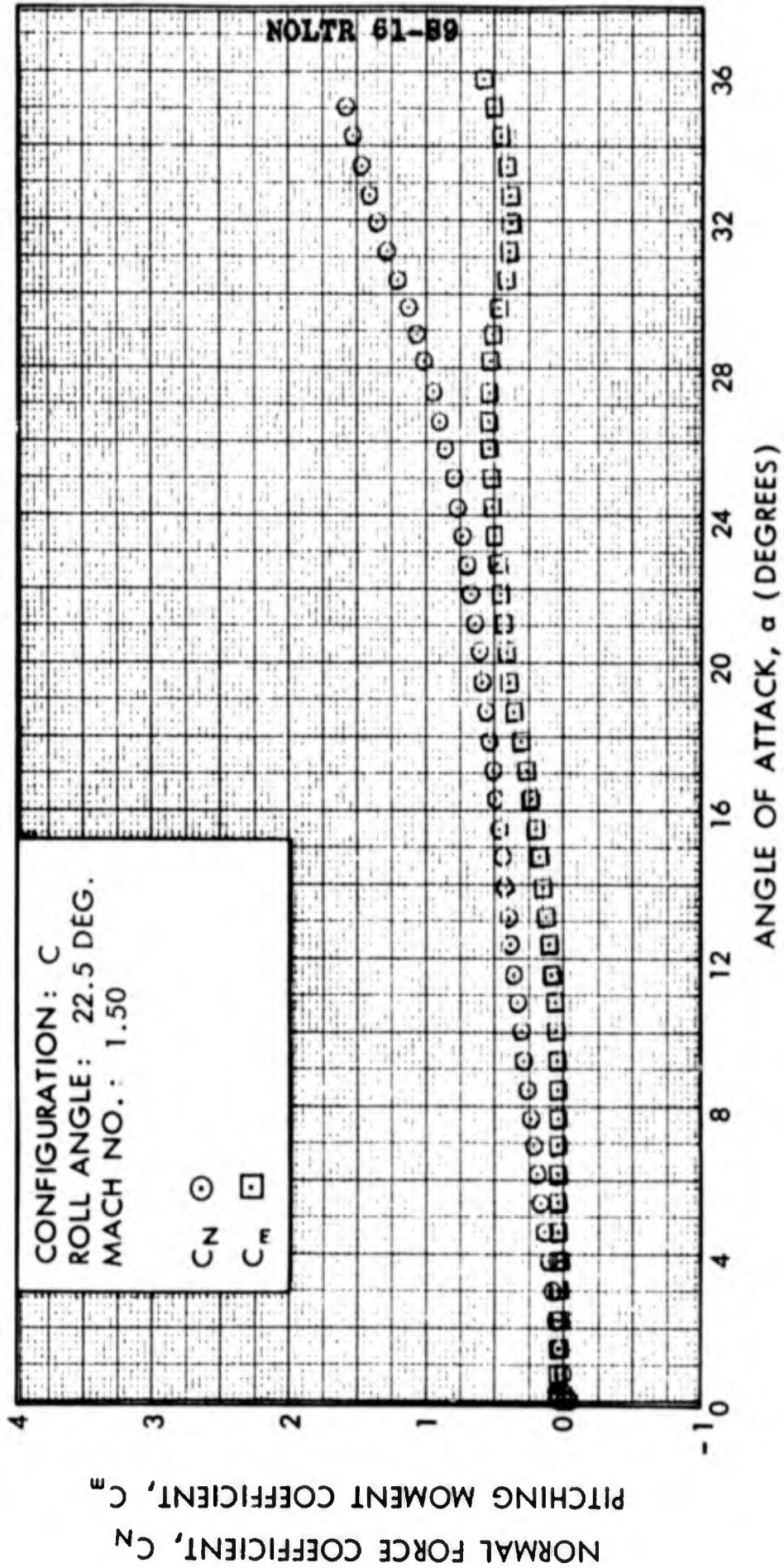


FIG. 27 NORMAL FORCE COEFFICIENT AND PITCHING MOMENT COEFFICIENT VERSUS ANGLE OF ATTACK

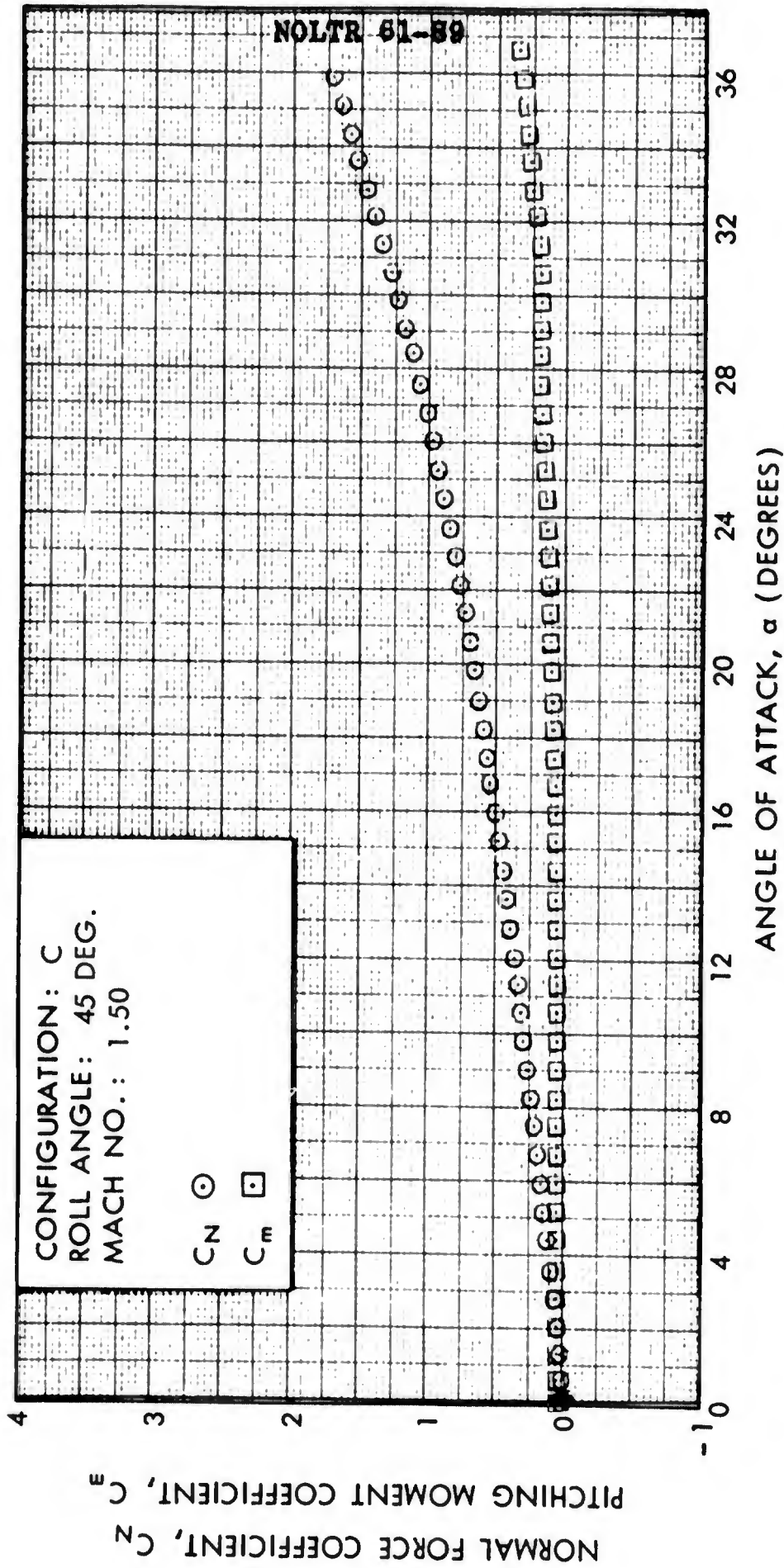


FIG. 28 NORMAL FORCE COEFFICIENT AND PITCHING MOMENT COEFFICIENT VERSUS ANGLE OF ATTACK

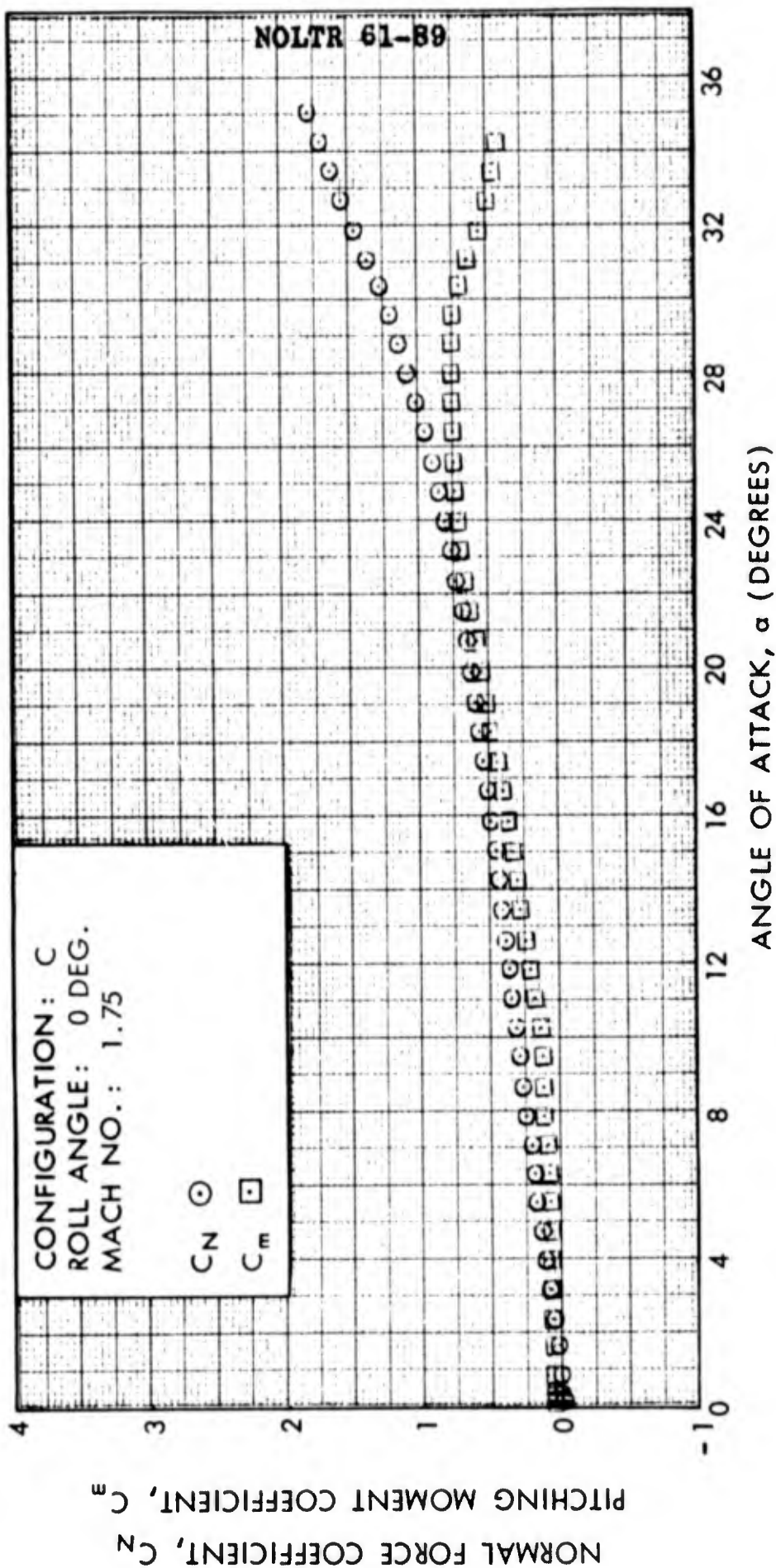


FIG. 29 NORMAL FORCE COEFFICIENT AND PITCHING MOMENT COEFFICIENT VERSUS ANGLE OF ATTACK

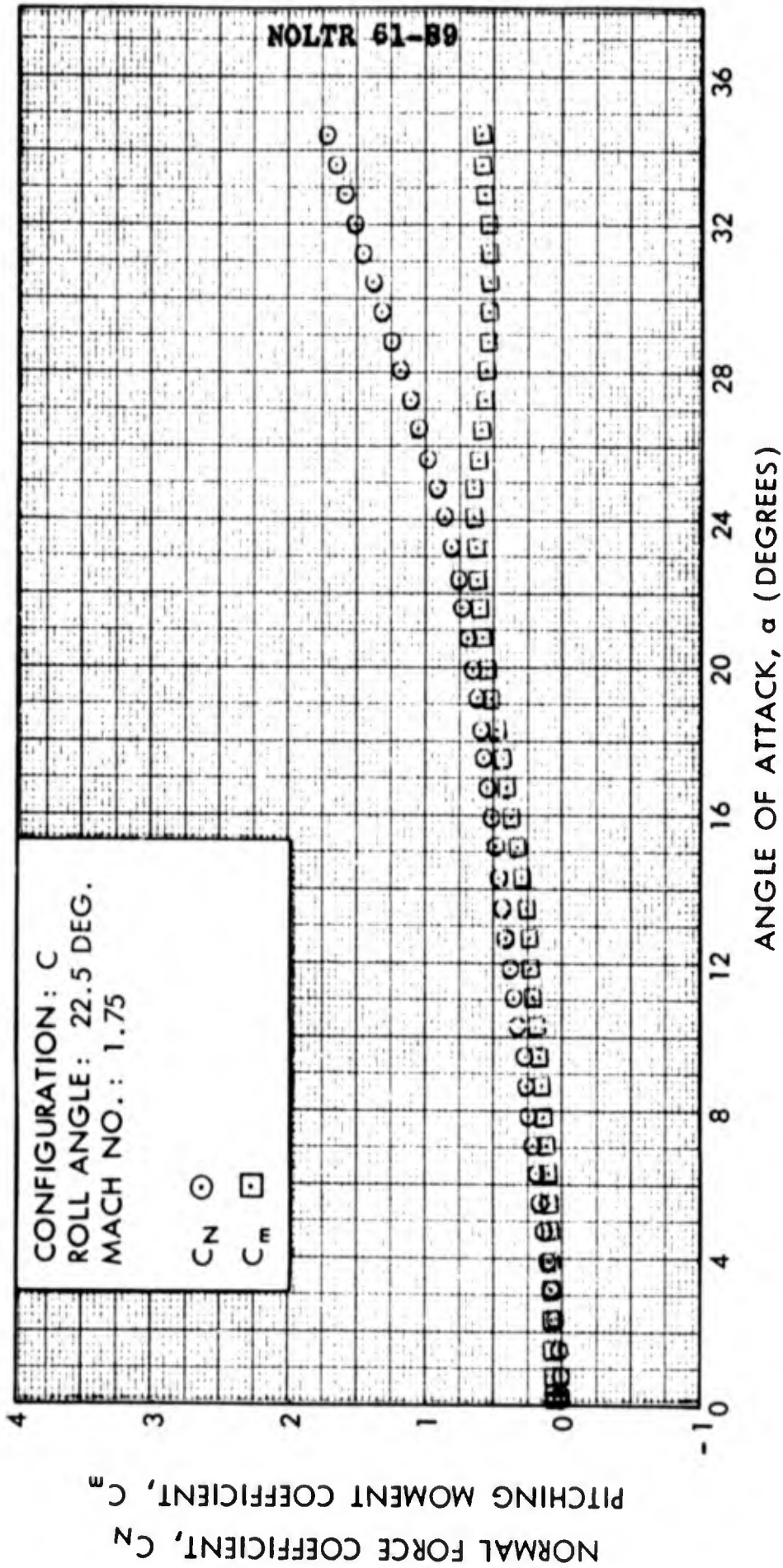


FIG. 30 NORMAL FORCE COEFFICIENT AND PITCHING MOMENT COEFFICIENT VERSUS ANGLE OF ATTACK

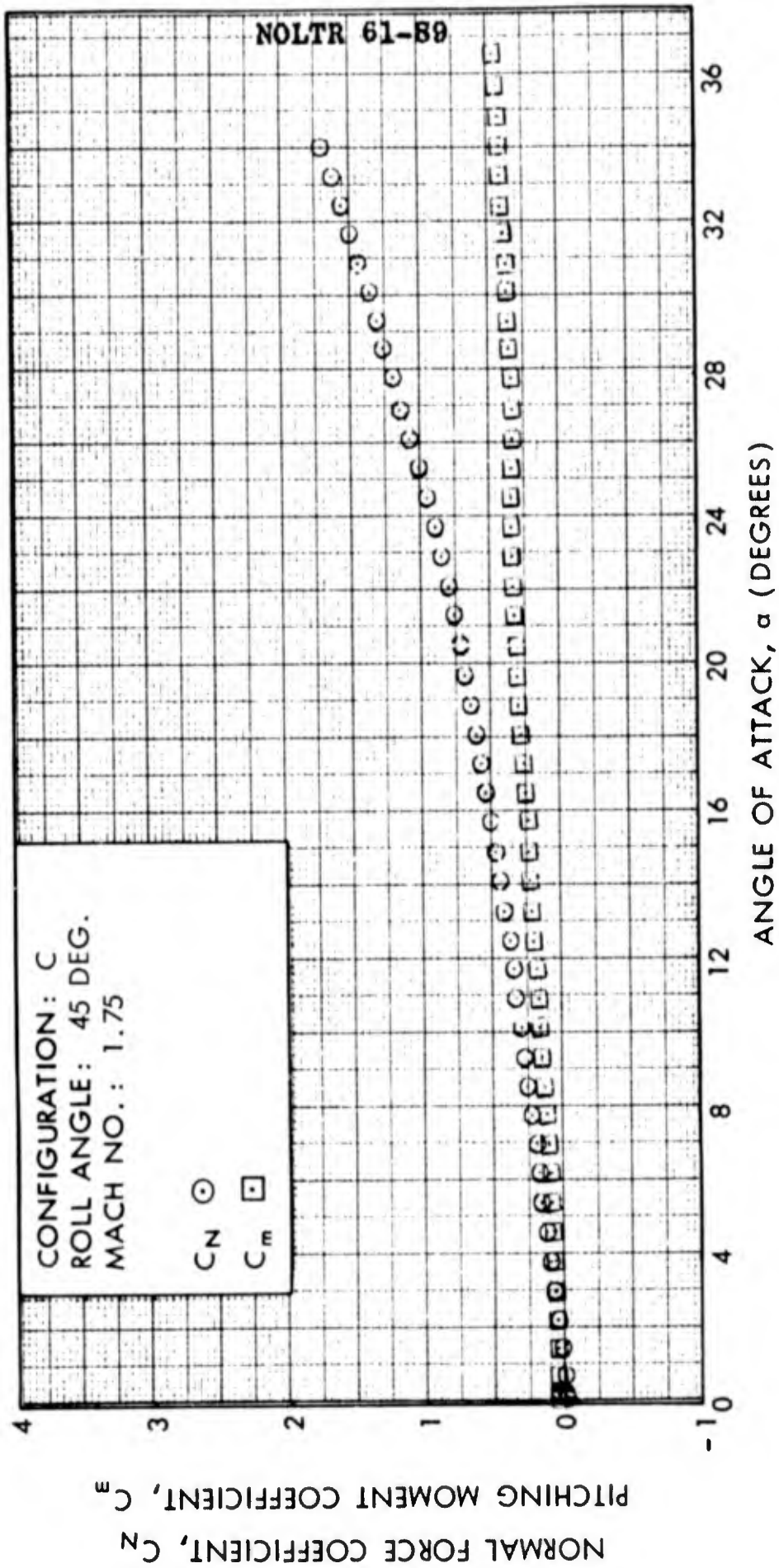


FIG. 31 NORMAL FORCE COEFFICIENT AND PITCHING MOMENT COEFFICIENT VERSUS ANGLE OF ATTACK

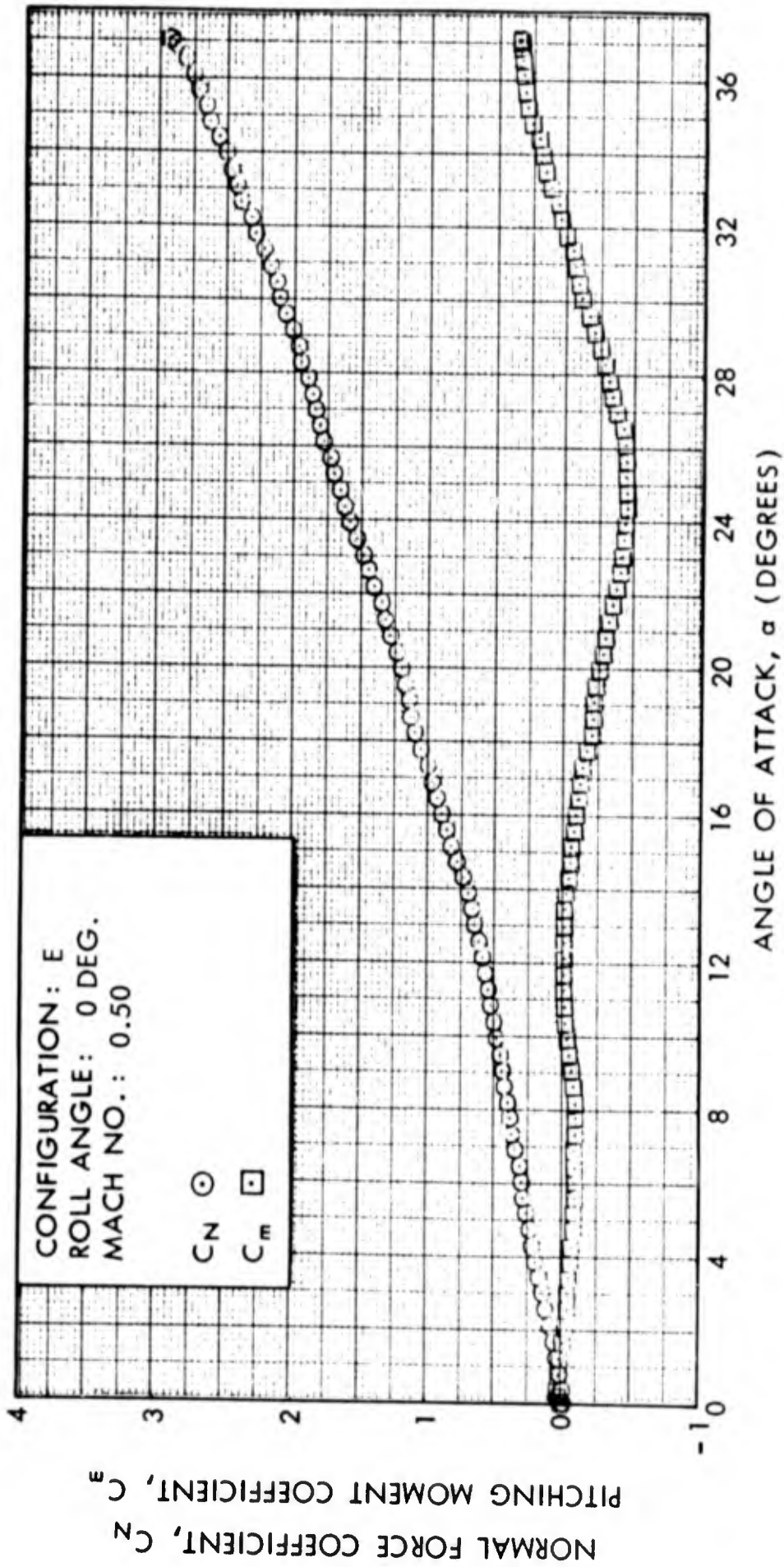


FIG. 32 NORMAL FORCE COEFFICIENT AND PITCHING MOMENT COEFFICIENT VERSUS ANGLE OF ATTACK

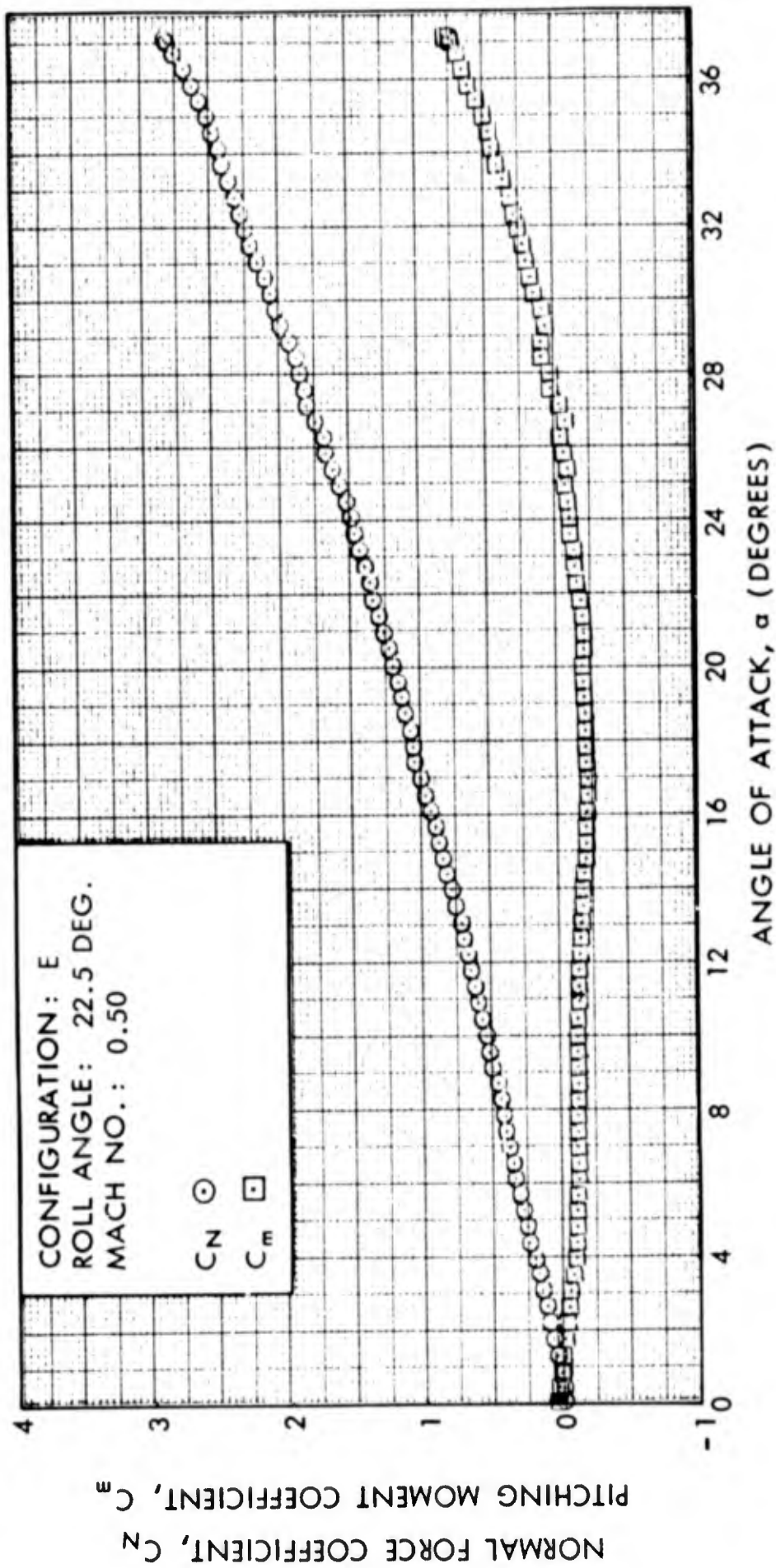


FIG. 33 NORMAL FORCE COEFFICIENT AND PITCHING MOMENT COEFFICIENT VERSUS ANGLE OF ATTACK

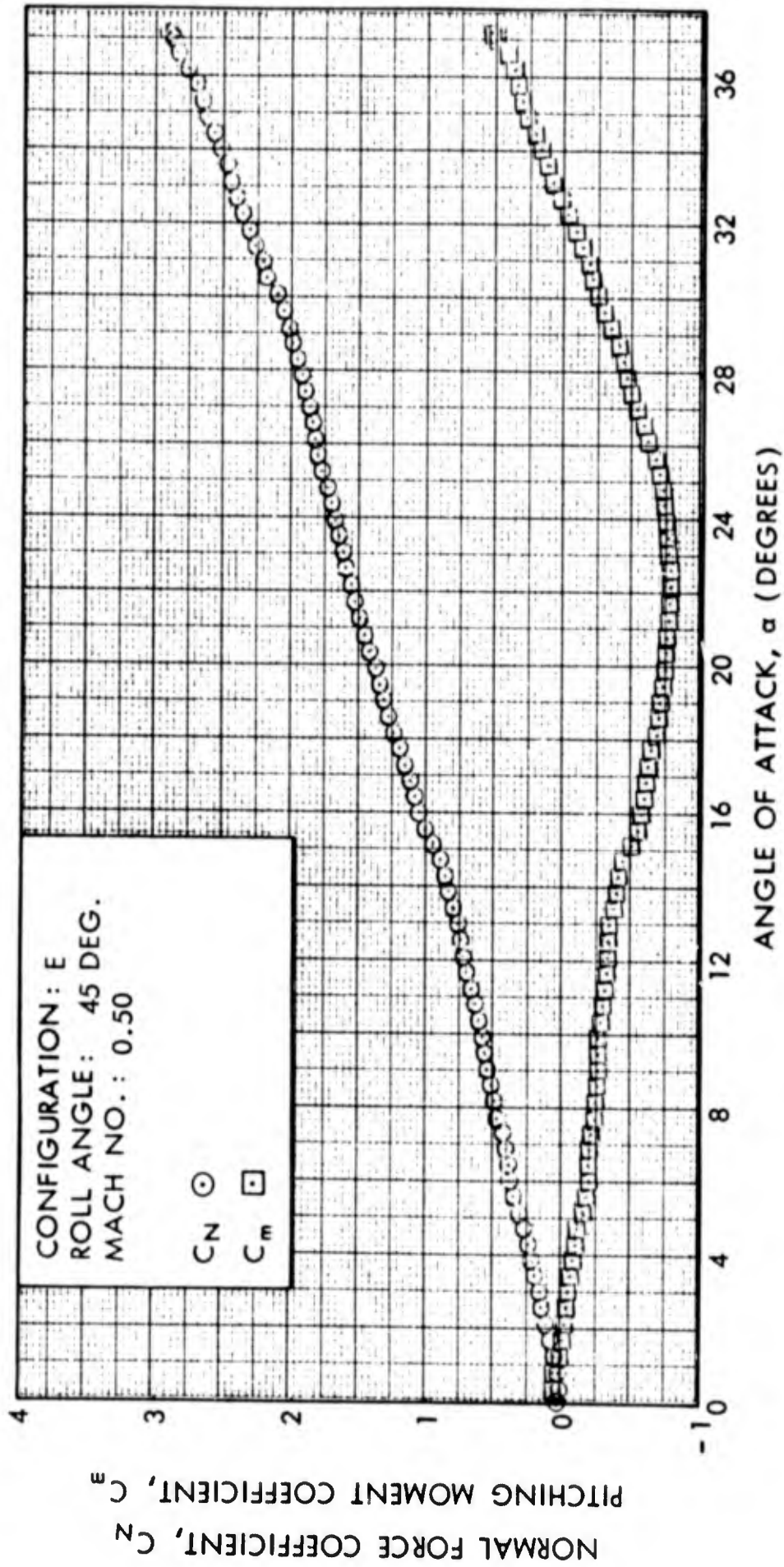


FIG. 34 NORMAL FORCE COEFFICIENT AND PITCHING MOMENT COEFFICIENT VERSUS ANGLE OF ATTACK

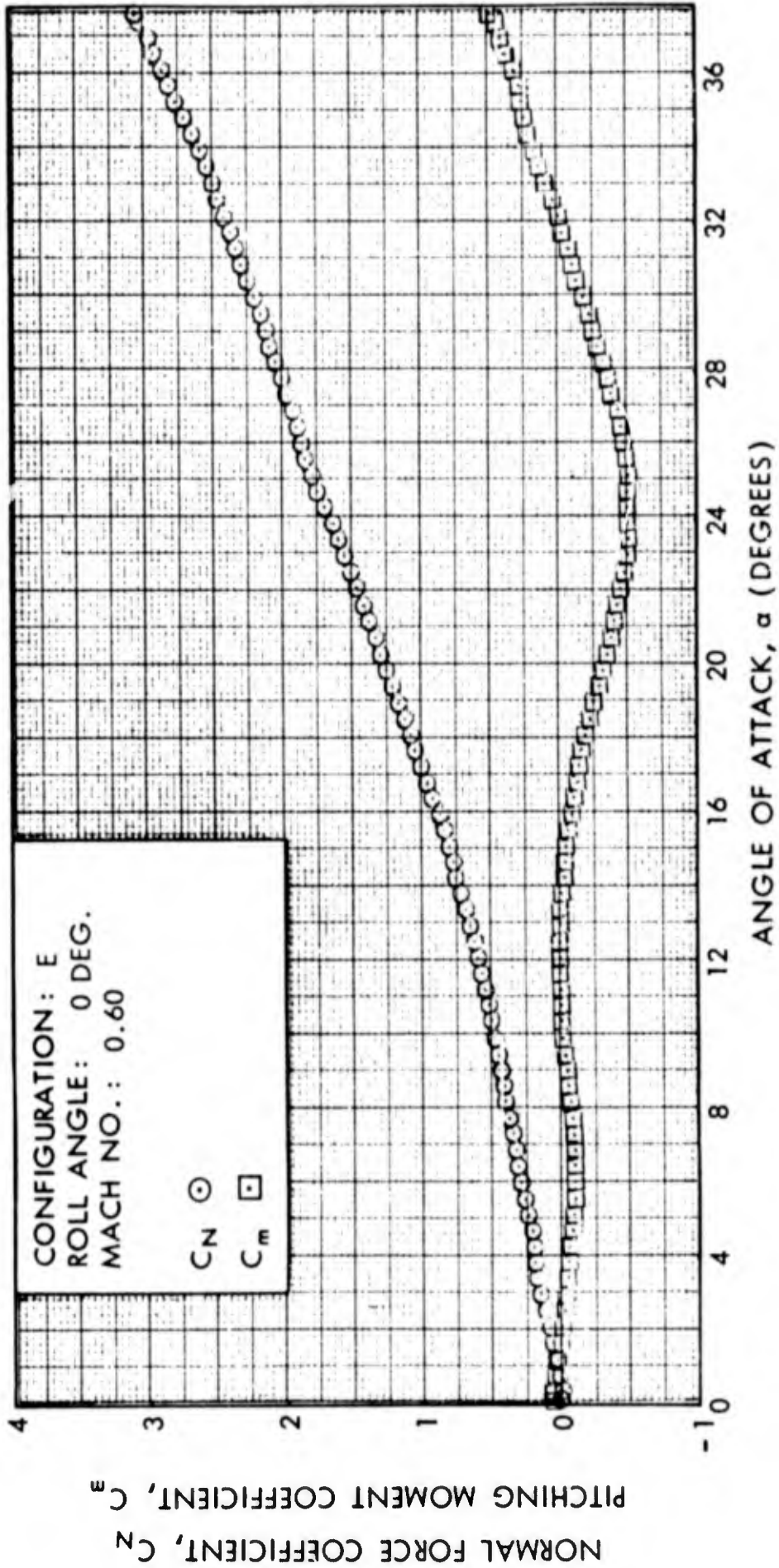


FIG. 35 NORMAL FORCE COEFFICIENT AND PITCHING MOMENT COEFFICIENT VERSUS ANGLE OF ATTACK

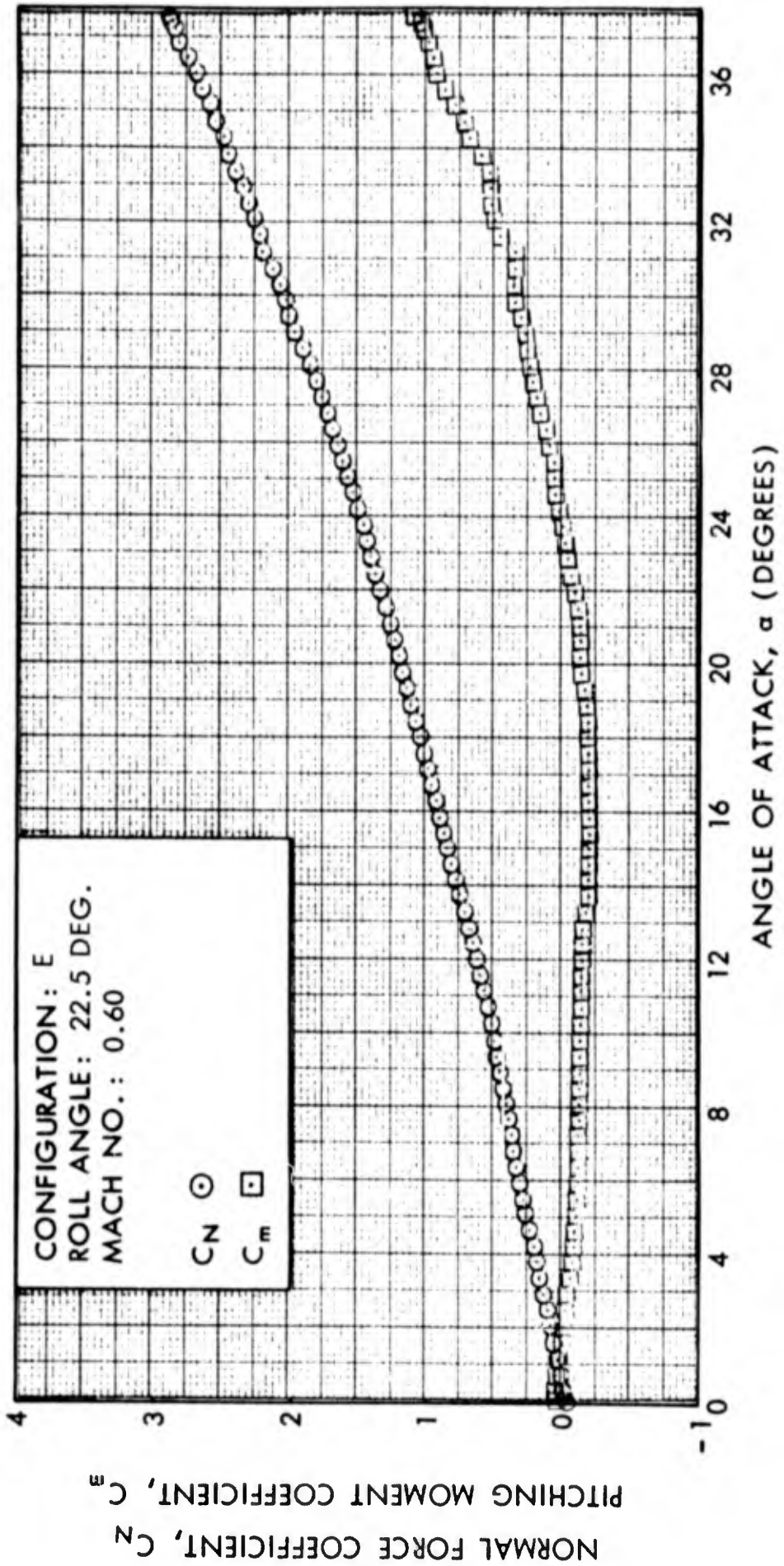


FIG. 36 NORMAL FORCE COEFFICIENT AND PITCHING MOMENT COEFFICIENT VERSUS ANGLE OF ATTACK

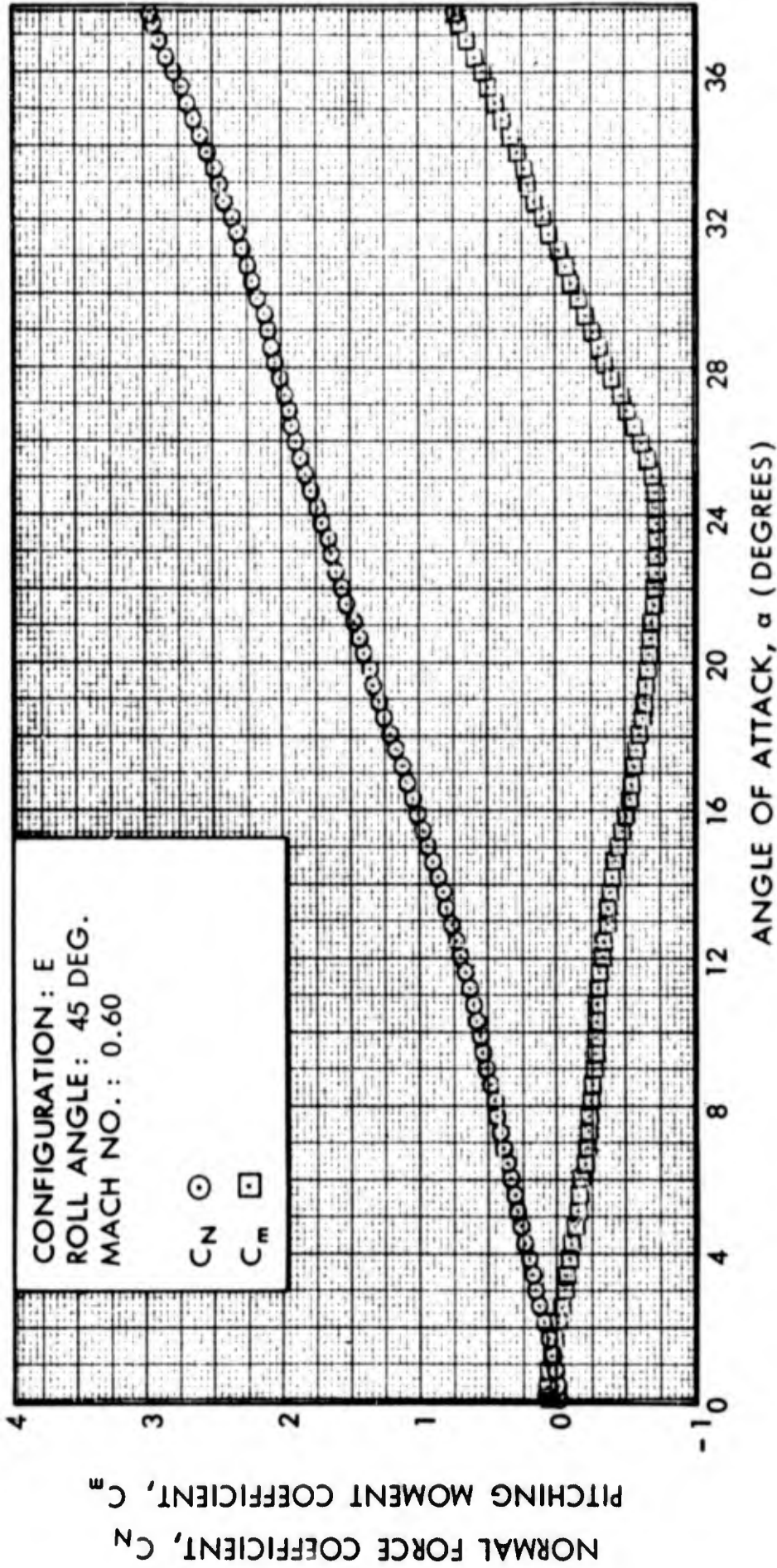


FIG. 37 NORMAL FORCE COEFFICIENT AND PITCHING MOMENT COEFFICIENT VERSUS ANGLE OF ATTACK

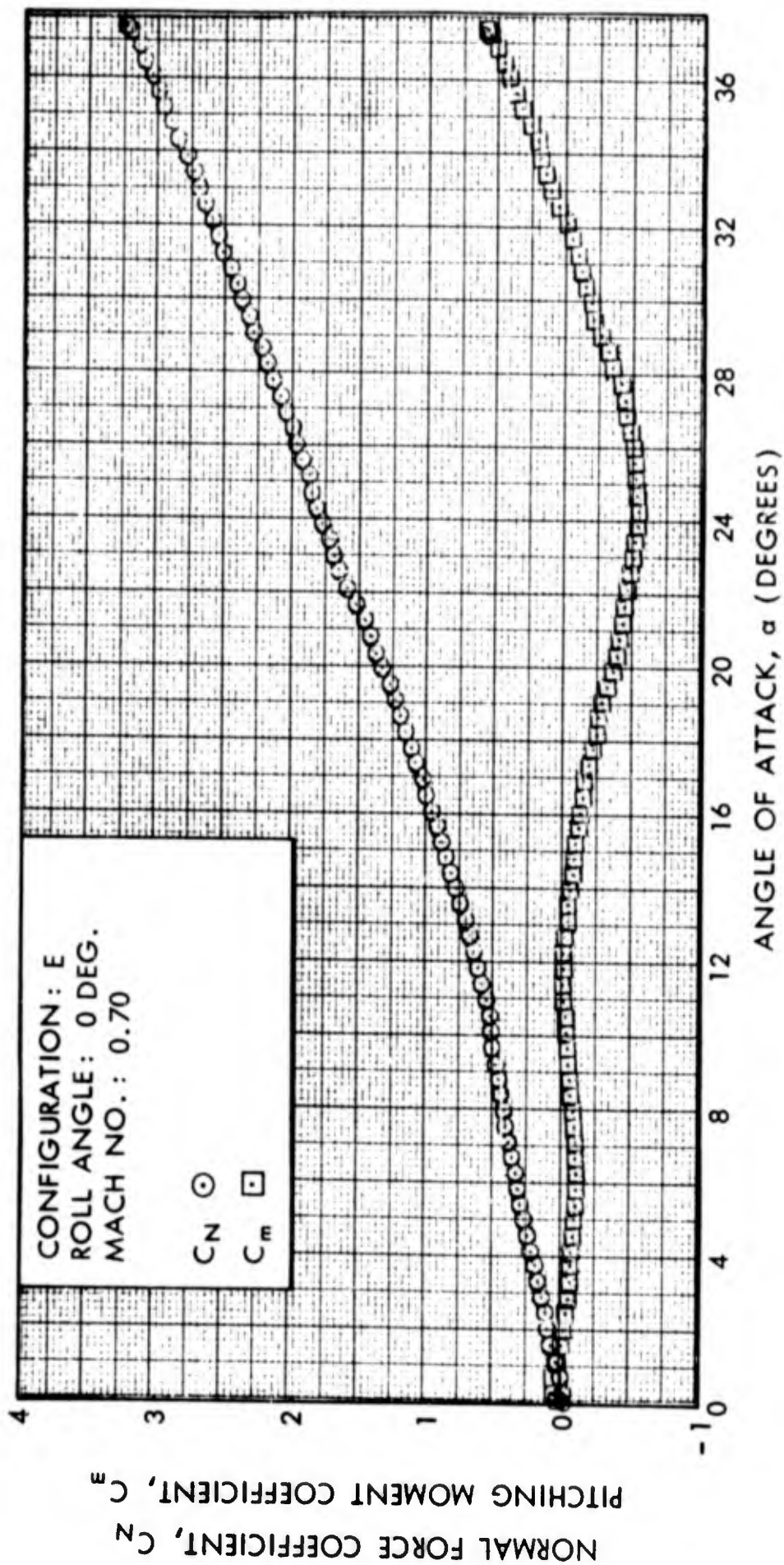


FIG. 38 NORMAL FORCE COEFFICIENT AND PITCHING MOMENT COEFFICIENT VERSUS ANGLE OF ATTACK

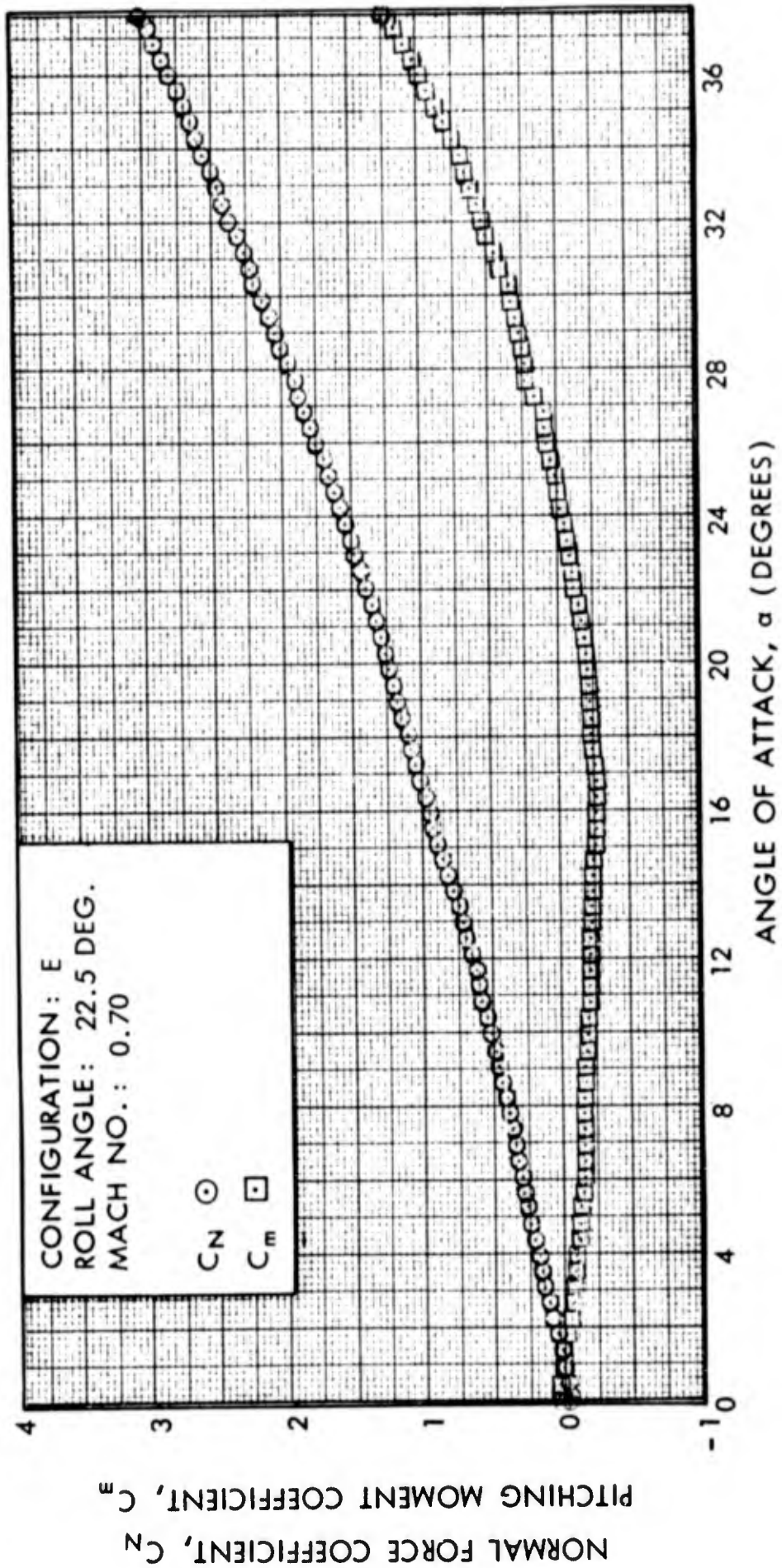


FIG. 39 NORMAL FORCE COEFFICIENT AND PITCHING MOMENT COEFFICIENT VERSUS ANGLE OF ATTACK

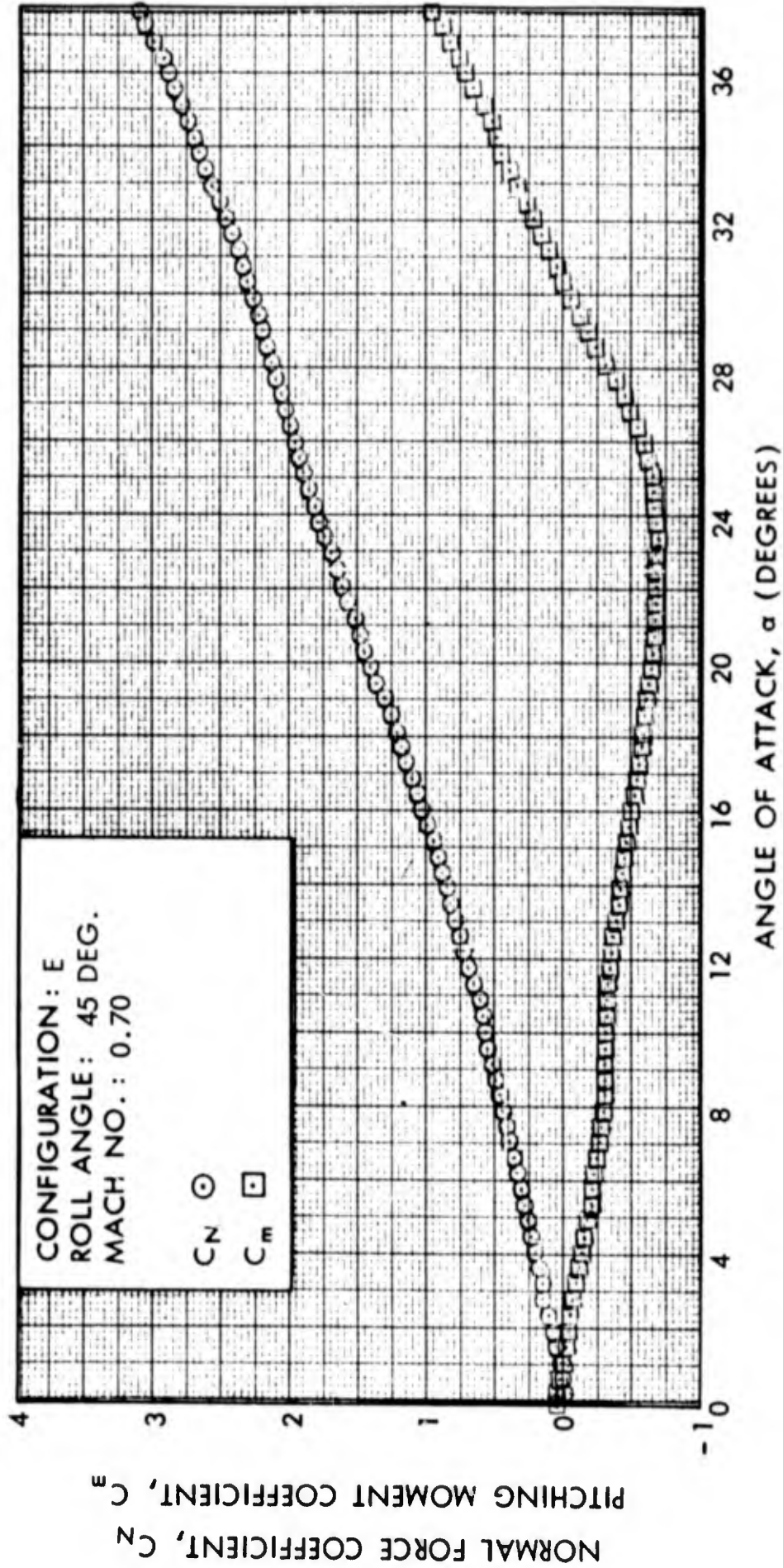


FIG. 40 NORMAL FORCE COEFFICIENT AND PITCHING MOMENT COEFFICIENT VERSUS ANGLE OF ATTACK

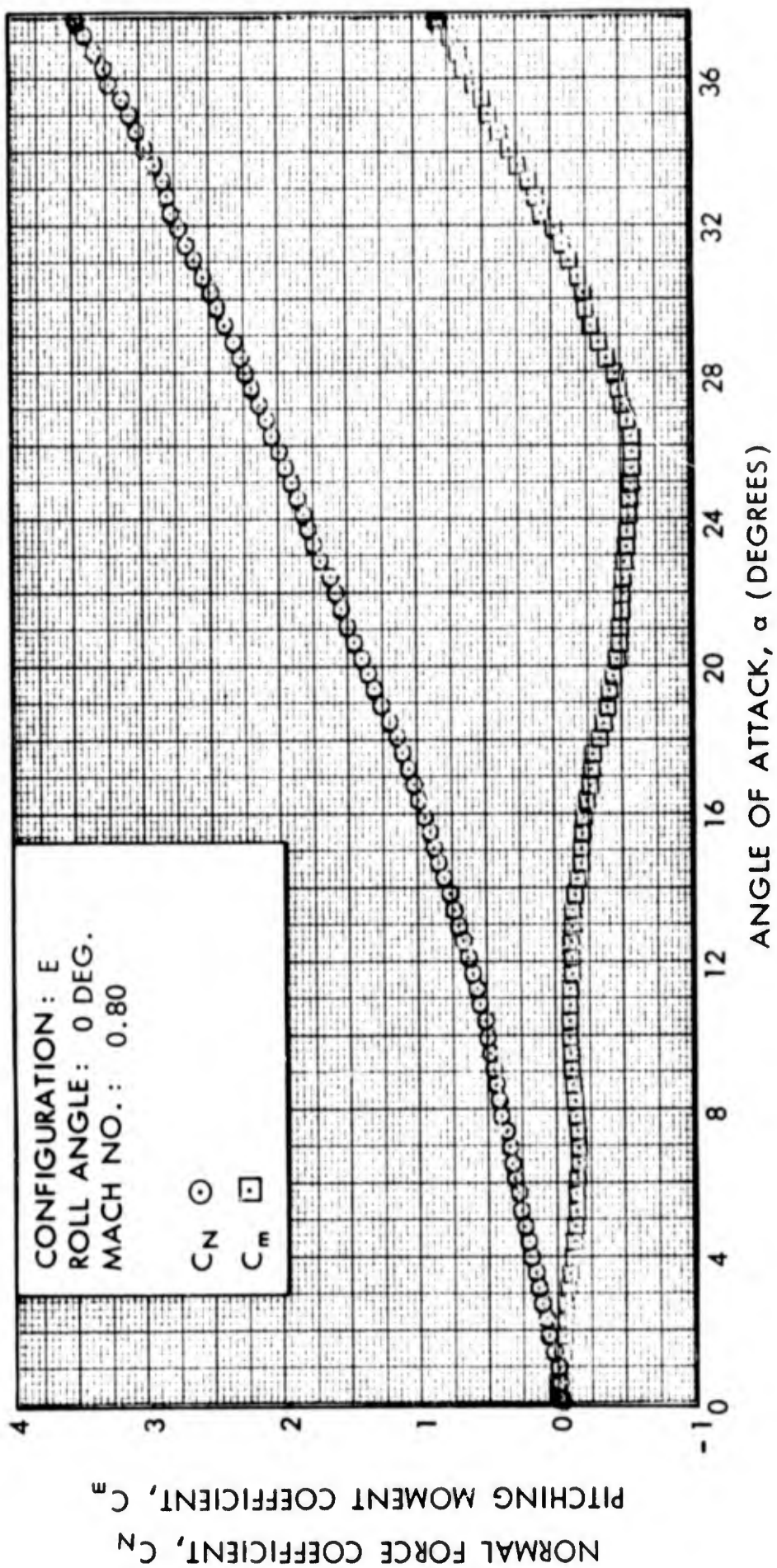


FIG. 41 NORMAL FORCE COEFFICIENT AND PITCHING MOMENT COEFFICIENT VERSUS ANGLE OF ATTACK

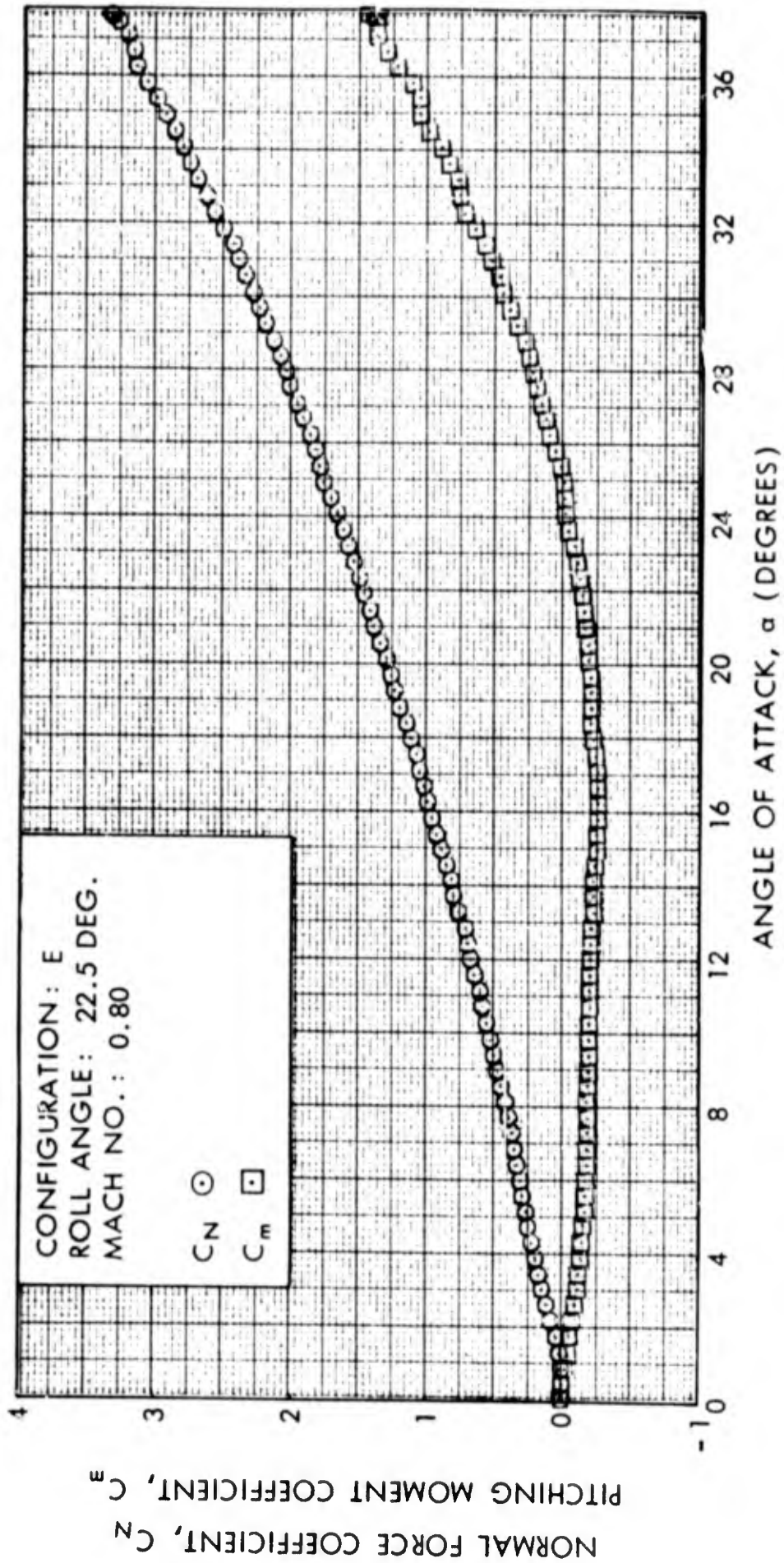


FIG. 42 NORMAL FORCE COEFFICIENT AND PITCHING MOMENT COEFFICIENT VERSUS ANGLE OF ATTACK

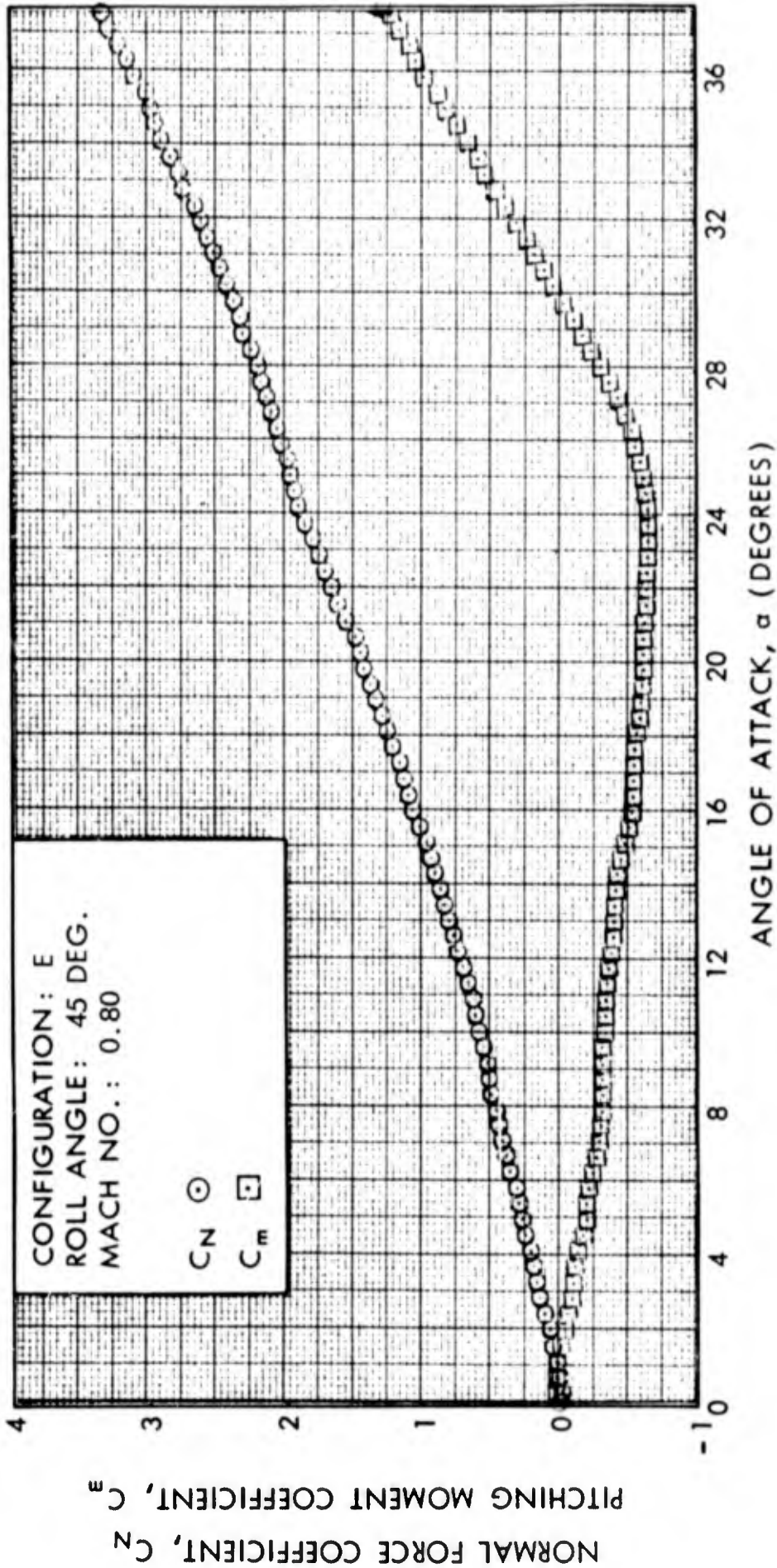


FIG. 43 NORMAL FORCE COEFFICIENT AND PITCHING MOMENT COEFFICIENT VERSUS ANGLE OF ATTACK

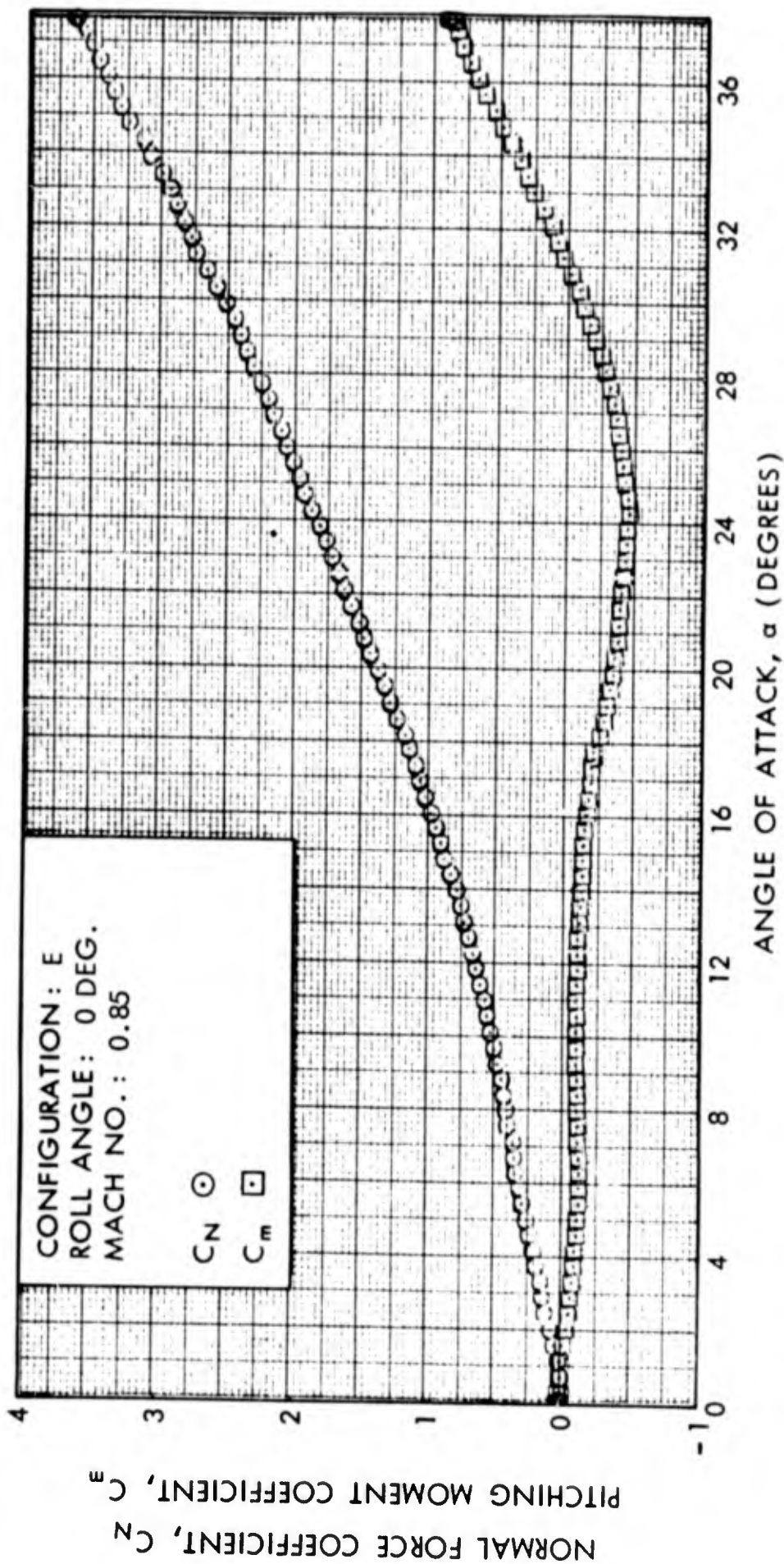


FIG. 44 NORMAL FORCE COEFFICIENT AND PITCHING MOMENT COEFFICIENT VERSUS ANGLE OF ATTACK

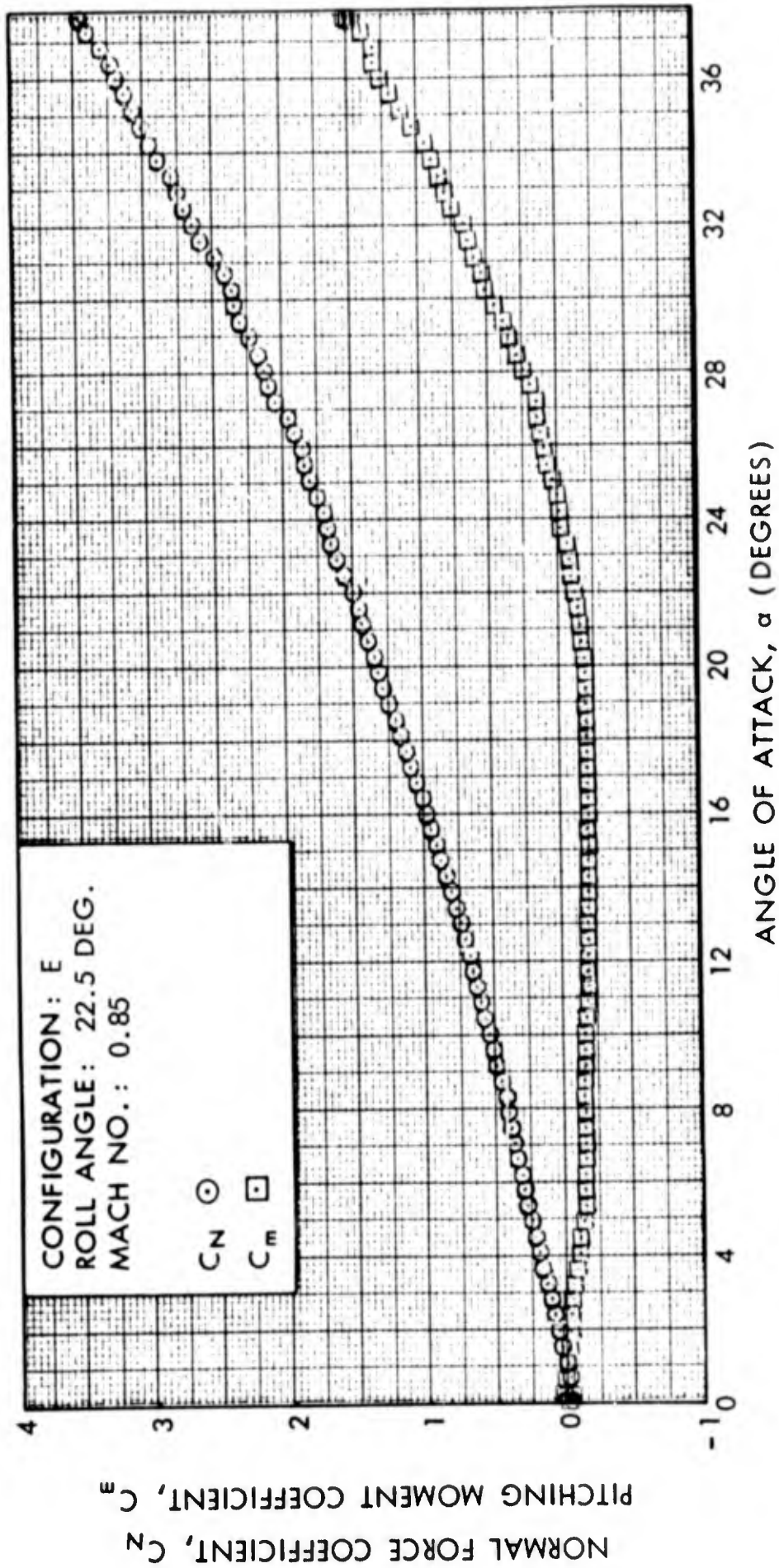


FIG. 45 NORMAL FORCE COEFFICIENT AND PITCHING MOMENT COEFFICIENT VERSUS ANGLE OF ATTACK

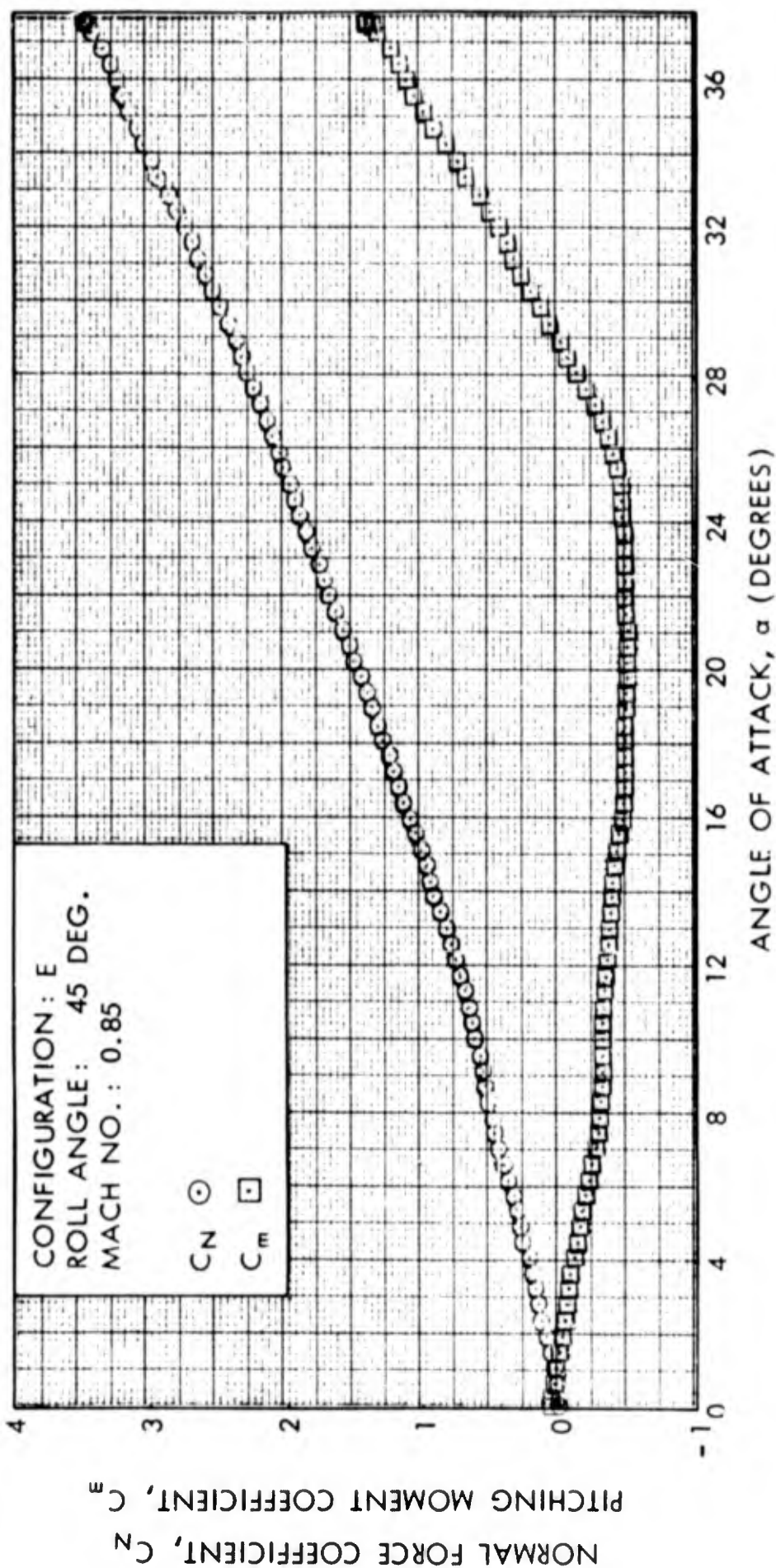


FIG. 46 NORMAL FORCE COEFFICIENT AND PITCHING MOMENT COEFFICIENT VERSUS ANGLE OF ATTACK

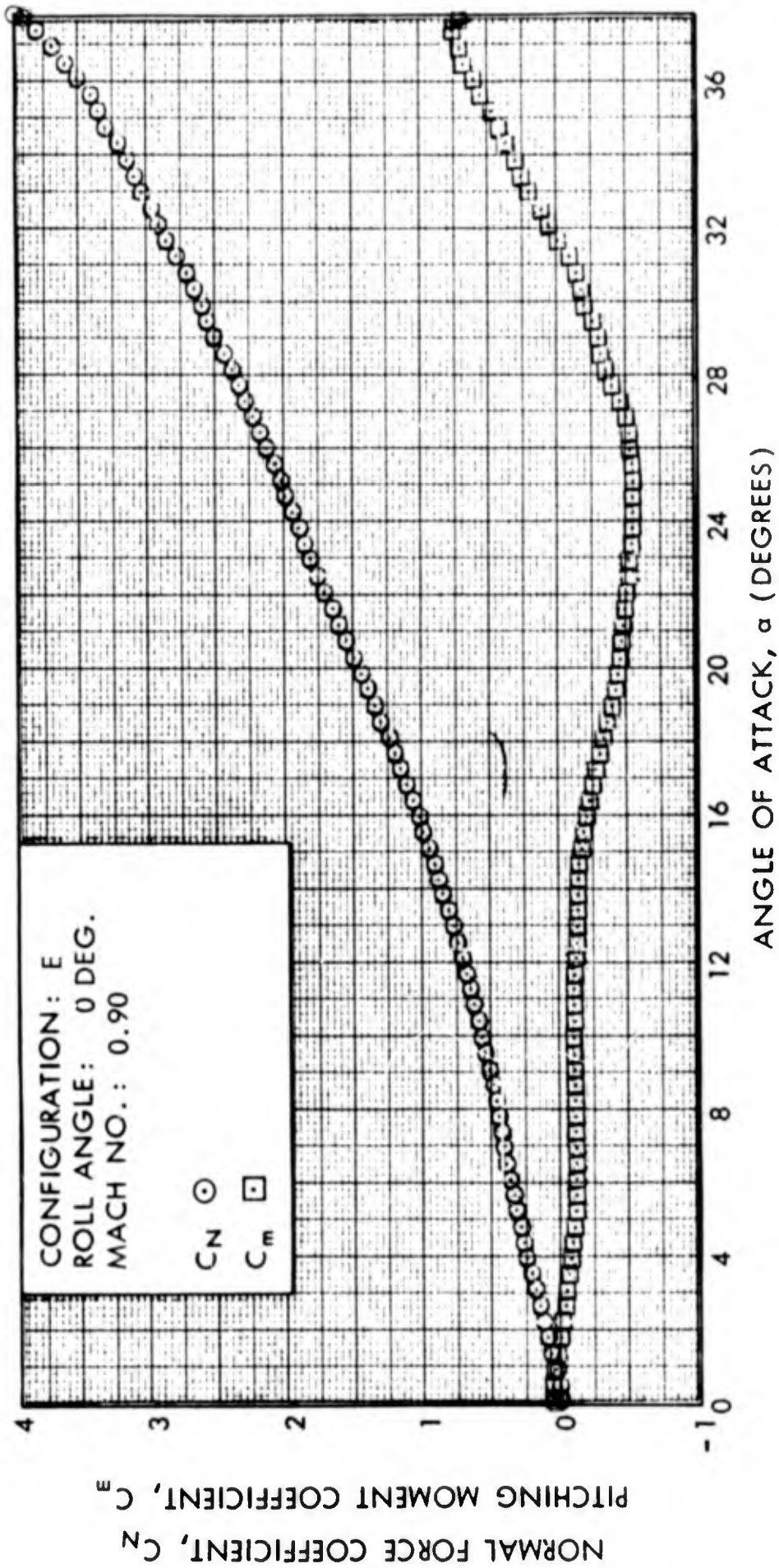


FIG. 47 NORMAL FORCE COEFFICIENT AND PITCHING MOMENT COEFFICIENT VERSUS ANGLE OF ATTACK

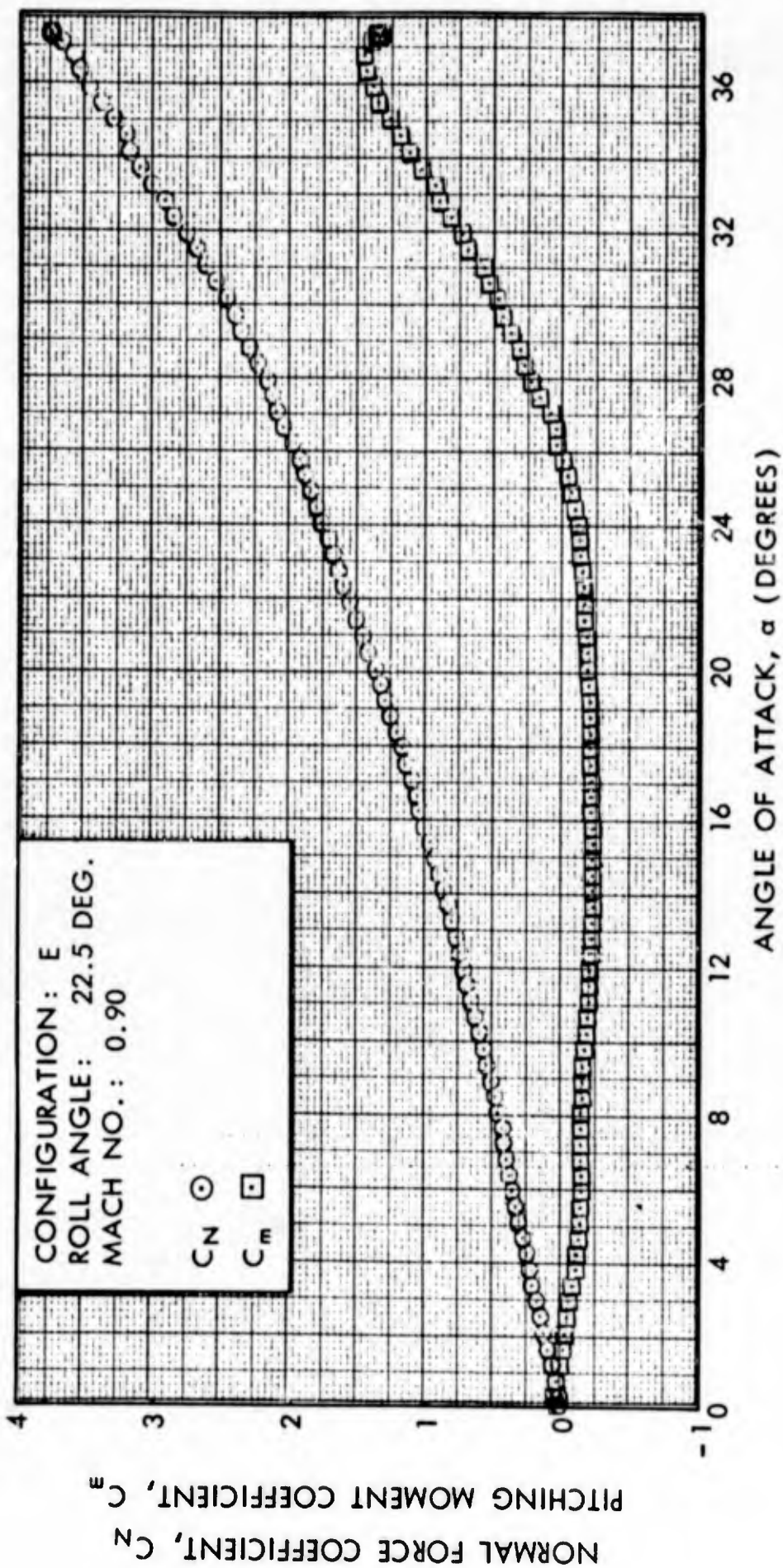


FIG. 48 NORMAL FORCE COEFFICIENT AND PITCHING  
MOMENT COEFFICIENT VERSUS ANGLE OF ATTACK

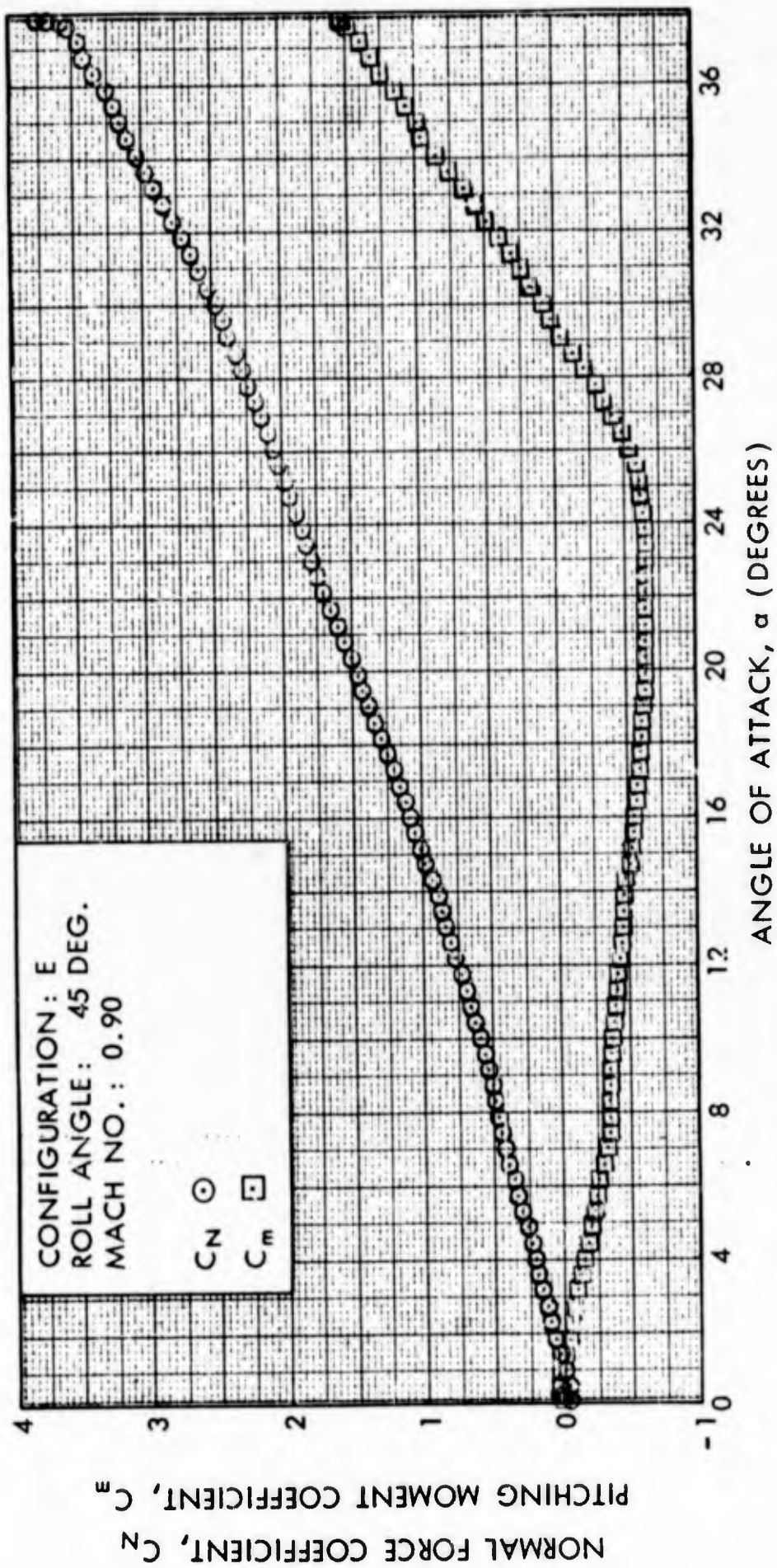


FIG. 49 NORMAL FORCE COEFFICIENT AND PITCHING MOMENT COEFFICIENT VERSUS ANGLE OF ATTACK

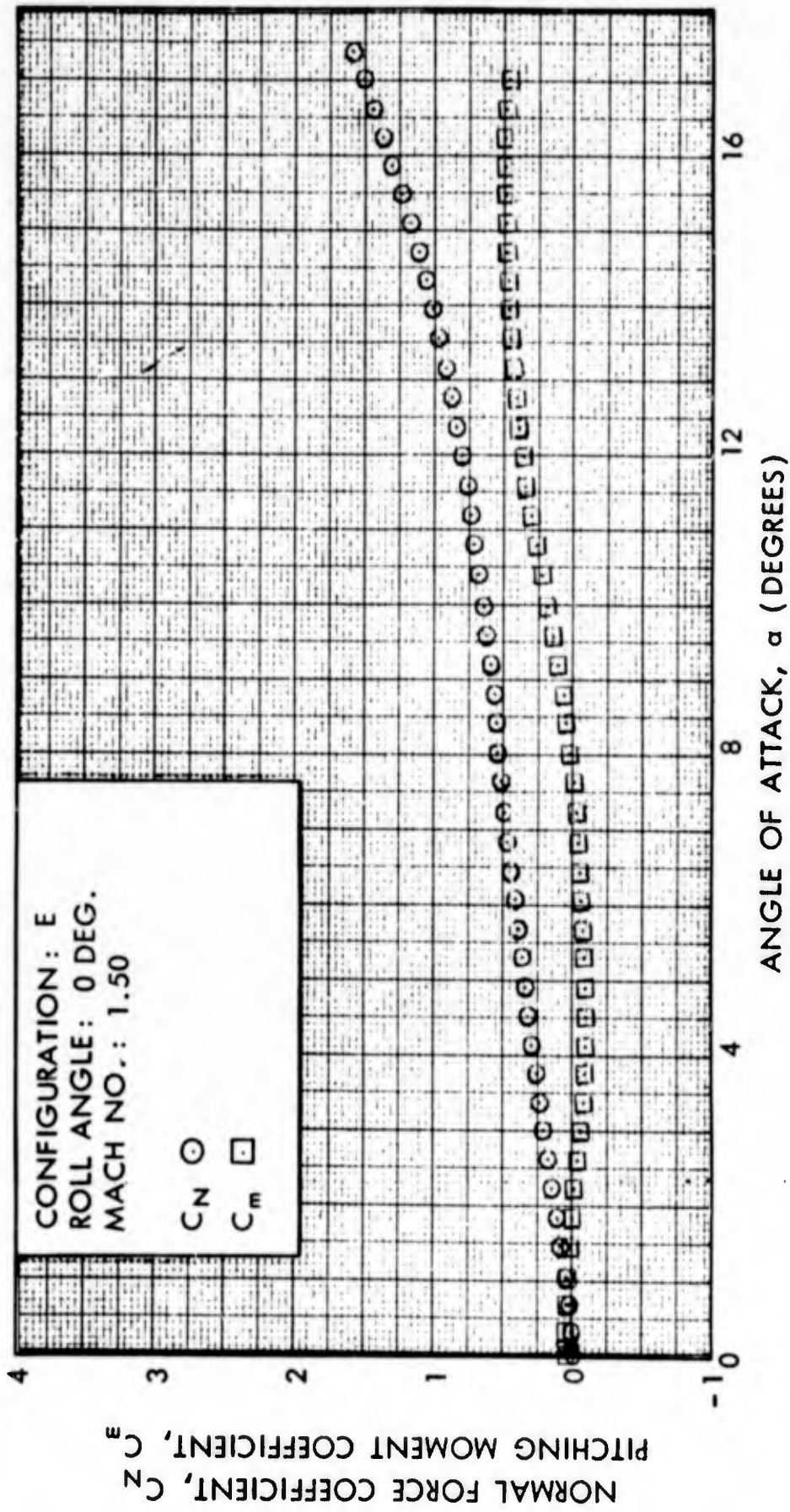


FIG. 50 NORMAL FORCE COEFFICIENT AND PITCHING  
MOMENT COEFFICIENT VERSUS ANGLE OF ATTACK

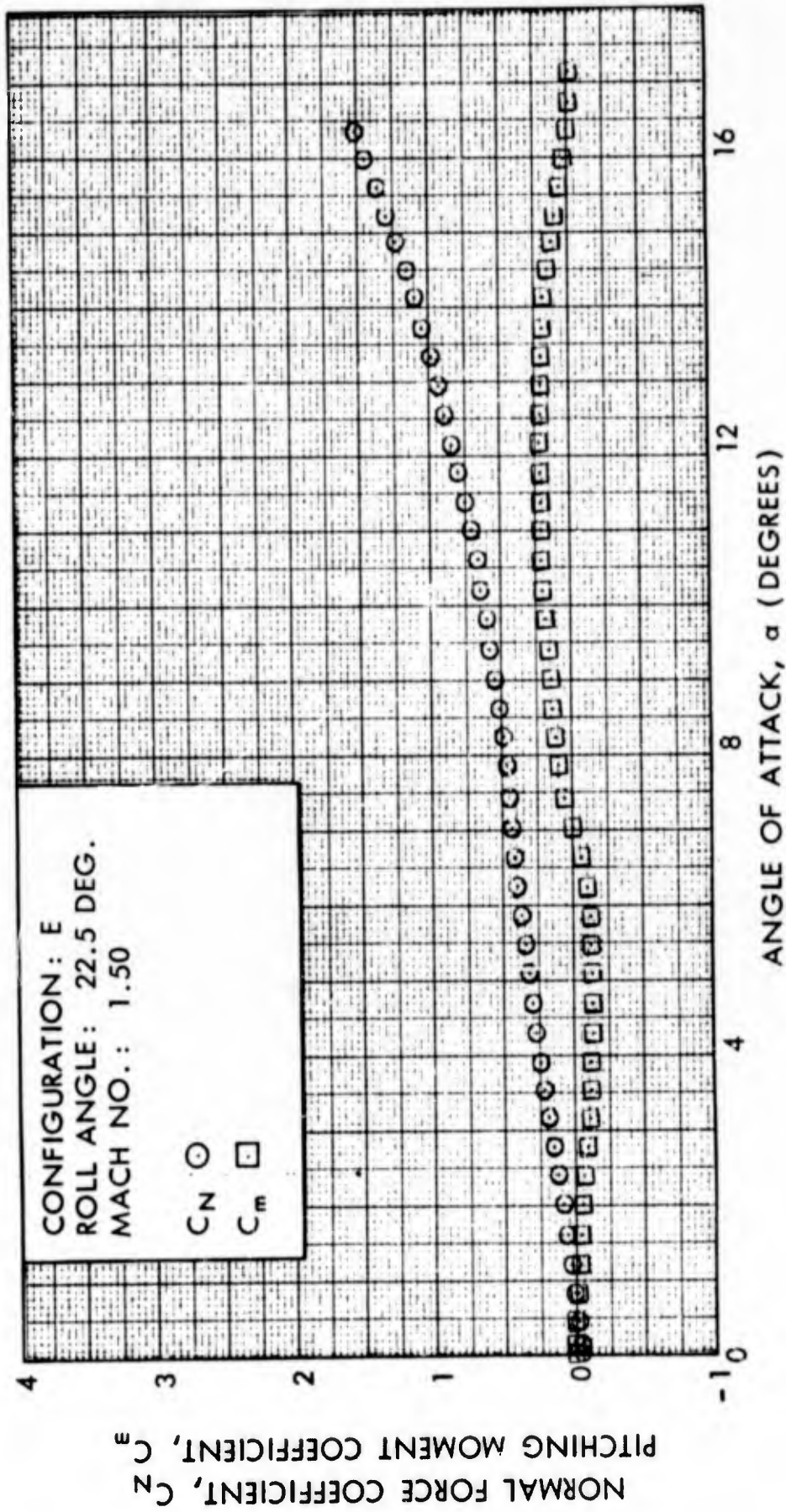


FIG. 51 NORMAL FORCE COEFFICIENT AND PITCHING MOMENT COEFFICIENT VERSUS ANGLE OF ATTACK

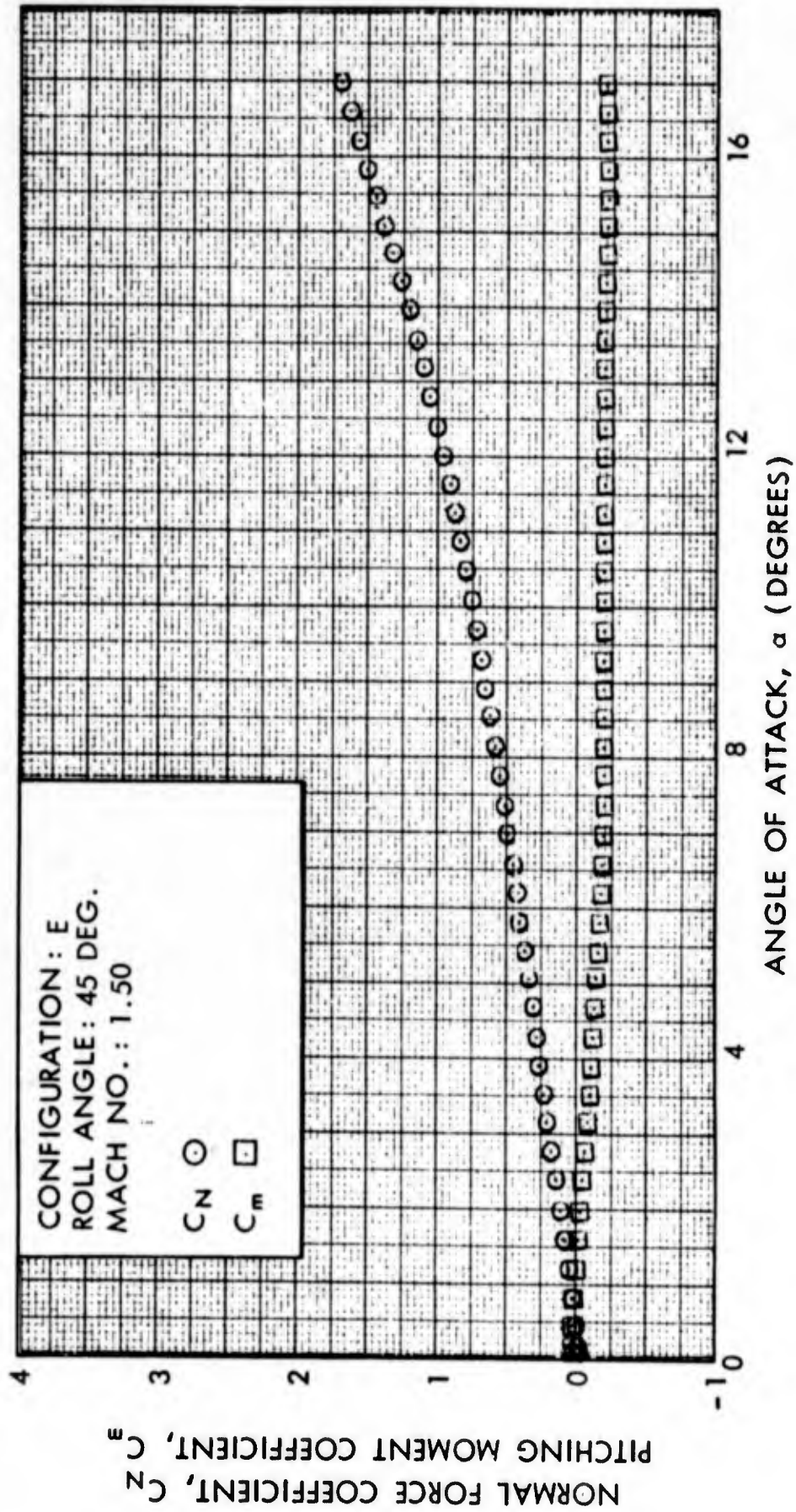


FIG. 52 NORMAL FORCE COEFFICIENT AND PITCHING MOMENT COEFFICIENT VERSUS ANGLE OF ATTACK

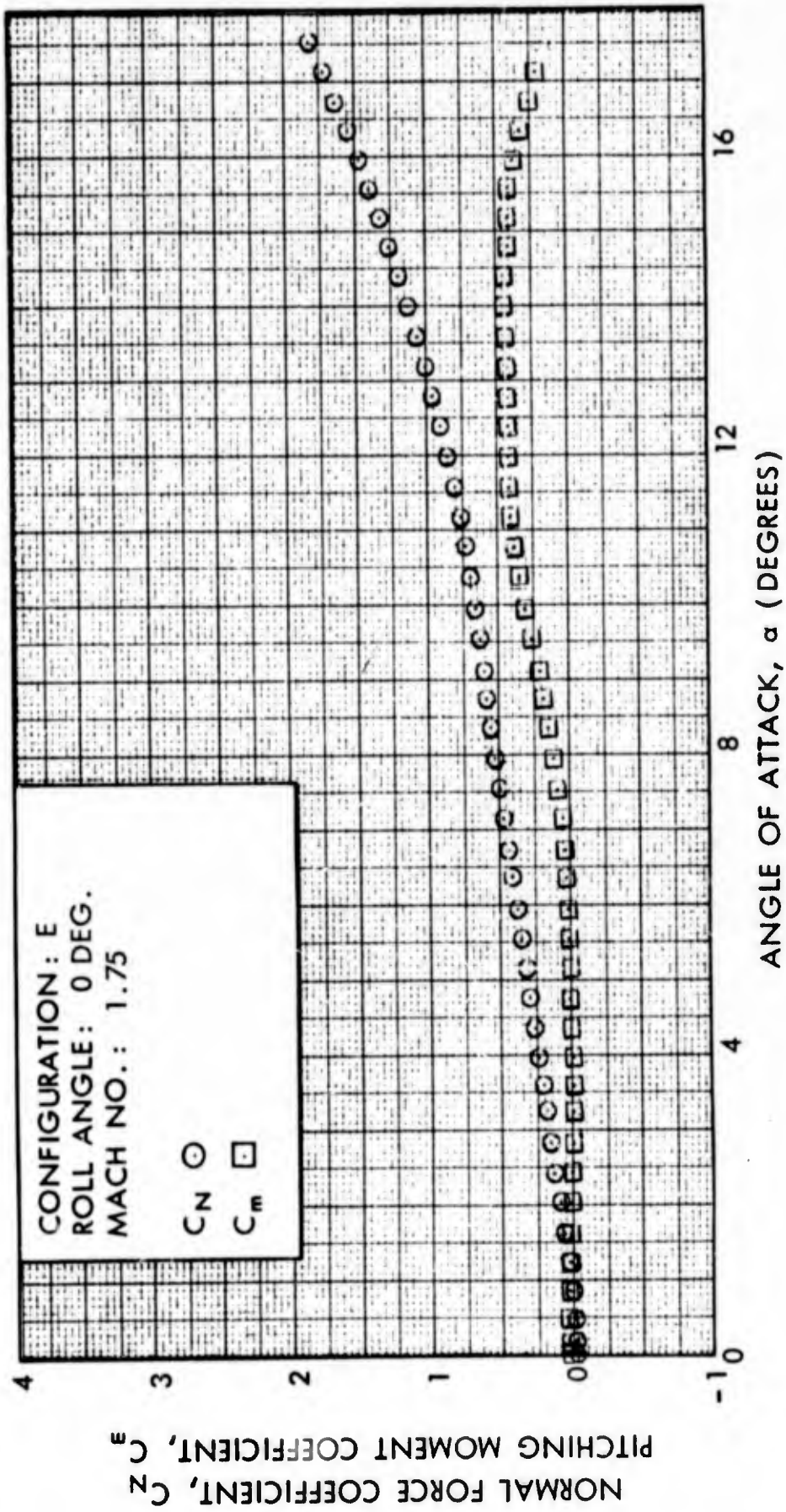


FIG. 53 NORMAL FORCE COEFFICIENT AND PITCHING MOMENT COEFFICIENT VERSUS ANGLE OF ATTACK

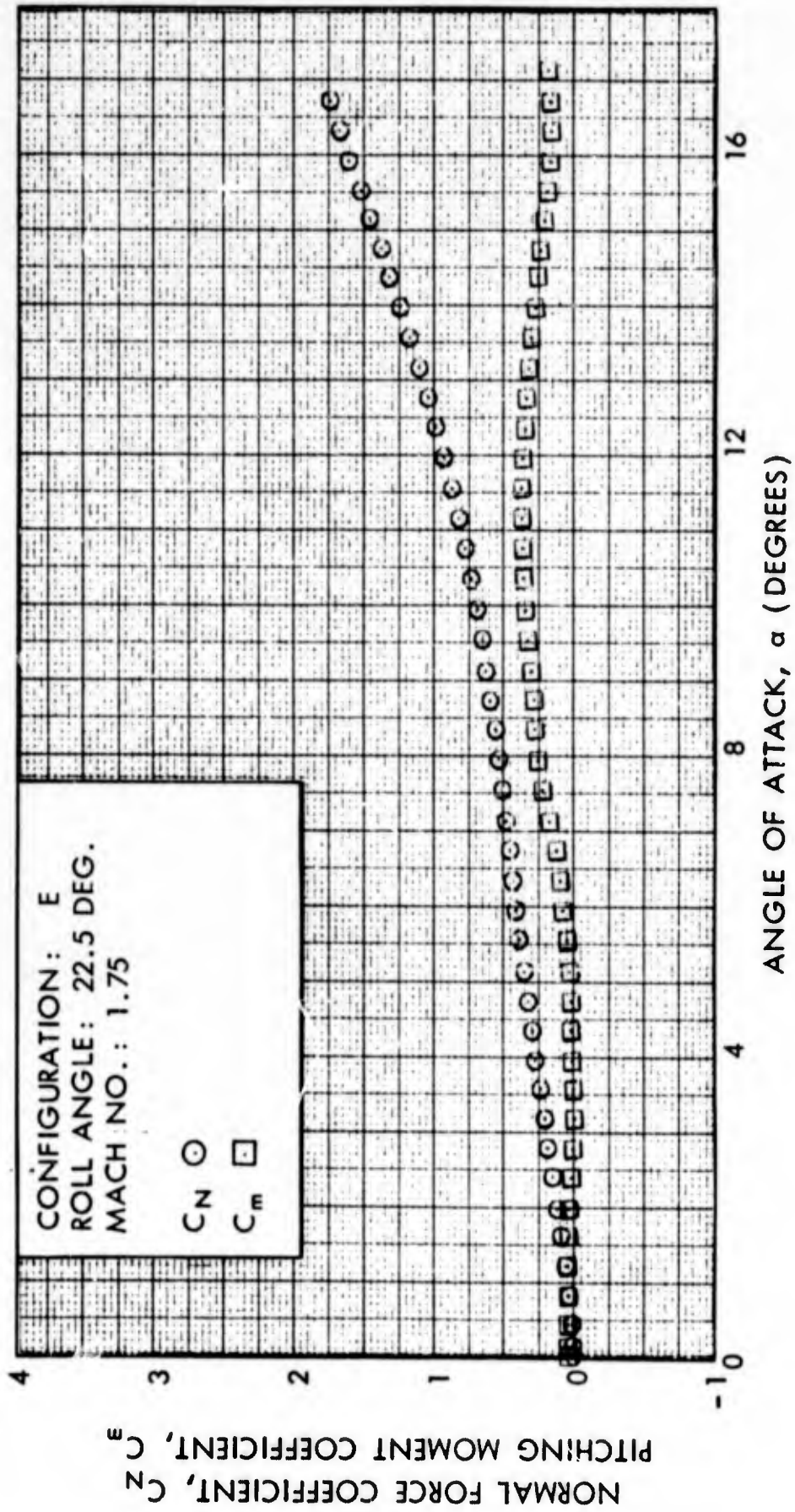


FIG. 54 NORMAL FORCE COEFFICIENT AND PITCHING MOMENT COEFFICIENT VERSUS ANGLE OF ATTACK

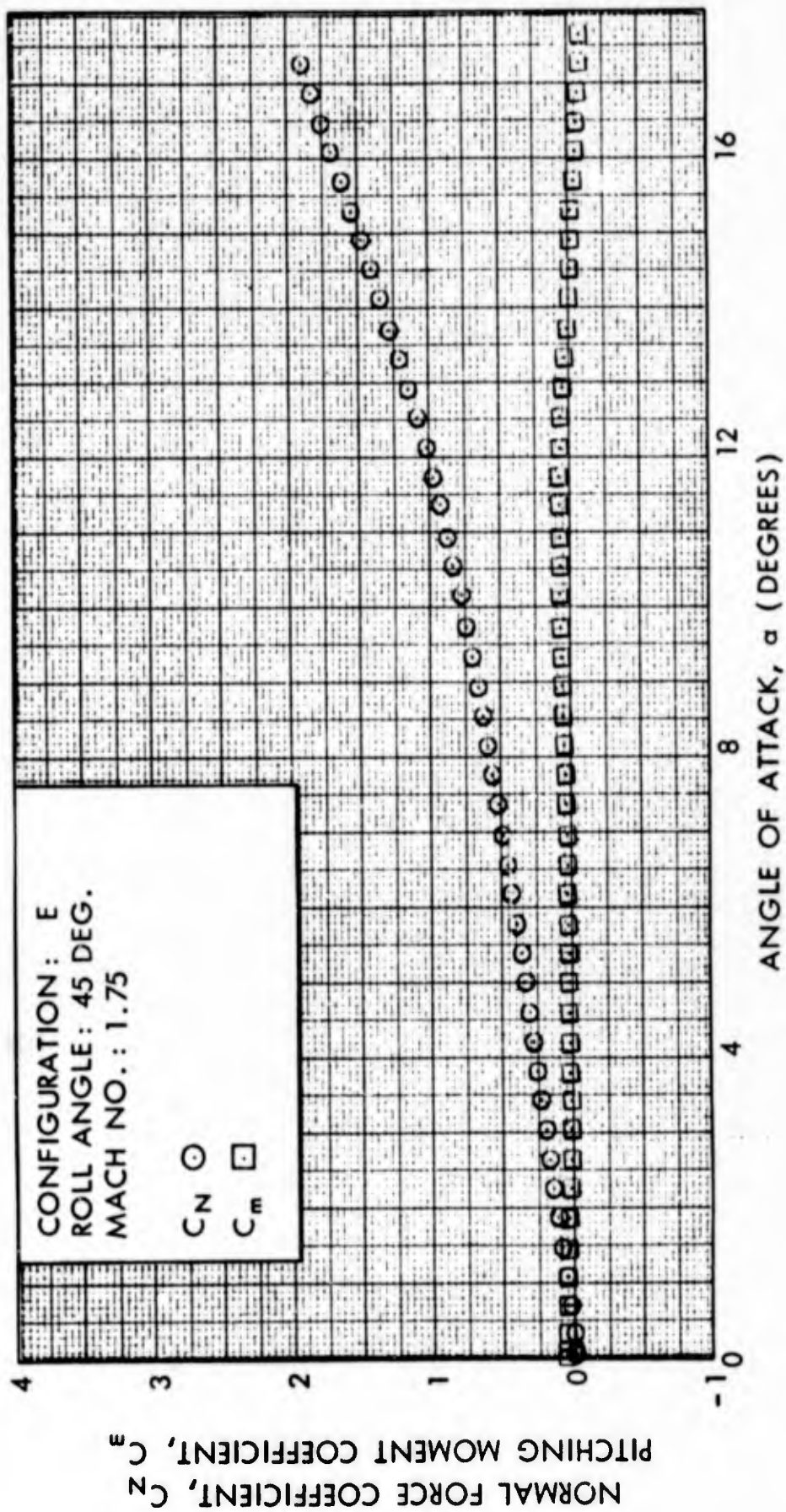


FIG. 55 NORMAL FORCE COEFFICIENT AND PITCHING MOMENT COEFFICIENT VERSUS ANGLE OF ATTACK

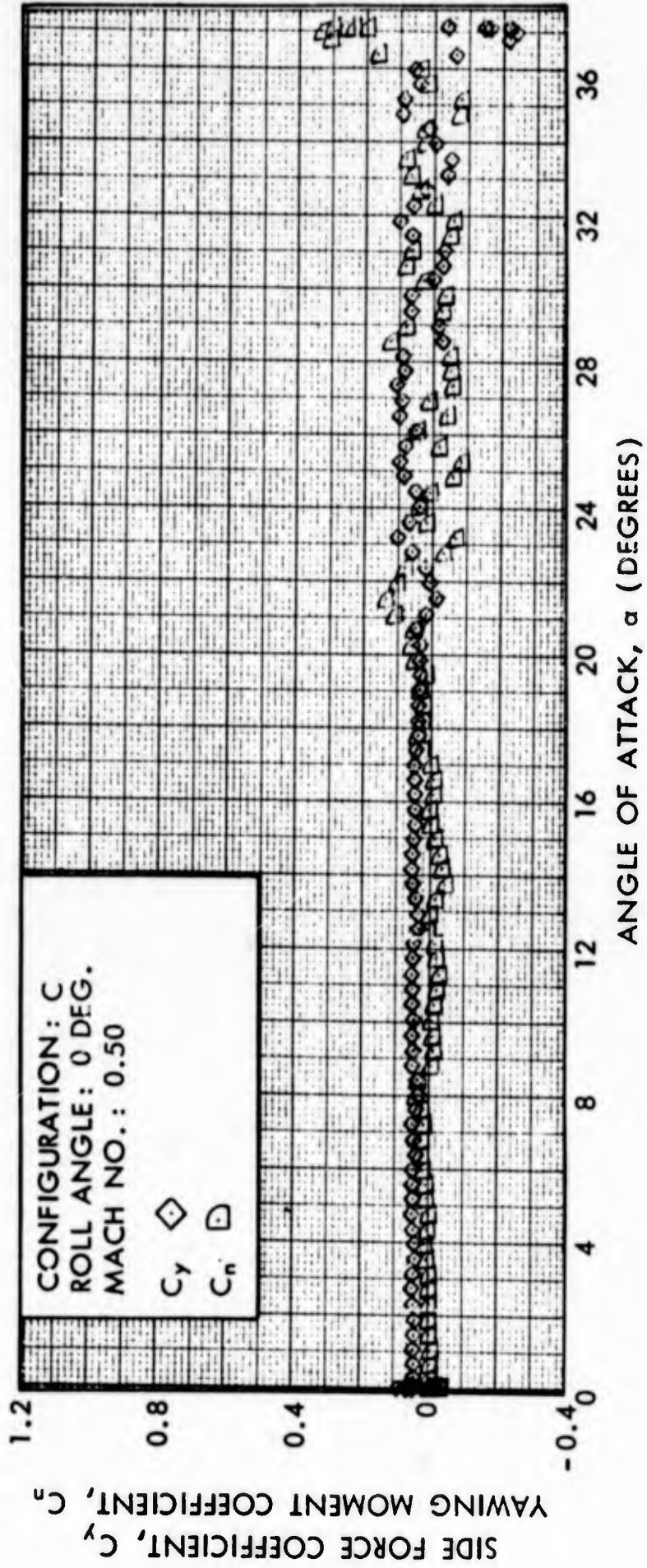


FIG. 56 .SIDE FORCE COEFFICIENT AND YAWING MOMENT COEFFICIENT VERSUS ANGLE OF ATTACK

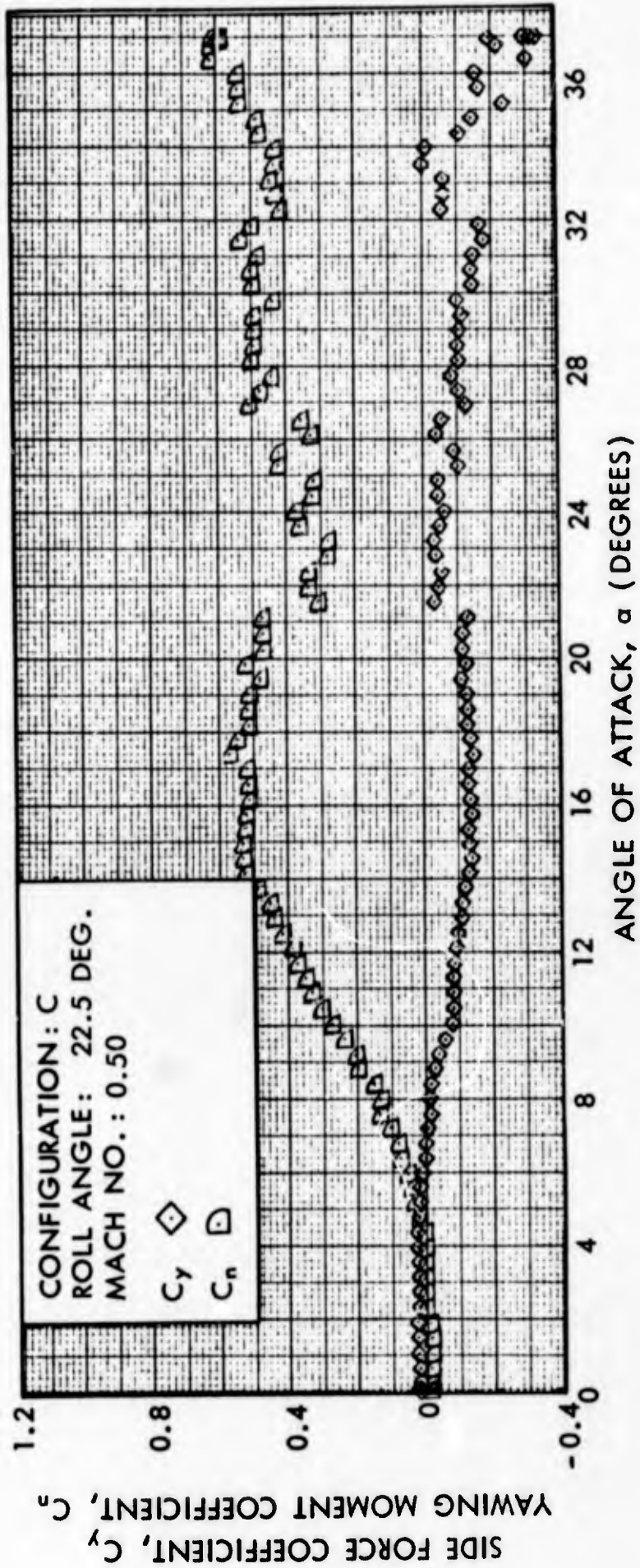


FIG. 57 SIDE FORCE COEFFICIENT AND YAWING MOMENT COEFFICIENT VERSUS ANGLE OF ATTACK

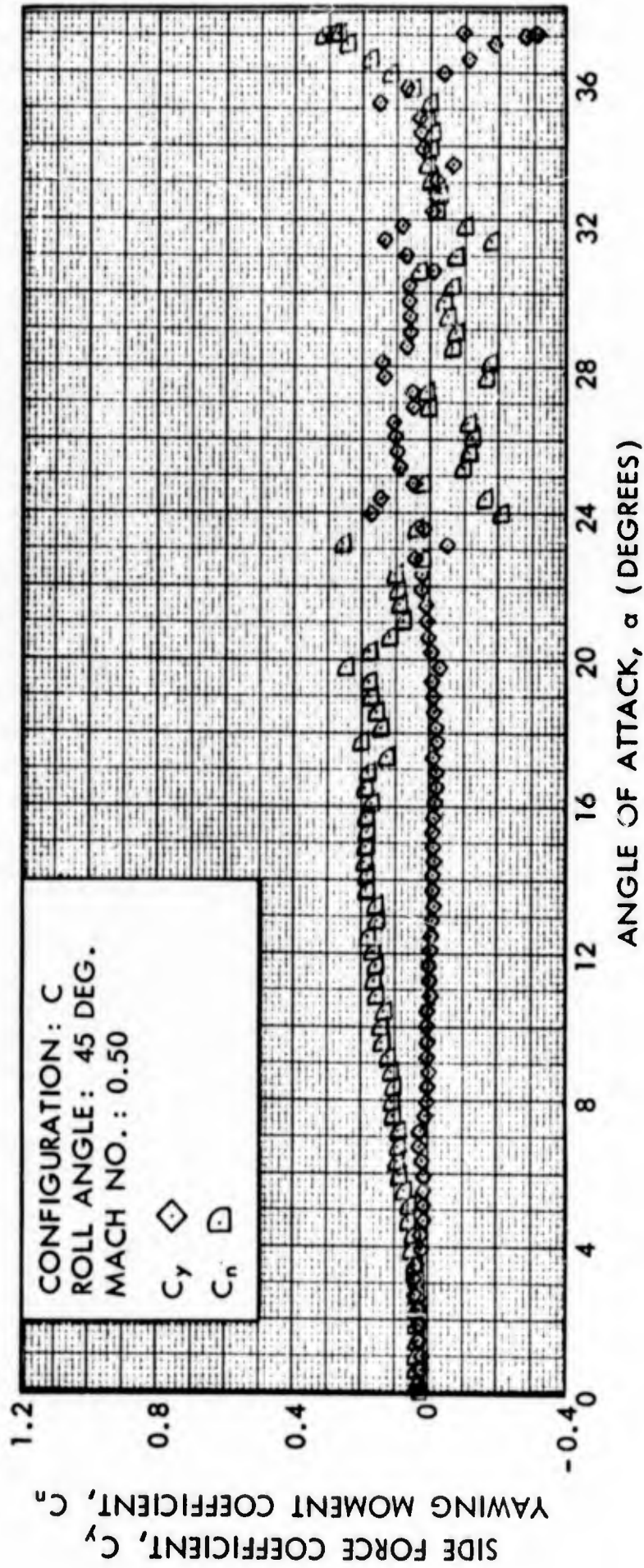


FIG. 58 SIDE FORCE COEFFICIENT AND YAWING MOMENT COEFFICIENT VERSUS ANGLE OF ATTACK

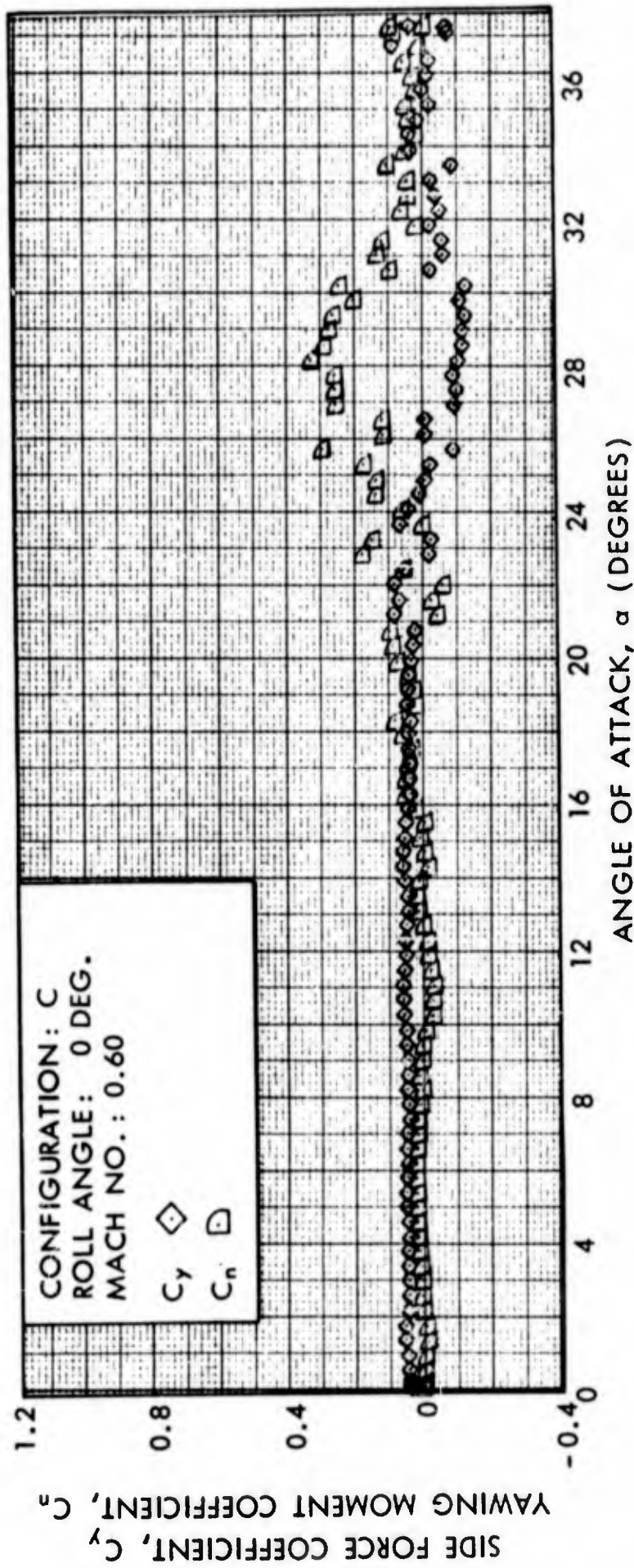


FIG. 59 SIDE FORCE COEFFICIENT AND YAWING MOMENT COEFFICIENT VERSUS ANGLE OF ATTACK

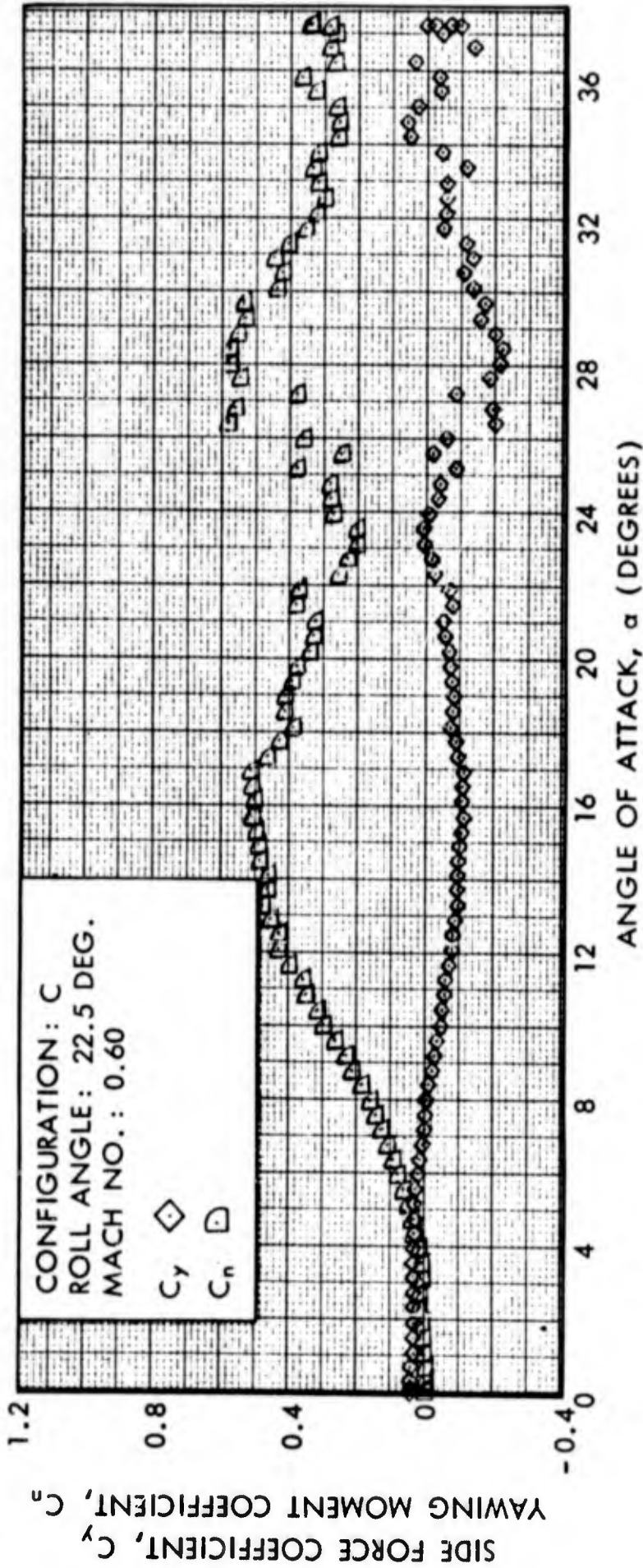


FIG. 60 SIDE FORCE COEFFICIENT AND YAWING MOMENT COEFFICIENT VERSUS ANGLE OF ATTACK

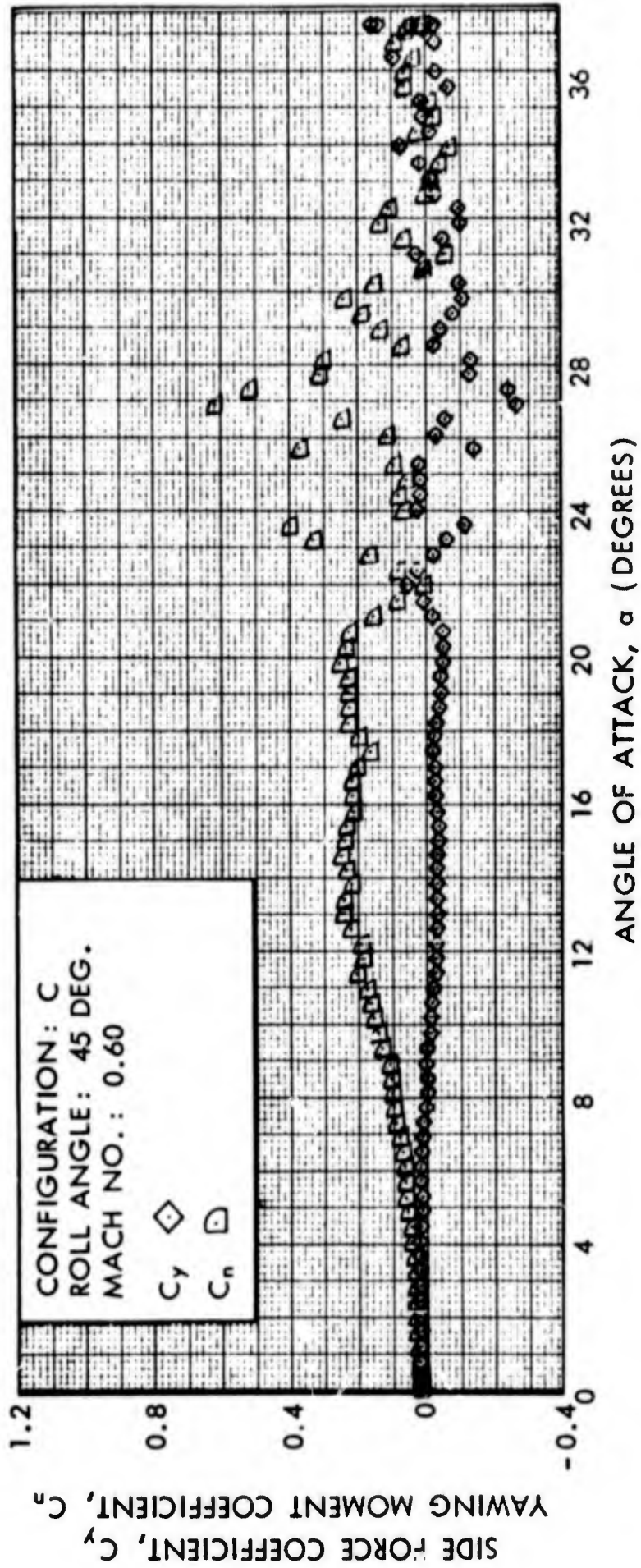


FIG. 61 SIDE FORCE COEFFICIENT AND YAWING MOMENT COEFFICIENT VERSUS ANGLE OF ATTACK

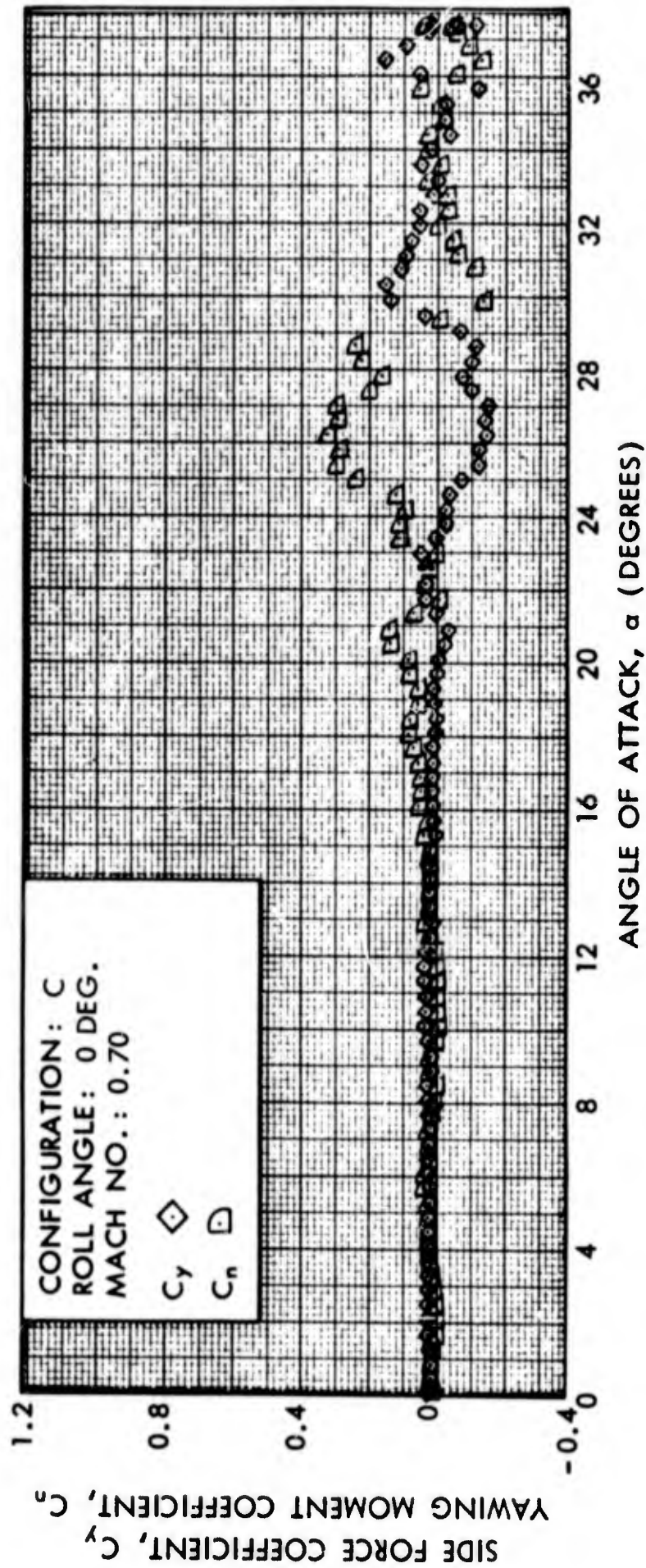


FIG. 62 SIDE FORCE COEFFICIENT AND YAWING MOMENT COEFFICIENT VERSUS ANGLE OF ATTACK

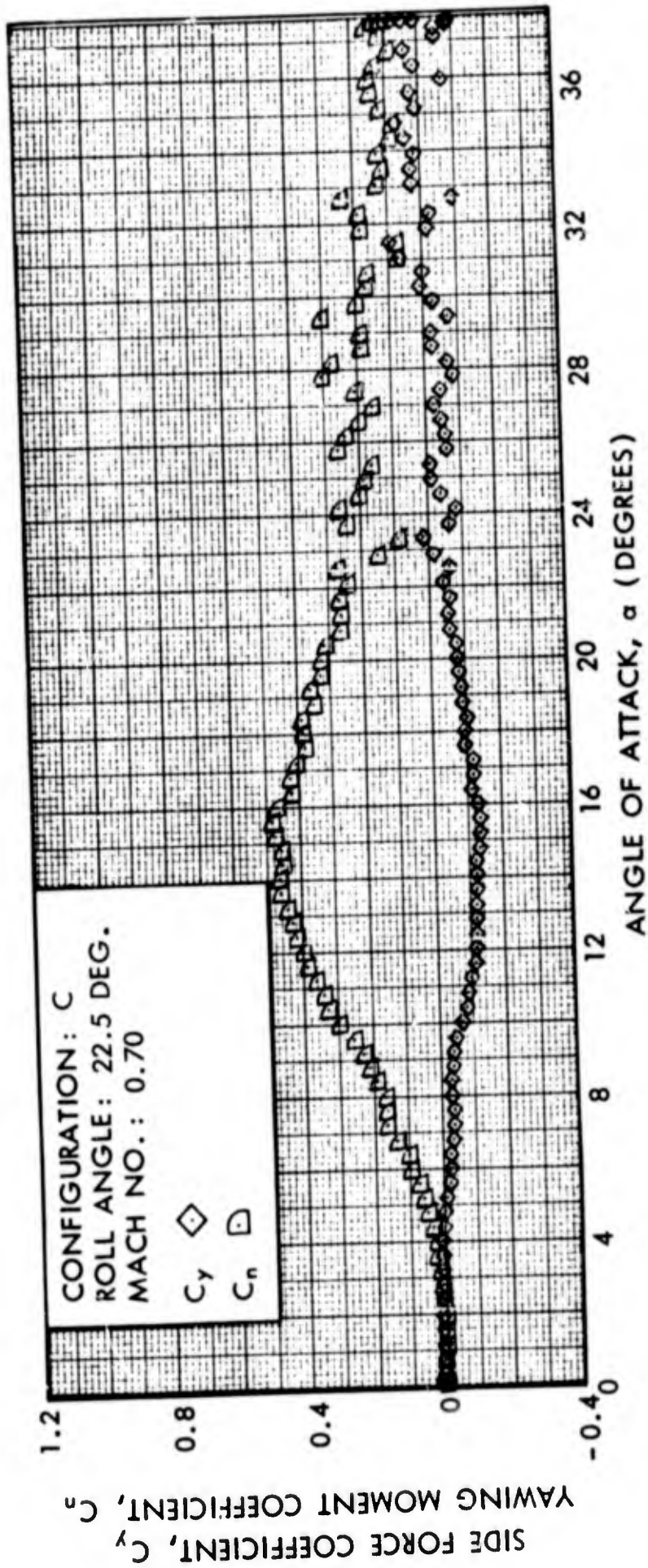


FIG. 63 SIDE FORCE COEFFICIENT AND YAWING MOMENT COEFFICIENT VERSUS ANGLE OF ATTACK

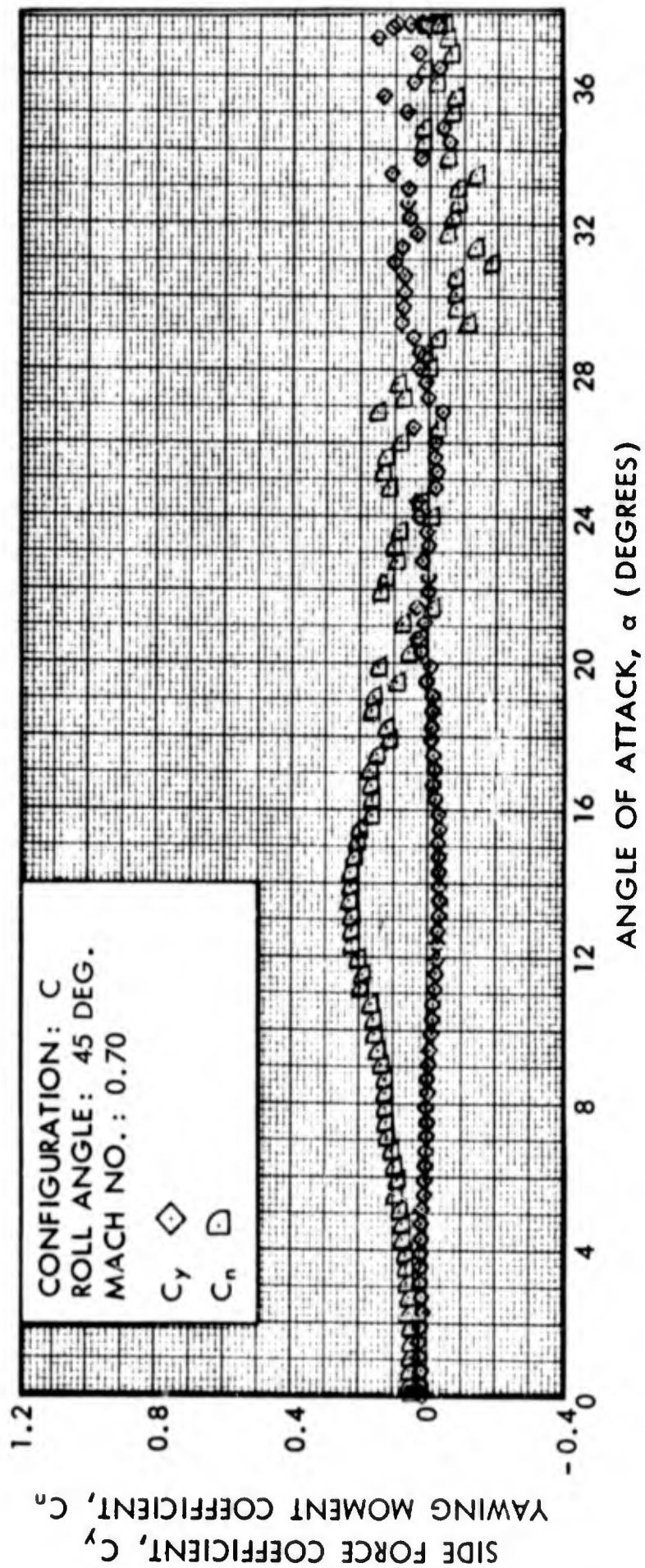


FIG. 64 SIDE FORCE COEFFICIENT AND YAWING MOMENT COEFFICIENT VERSUS ANGLE OF ATTACK

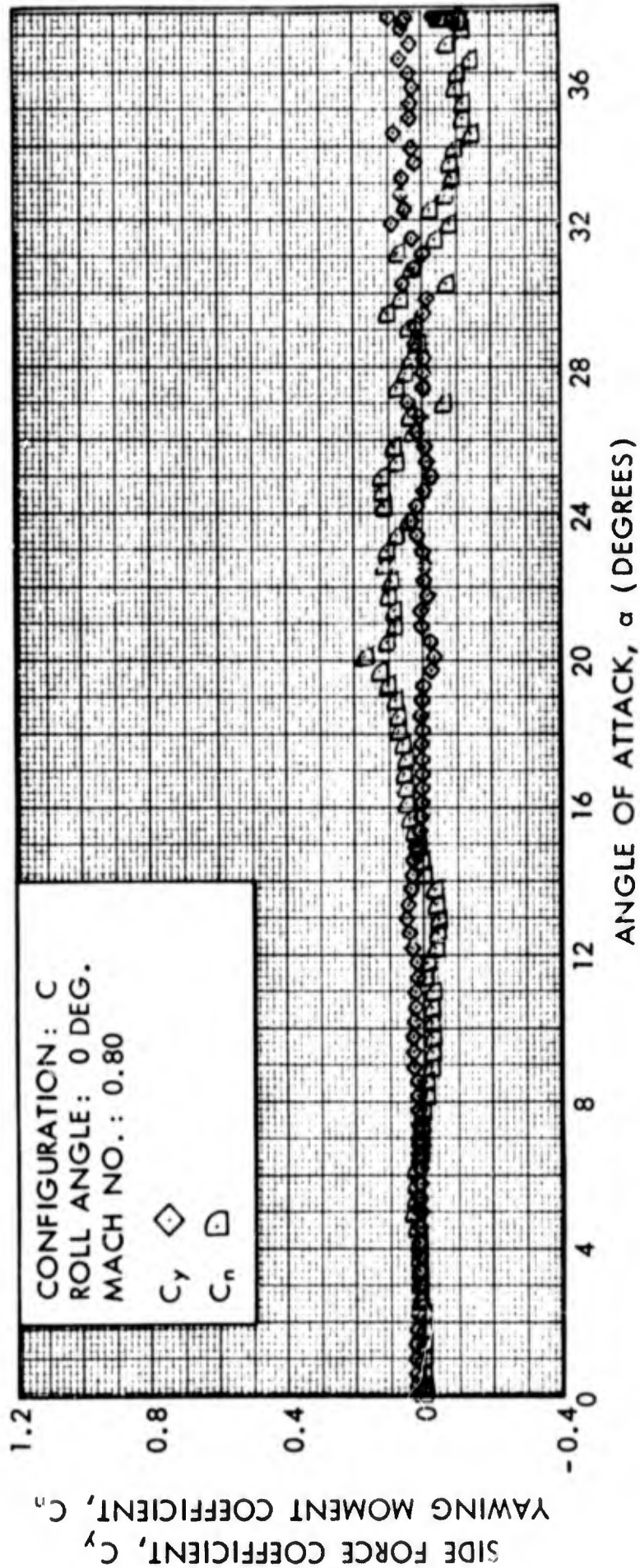


FIG. 65 SIDE FORCE COEFFICIENT AND YAWING MOMENT COEFFICIENT VERSUS ANGLE OF ATTACK

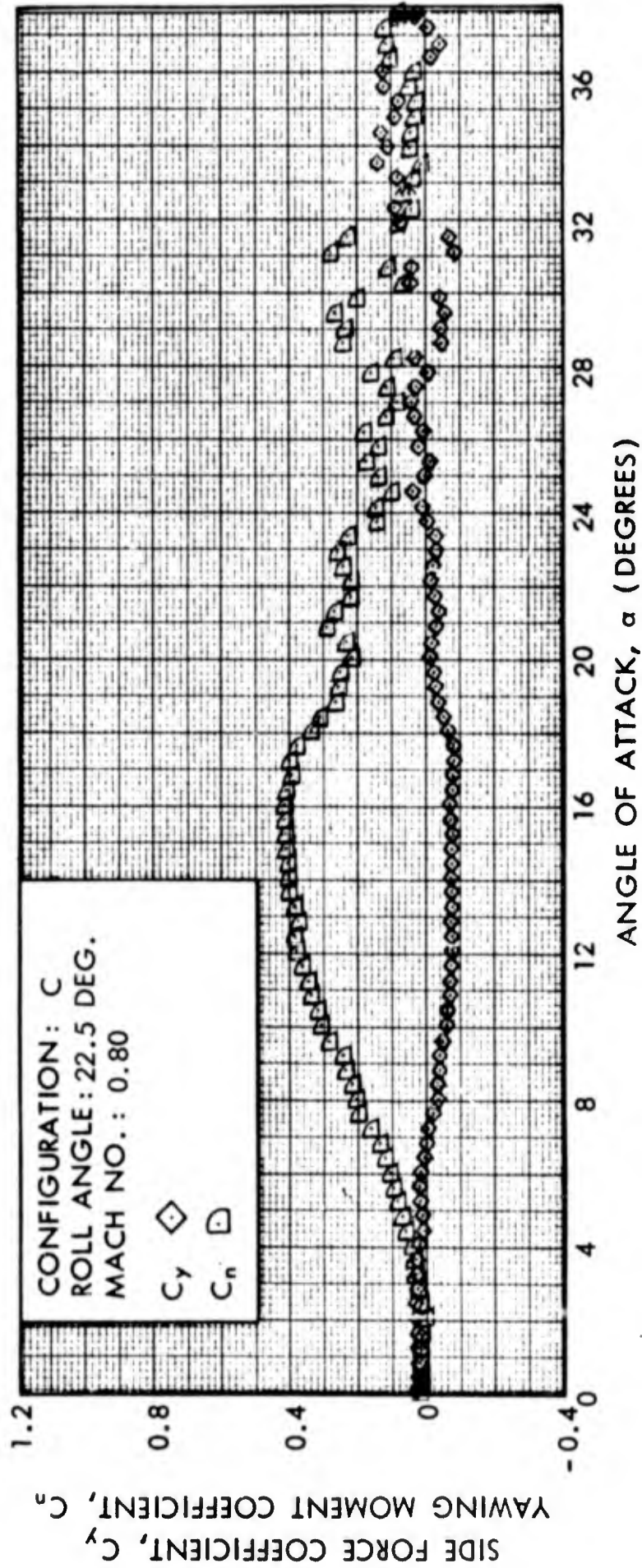


FIG. 66 SIDE FORCE COEFFICIENT AND YAWING MOMENT COEFFICIENT VERSUS ANGLE OF ATTACK

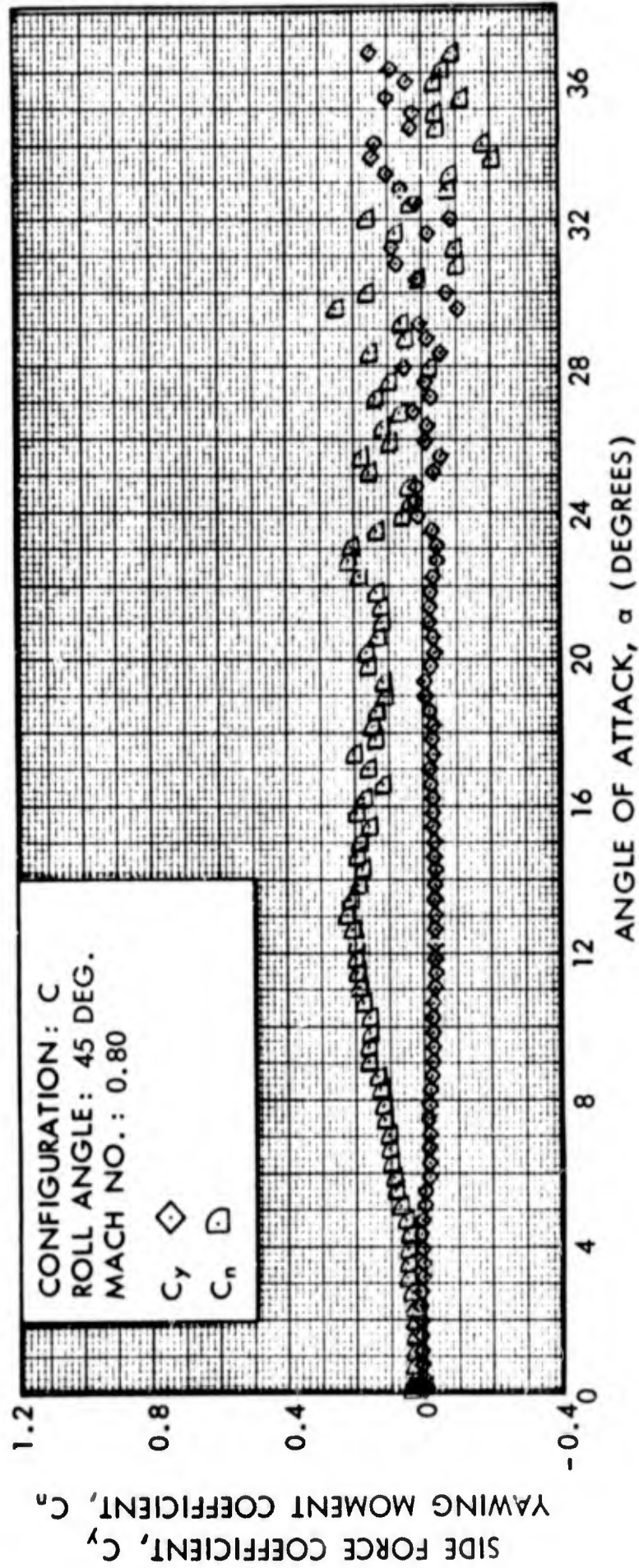


FIG. 67 SIDE FORCE COEFFICIENT AND YAWING MOMENT COEFFICIENT VERSUS ANGLE OF ATTACK

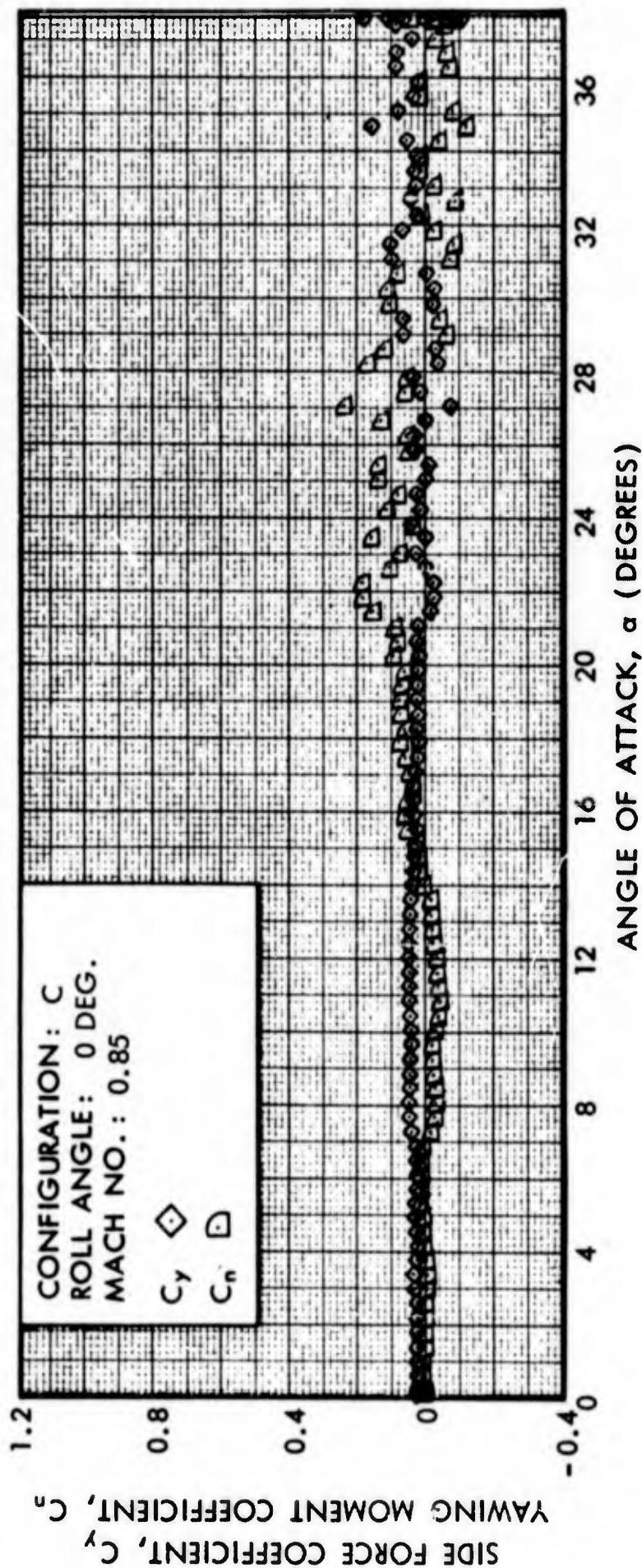


FIG. 68 SIDE FORCE COEFFICIENT AND YAWING MOMENT COEFFICIENT VERSUS ANGLE OF ATTACK

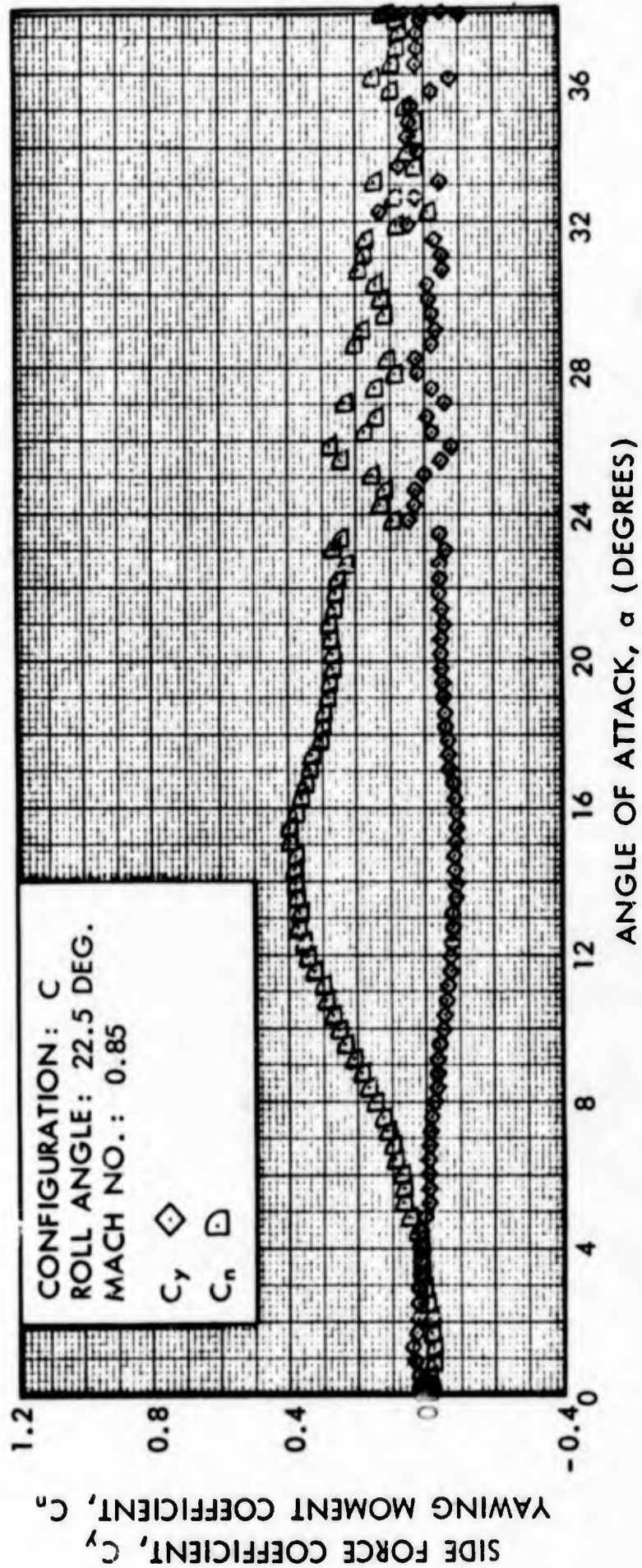


FIG. 69 SIDE FORCE COEFFICIENT AND YAWING MOMENT COEFFICIENT VERSUS ANGLE OF ATTACK

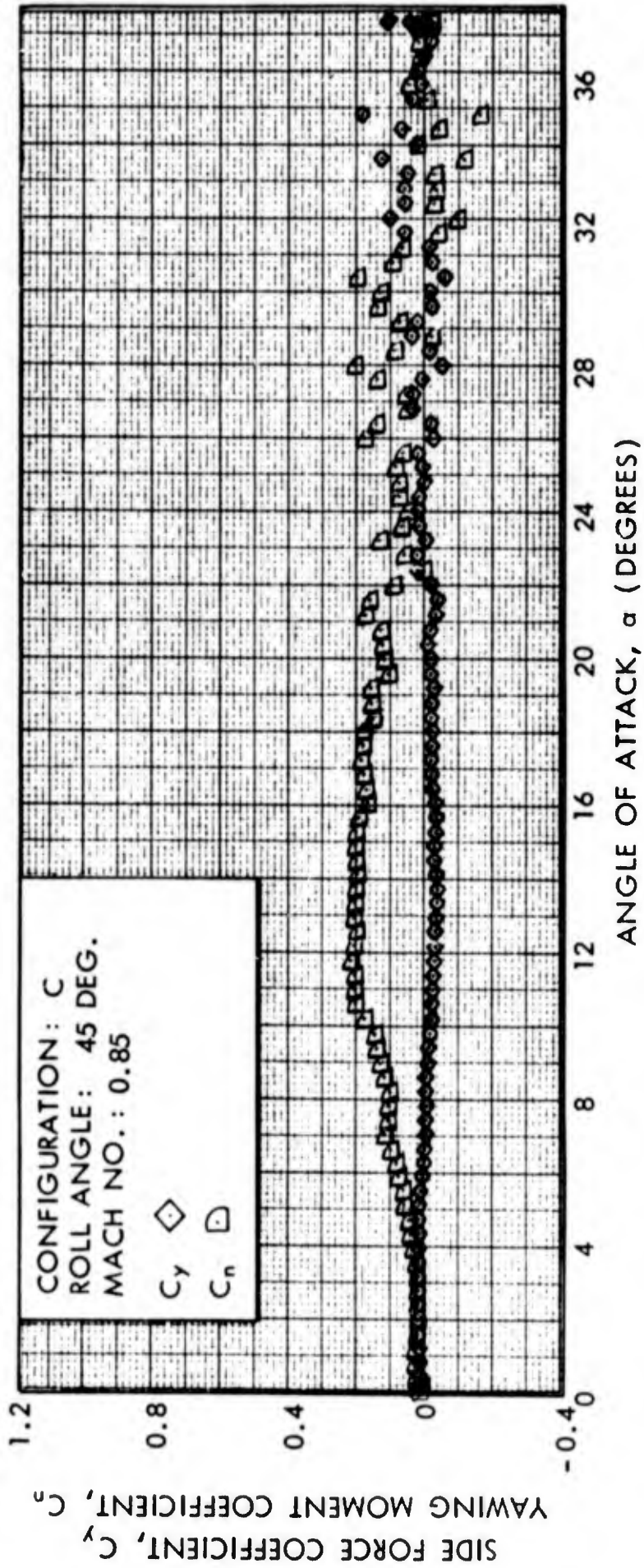


FIG. 70 SIDE FORCE COEFFICIENT AND YAWING MOMENT COEFFICIENT VERSUS ANGLE OF ATTACK

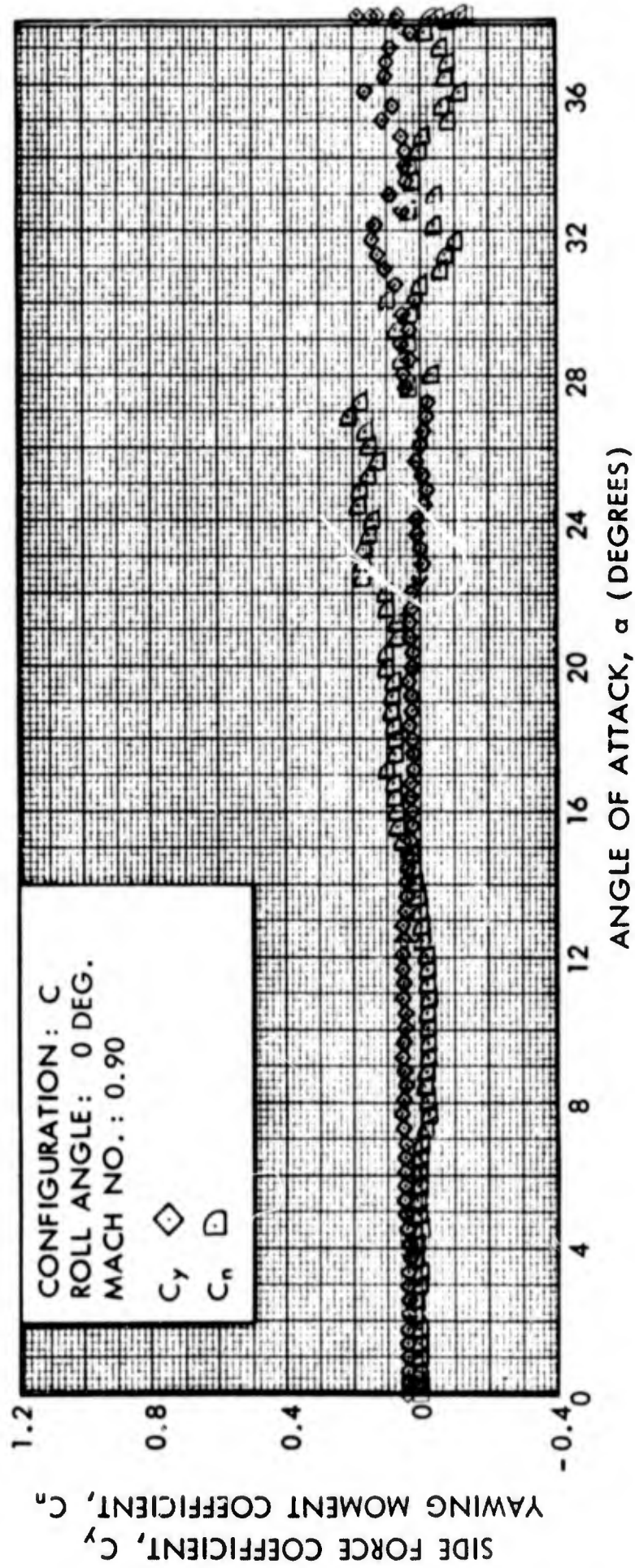


FIG. 71 SIDE FORCE COEFFICIENT AND YAWING MOMENT COEFFICIENT VERSUS ANGLE OF ATTACK

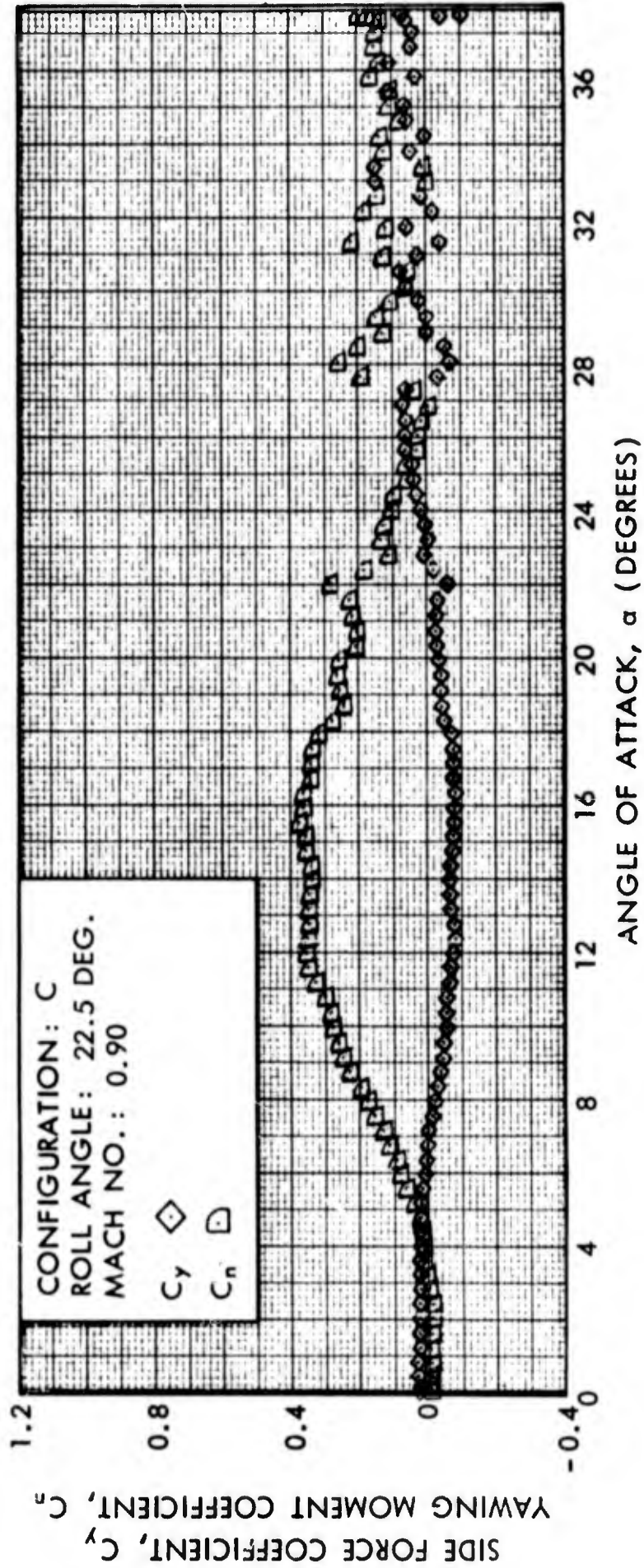


FIG. 72 SIDE FORCE COEFFICIENT AND YAWING MOMENT COEFFICIENT VERSUS ANGLE OF ATTACK

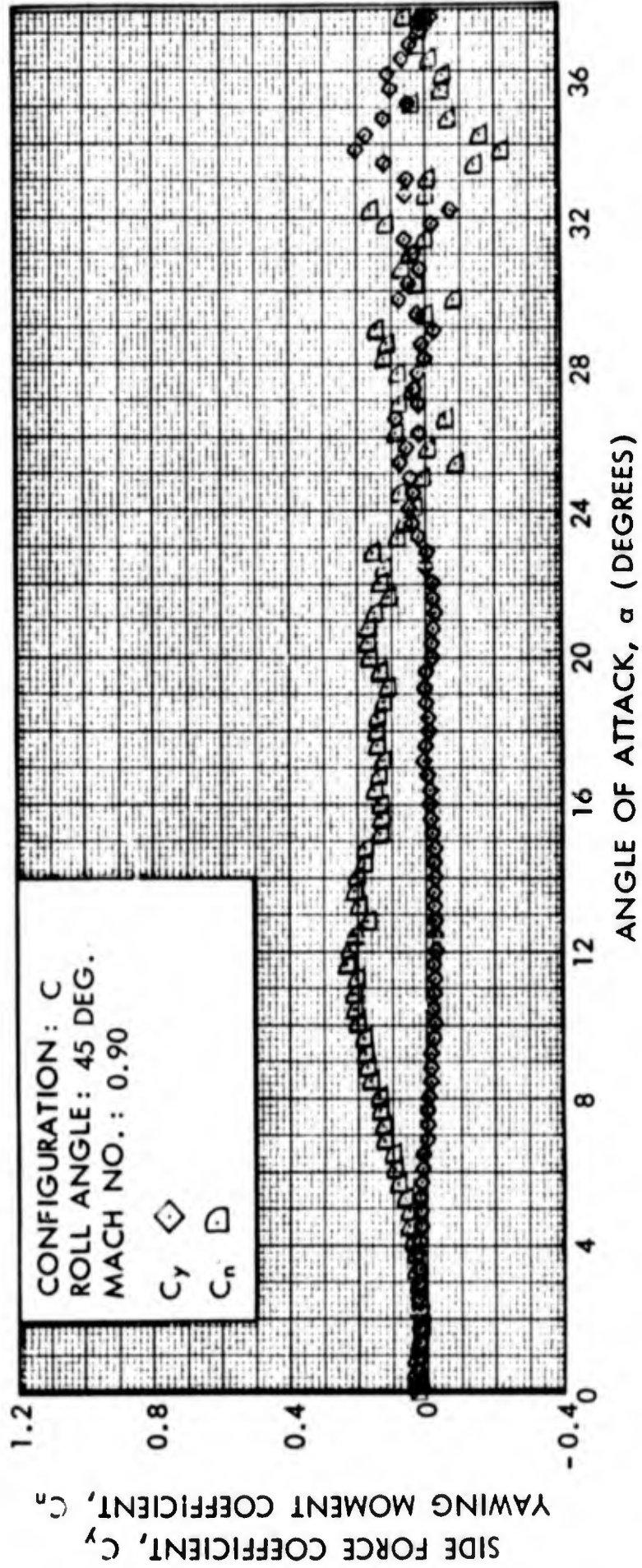


FIG. 73 SIDE FORCE COEFFICIENT AND YAWING MOMENT COEFFICIENT VERSUS ANGLE OF ATTACK

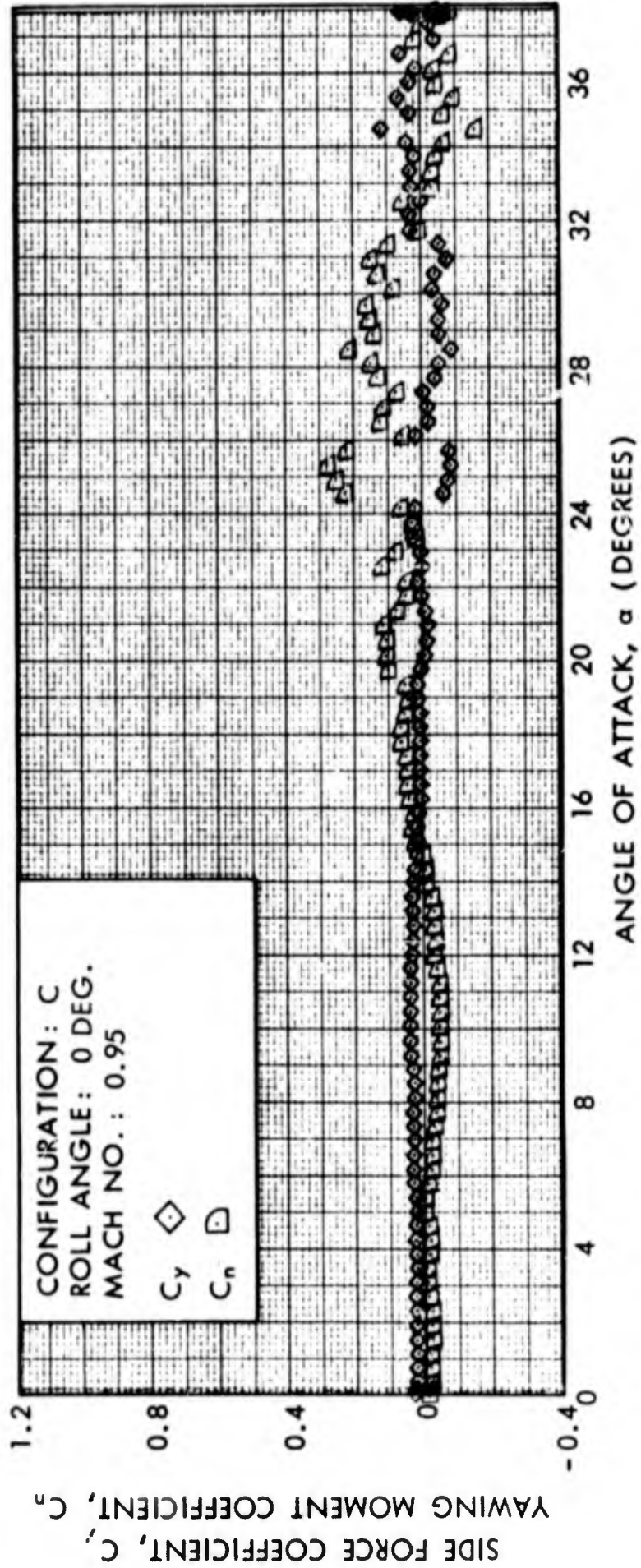


FIG. 74 SIDE FORCE COEFFICIENT AND YAWING MOMENT COEFFICIENT VERSUS ANGLE OF ATTACK

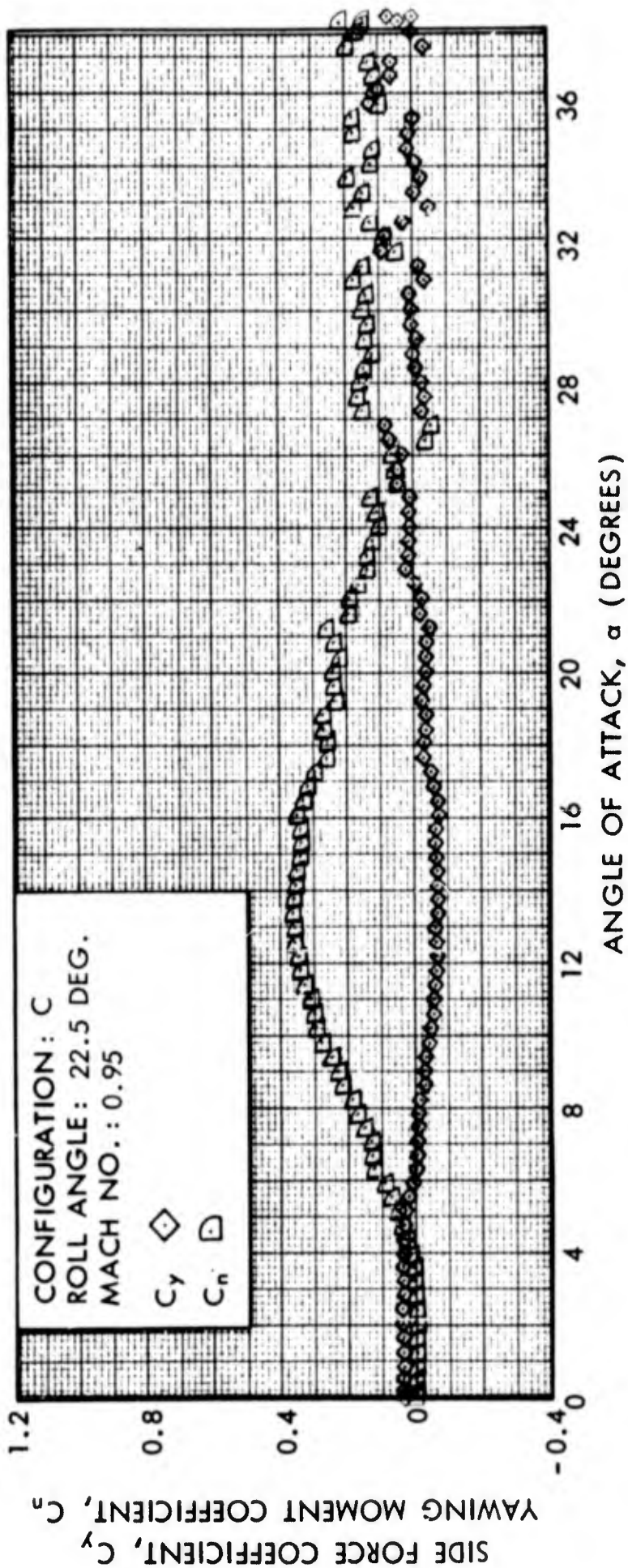


FIG. 75 SIDE FORCE COEFFICIENT AND YAWING MOMENT COEFFICIENT VERSUS ANGLE OF ATTACK

SIDE FORCE COEFFICIENT,  $C_y$   
YAWING MOMENT COEFFICIENT,  $C_n$

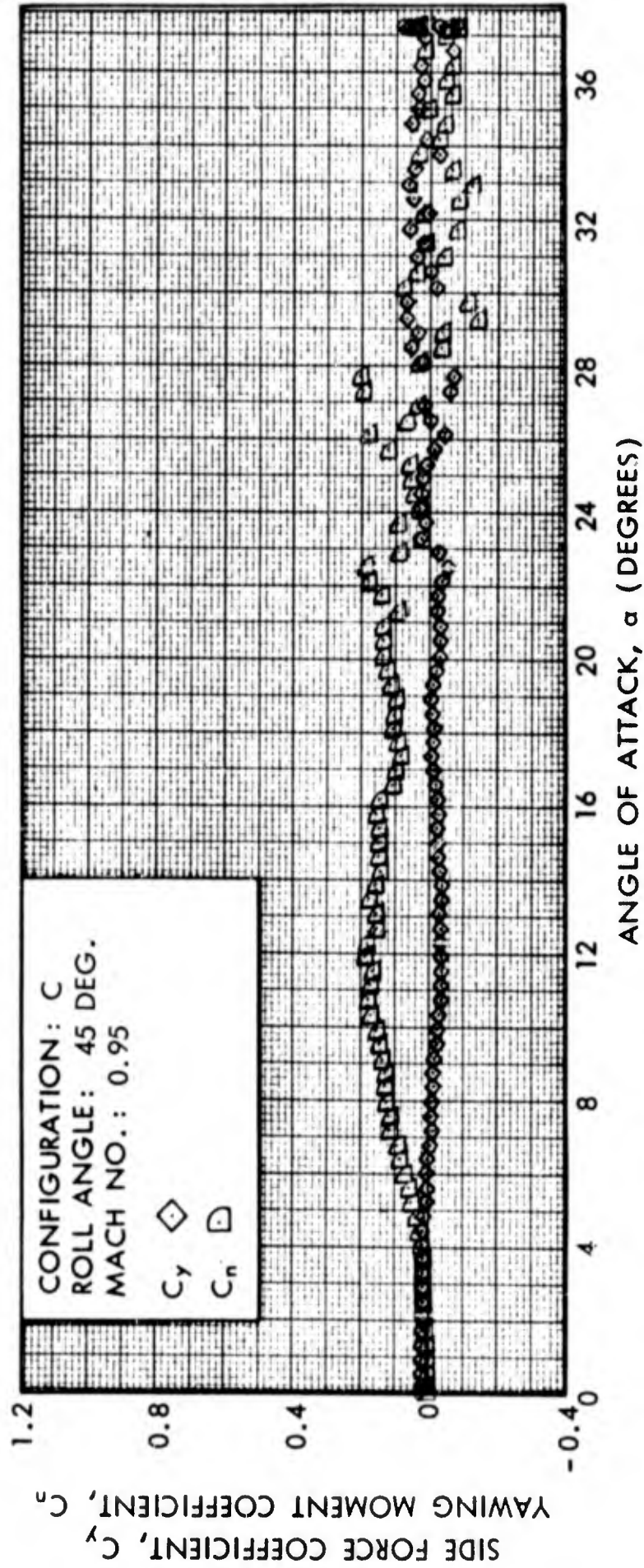


FIG. 76 SIDE FORCE COEFFICIENT AND YAWING MOMENT COEFFICIENT VERSUS ANGLE OF ATTACK

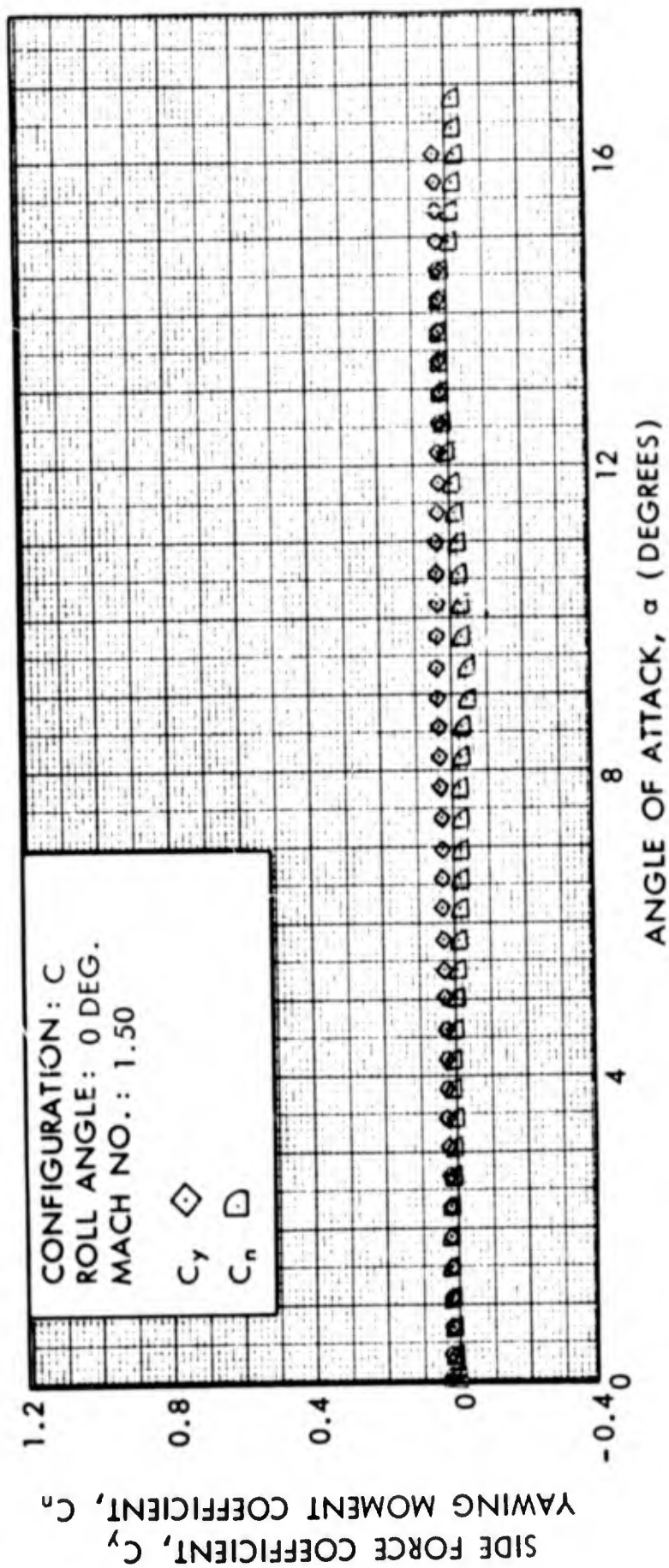


FIG. 77 SIDE FORCE COEFFICIENT AND YAWING MOMENT COEFFICIENT VERSUS ANGLE OF ATTACK

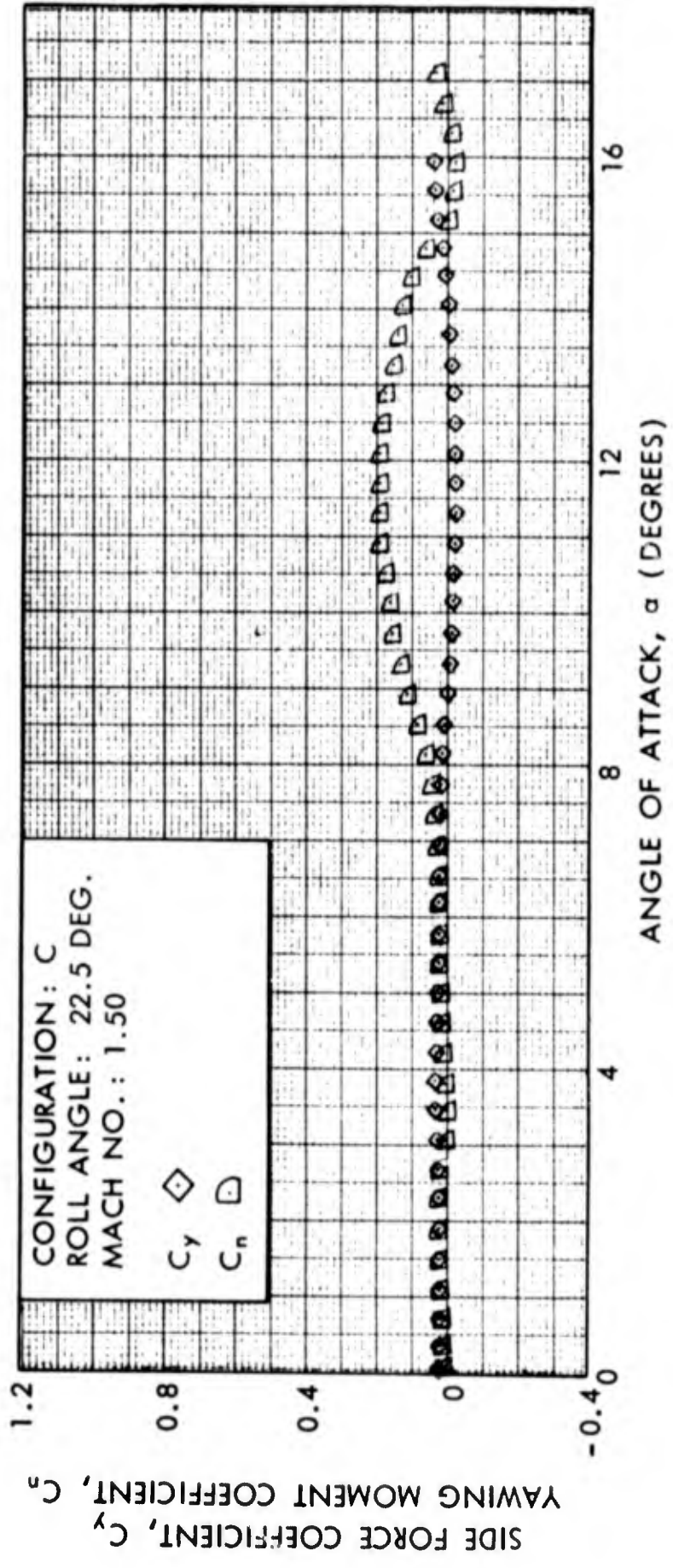


FIG. 78 SIDE FORCE COEFFICIENT AND YAWING MOMENT COEFFICIENT VERSUS ANGLE OF ATTACK

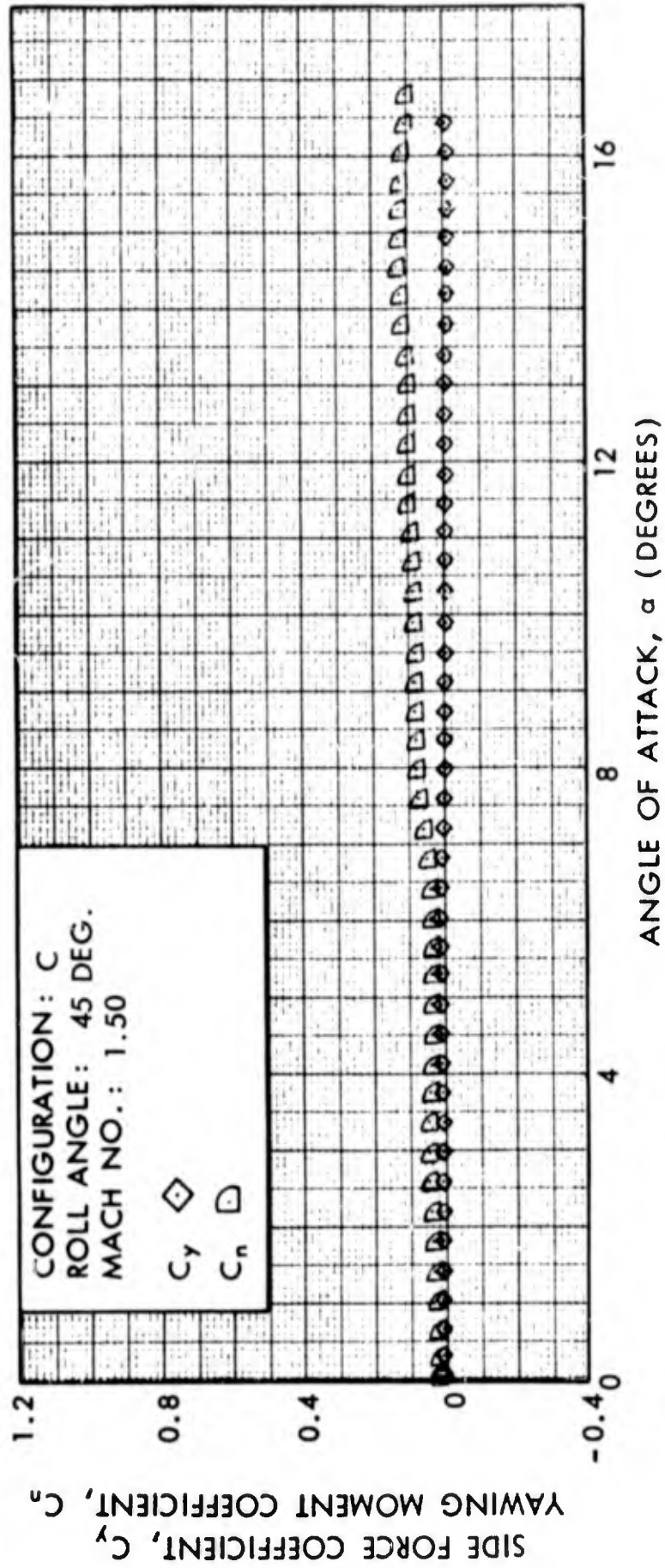


FIG. 79 SIDE FORCE COEFFICIENT AND YAWING MOMENT COEFFICIENT VERSUS ANGLE OF ATTACK

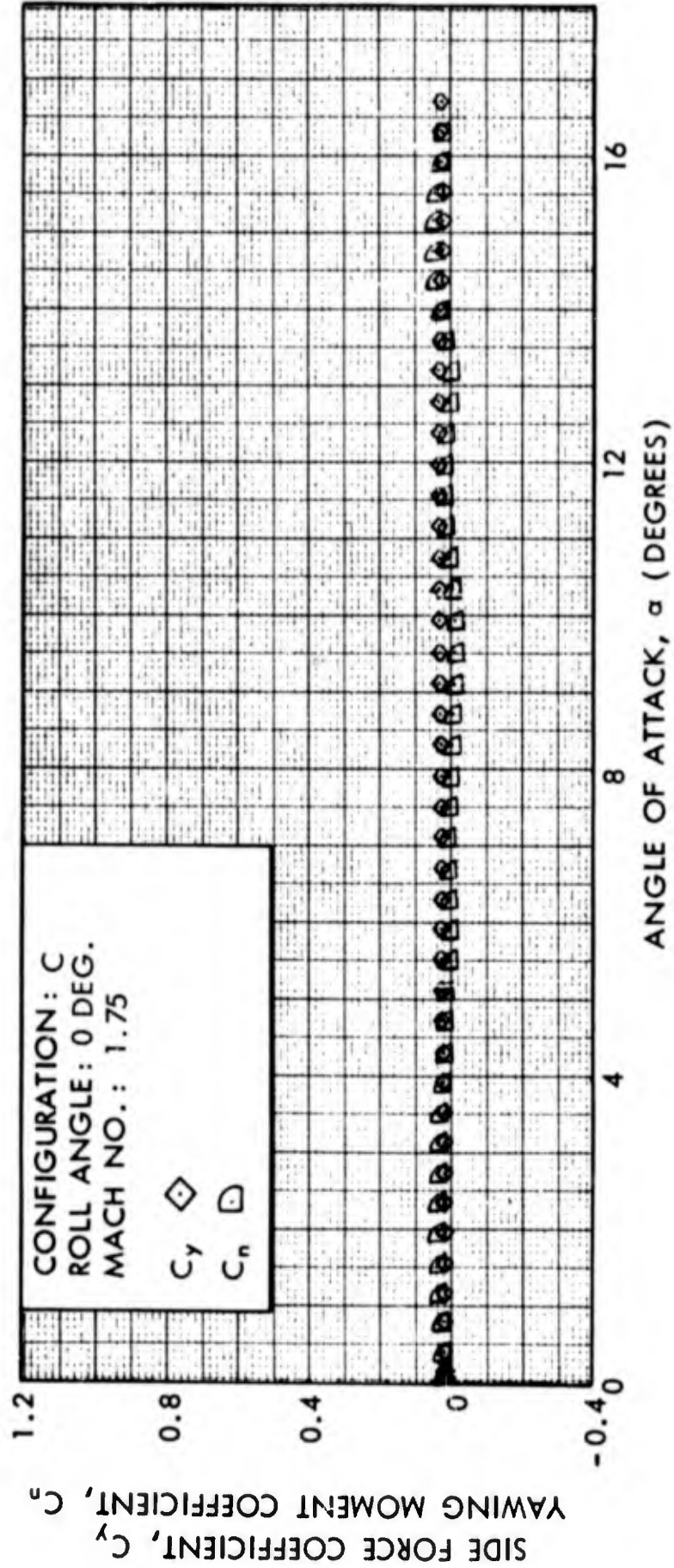


FIG. 80 SIDE FORCE COEFFICIENT AND YAWING MOMENT COEFFICIENT VERSUS ANGLE OF ATTACK

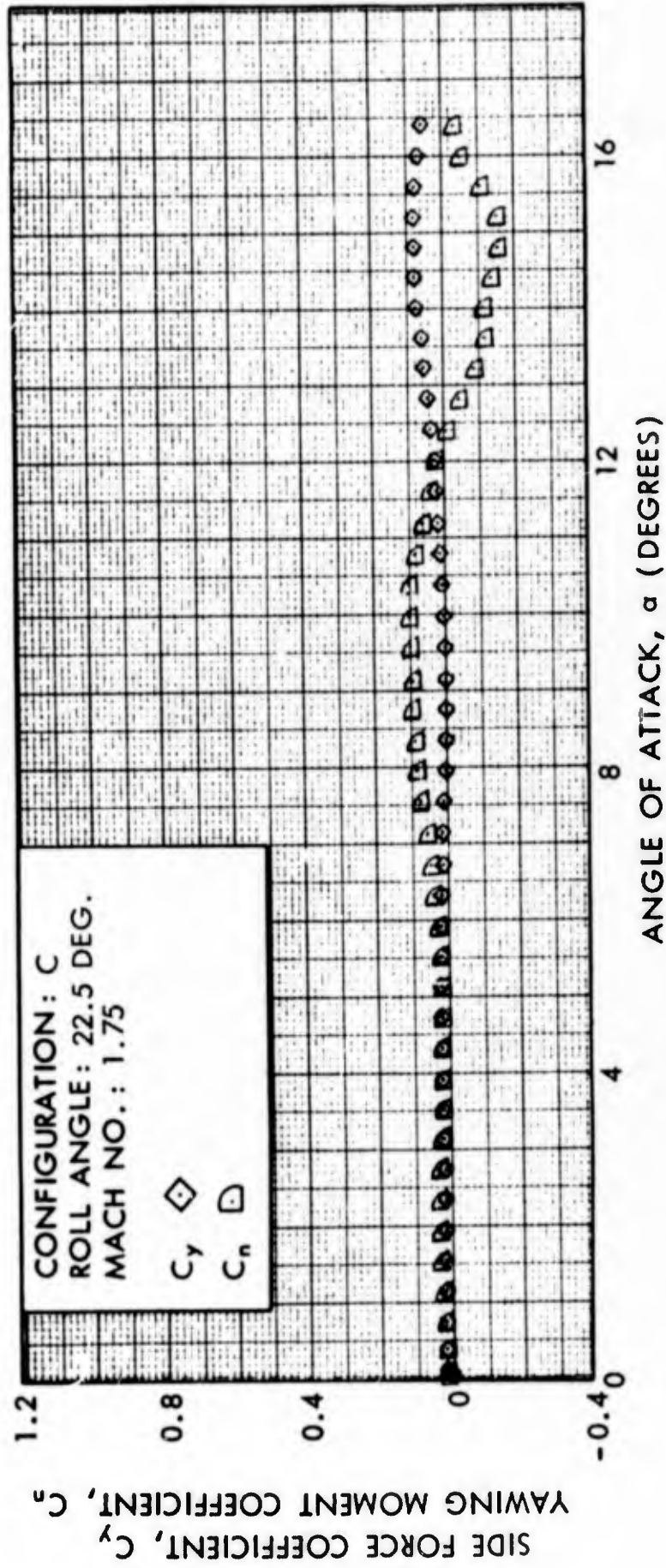


FIG. 81 SIDE FORCE COEFFICIENT AND YAWING MOMENT COEFFICIENT VERSUS ANGLE OF ATTACK

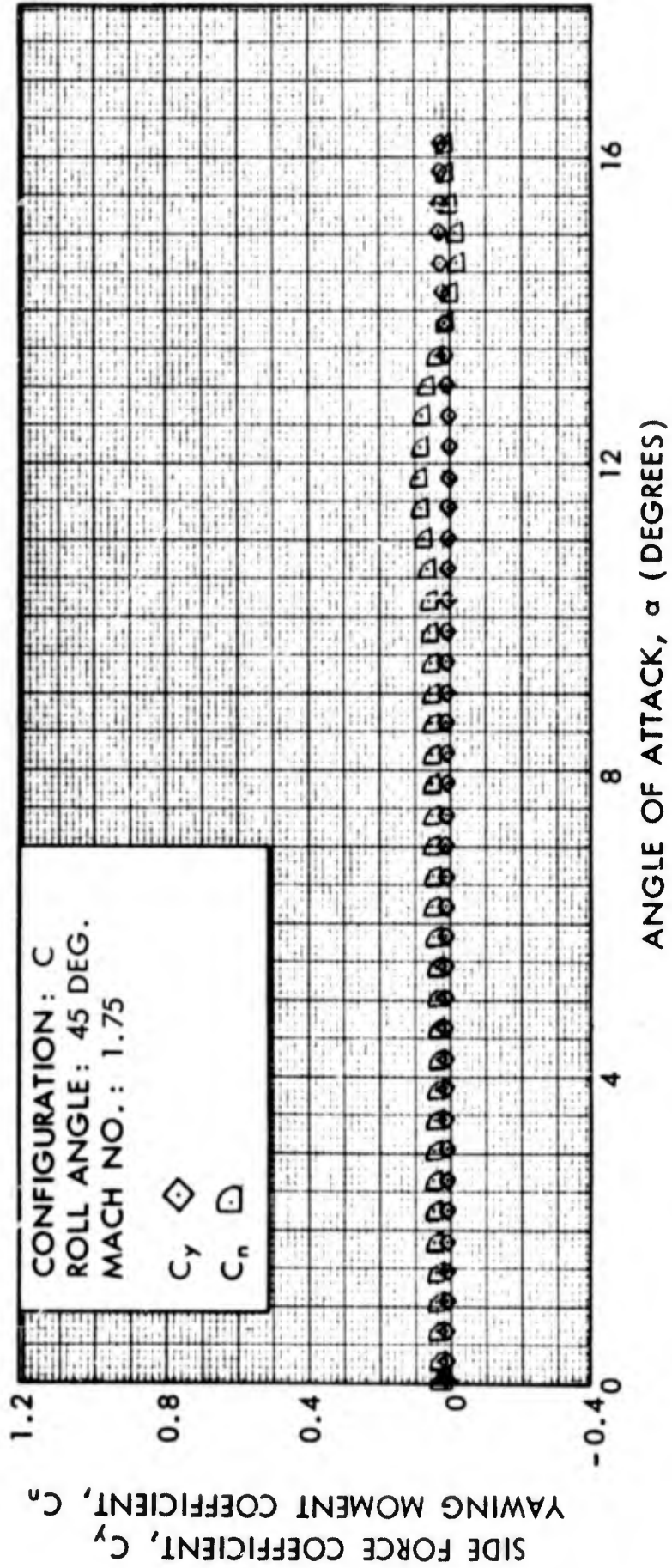


FIG. 82 SIDE FORCE COEFFICIENT AND YAWING MOMENT COEFFICIENT VERSUS ANGLE OF ATTACK

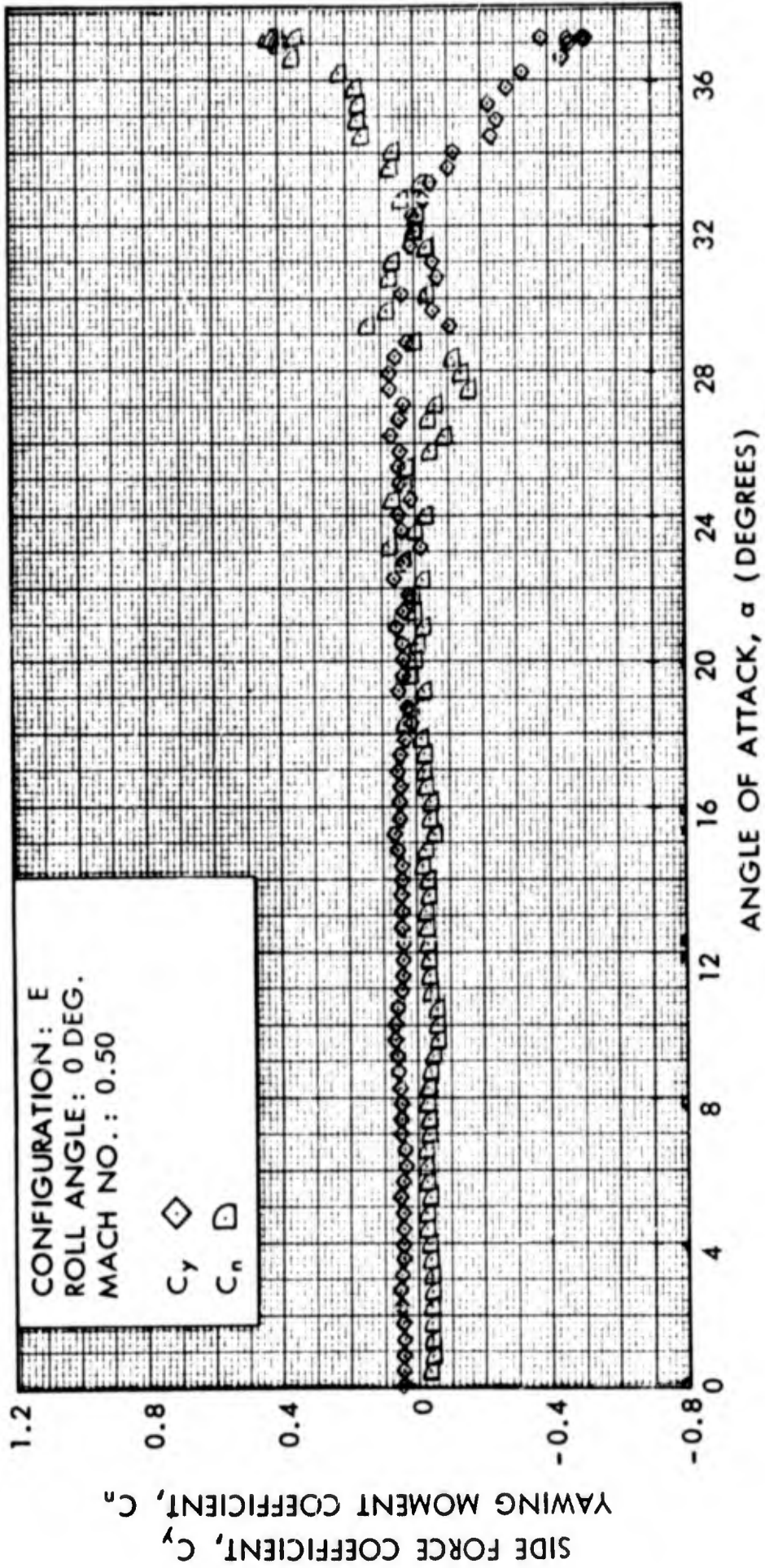


FIG. 83 SIDE FORCE COEFFICIENT AND YAWING MOMENT COEFFICIENT VERSUS ANGLE OF ATTACK

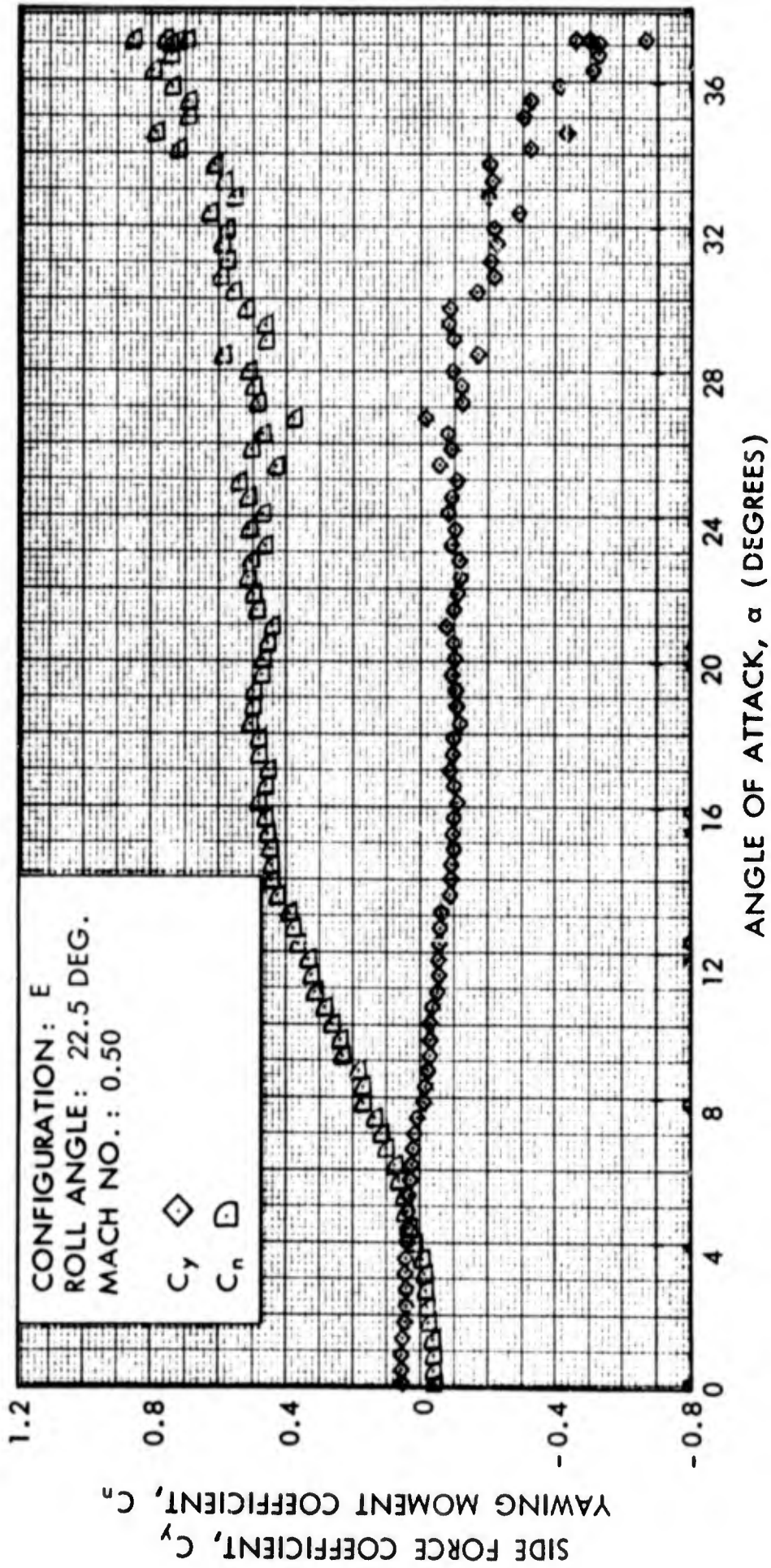


FIG. 84 SIDE FORCE COEFFICIENT AND YAWING MOMENT COEFFICIENT VERSUS ANGLE OF ATTACK

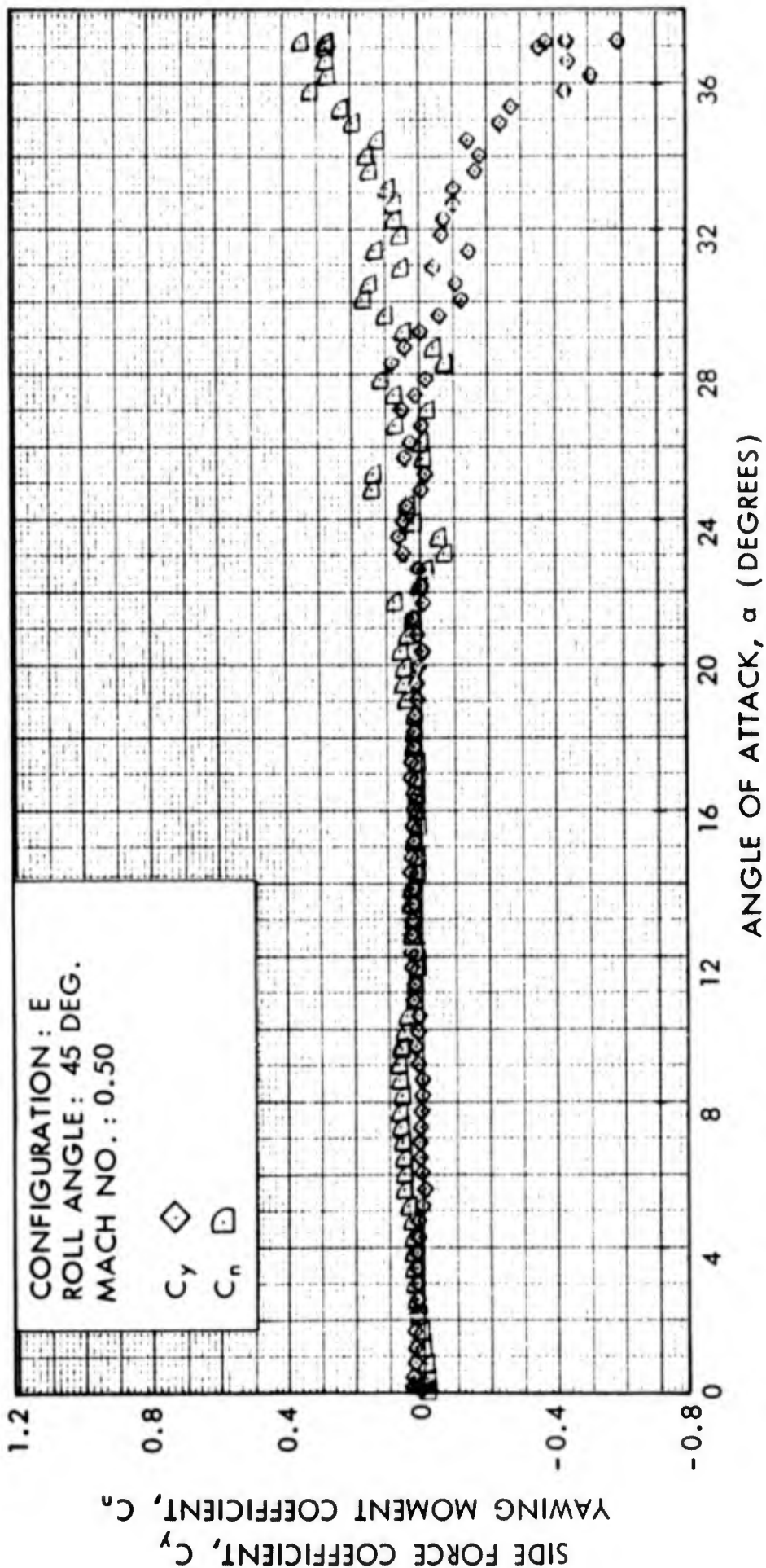


FIG. 85 SIDE FORCE COEFFICIENT AND YAWING MOMENT COEFFICIENT VERSUS ANGLE OF ATTACK

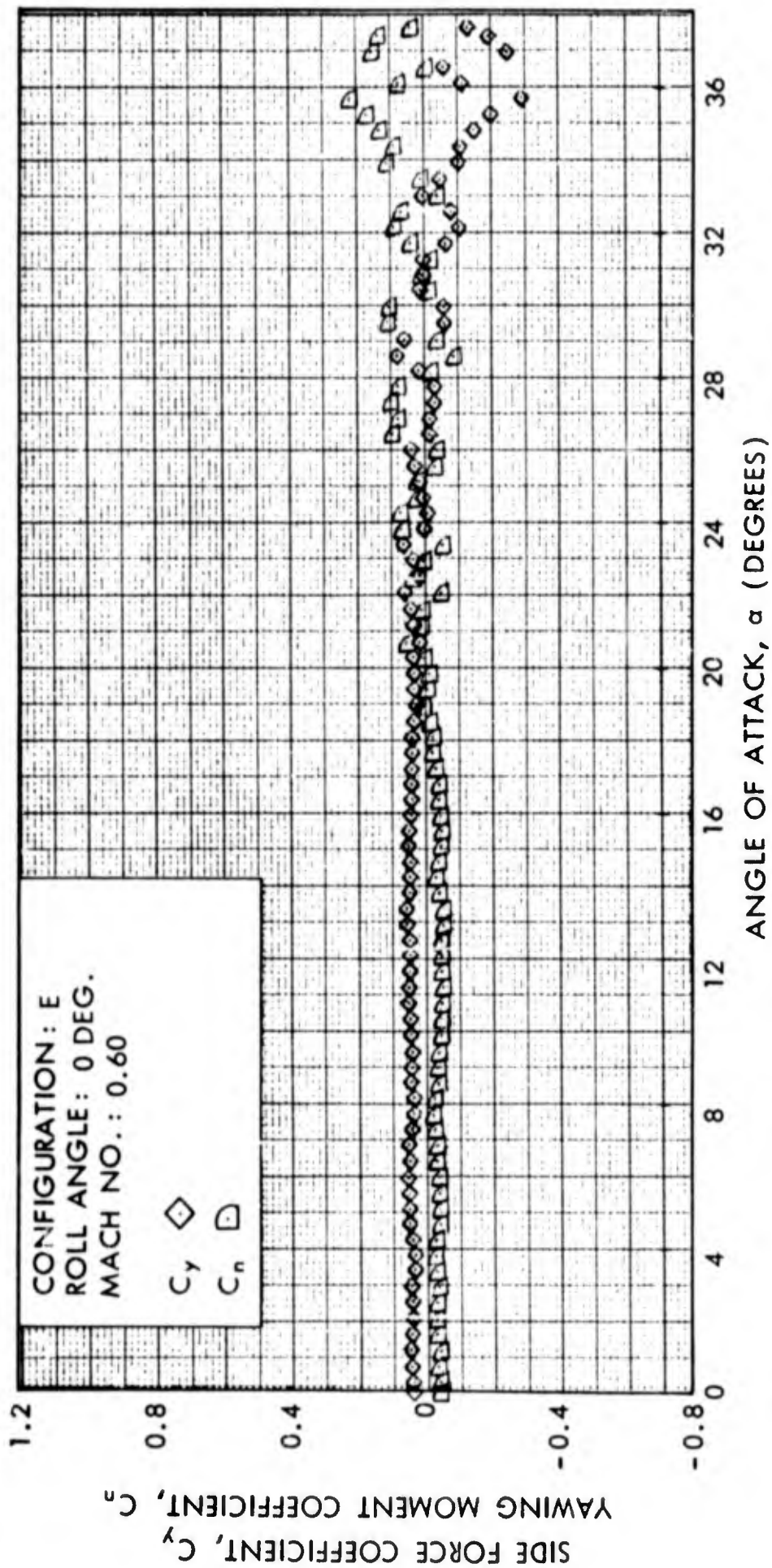


FIG. 86 SIDE FORCE COEFFICIENT AND YAWING MOMENT COEFFICIENT VERSUS ANGLE OF ATTACK

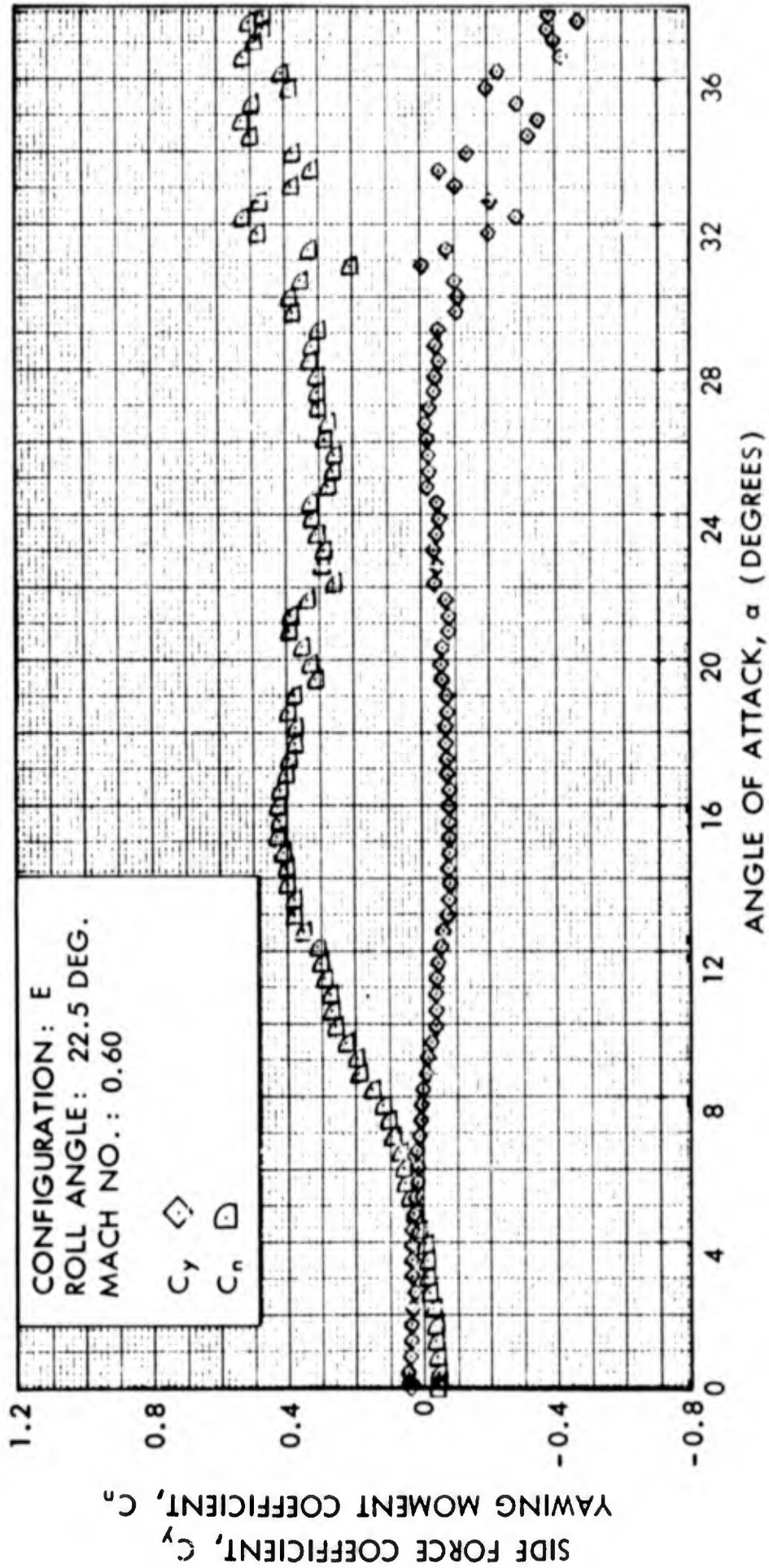


FIG. 87 SIDE FORCE COEFFICIENT AND YAWING MOMENT COEFFICIENT VERSUS ANGLE OF ATTACK

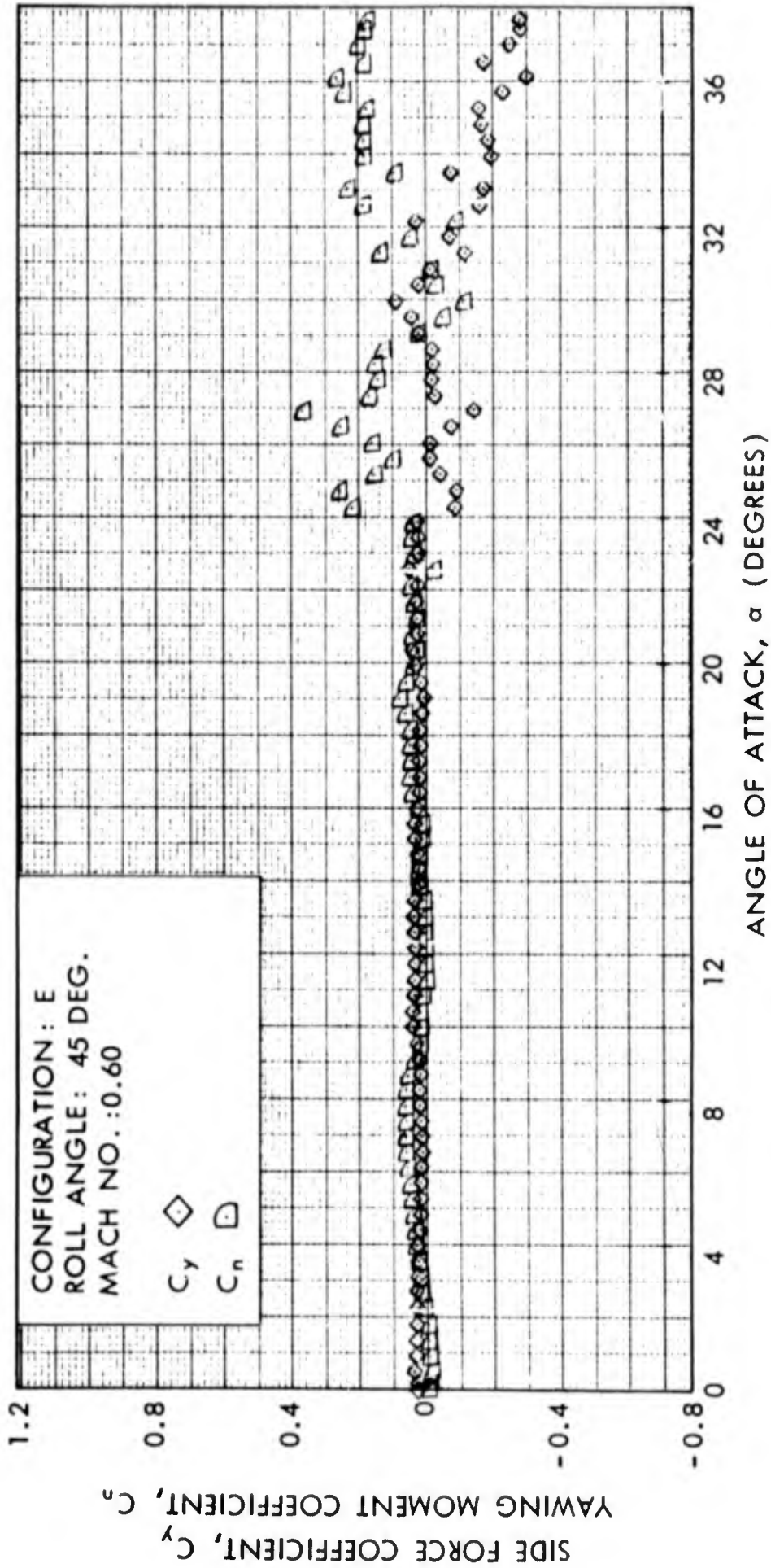


FIG. 88 SIDE FORCE COEFFICIENT AND YAWING MOMENT COEFFICIENT VERSUS ANGLE OF ATTACK

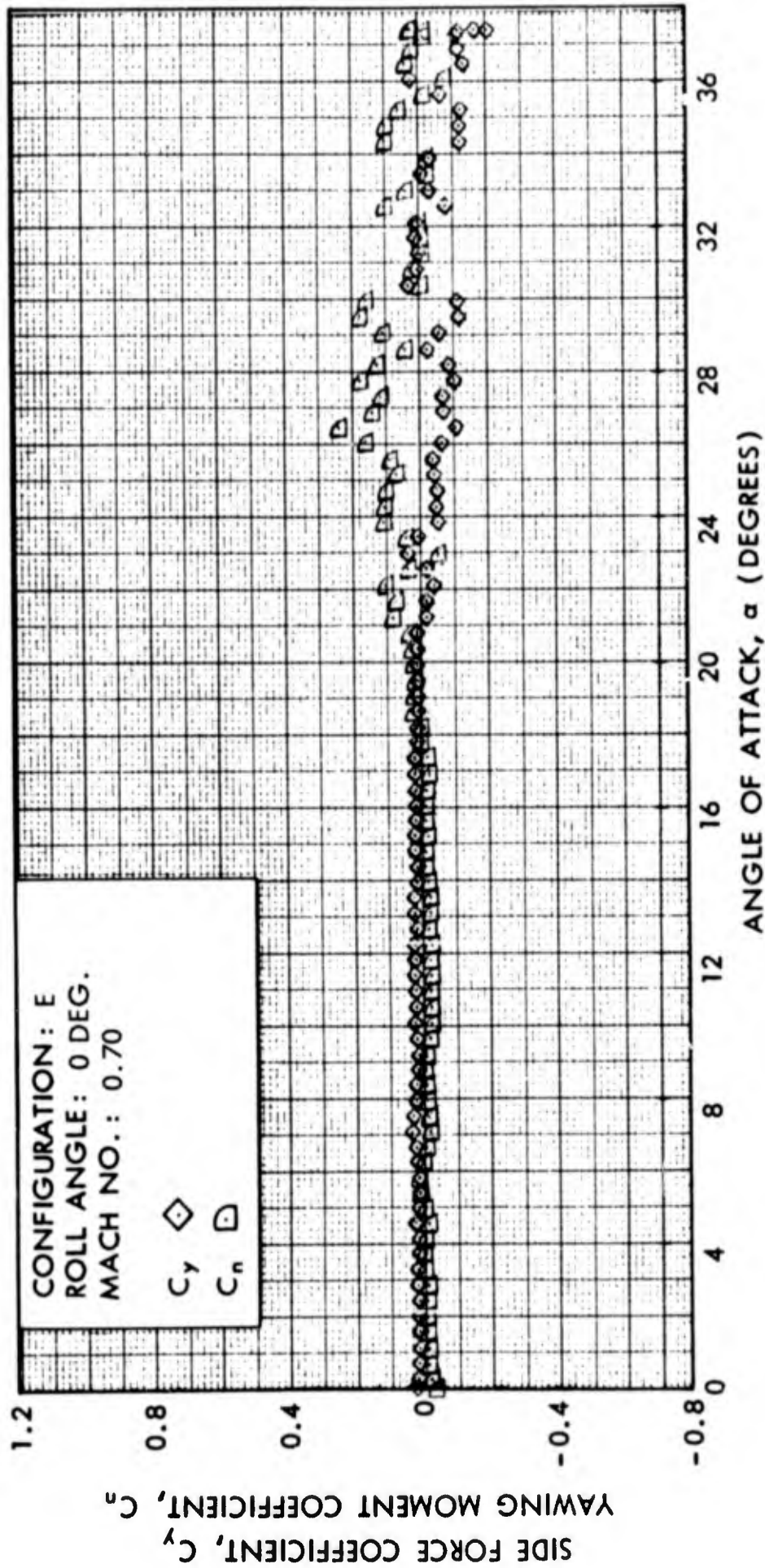


FIG. 89 SIDE FORCE COEFFICIENT AND YAWING MOMENT COEFFICIENT VERSUS ANGLE OF ATTACK

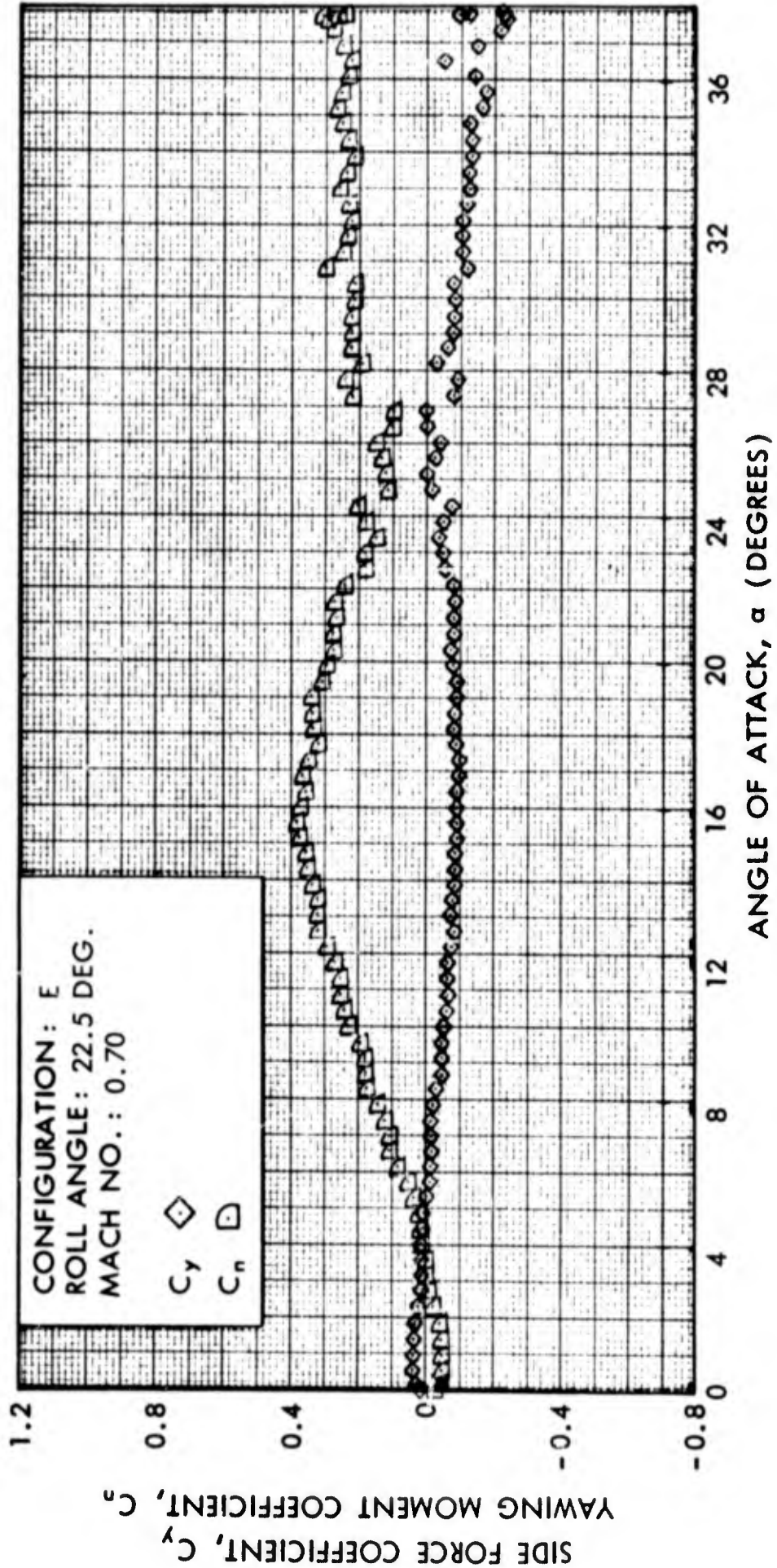


FIG. 90 SIDE FORCE COEFFICIENT AND YAWING MOMENT COEFFICIENT VERSUS ANGLE OF ATTACK

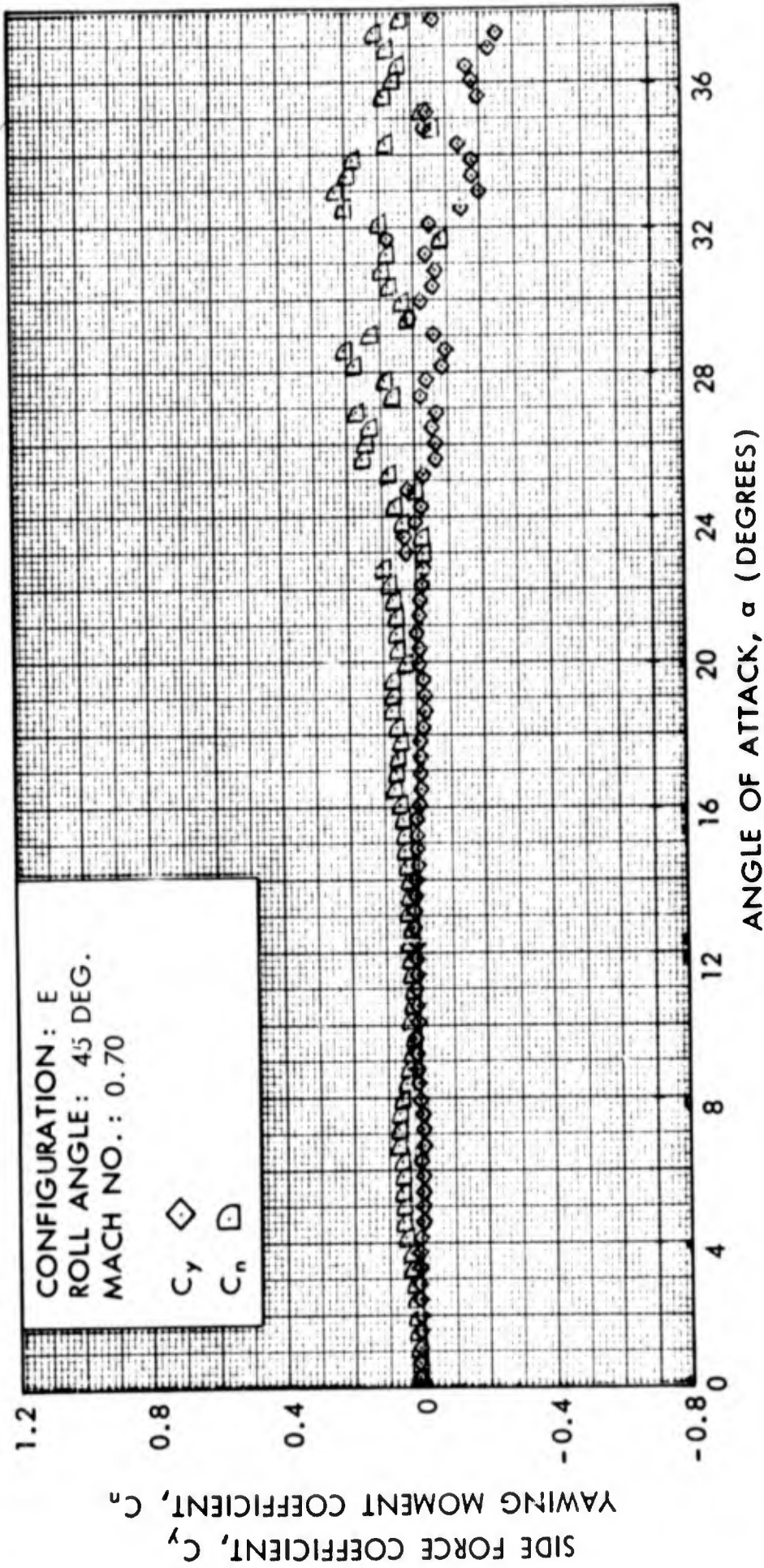


FIG. 91 SIDE FORCE COEFFICIENT AND YAWING MOMENT COEFFICIENT VERSUS ANGLE OF ATTACK

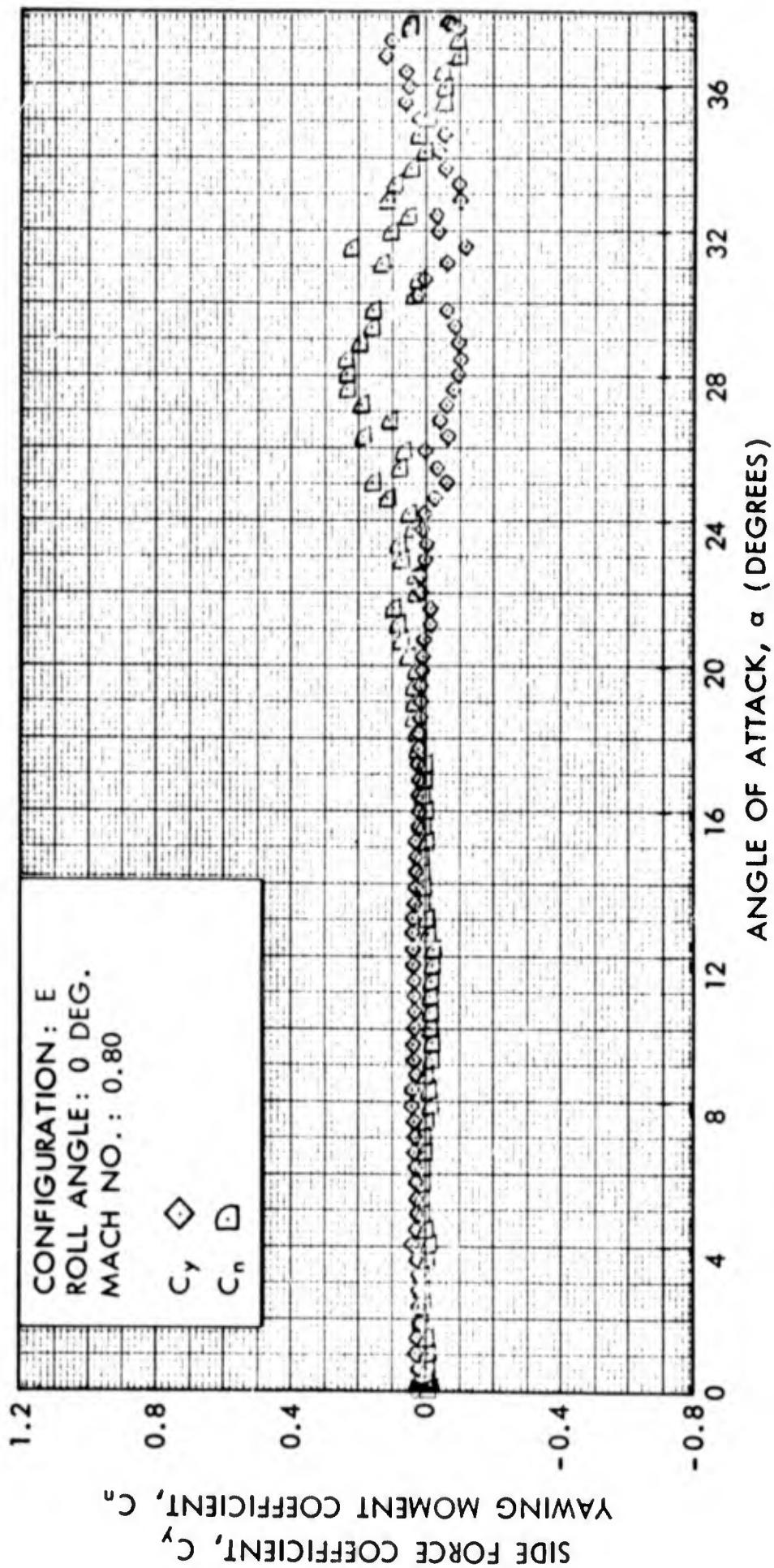


FIG. 92 SIDE FORCE COEFFICIENT AND YAWING MOMENT COEFFICIENT VERSUS ANGLE OF ATTACK

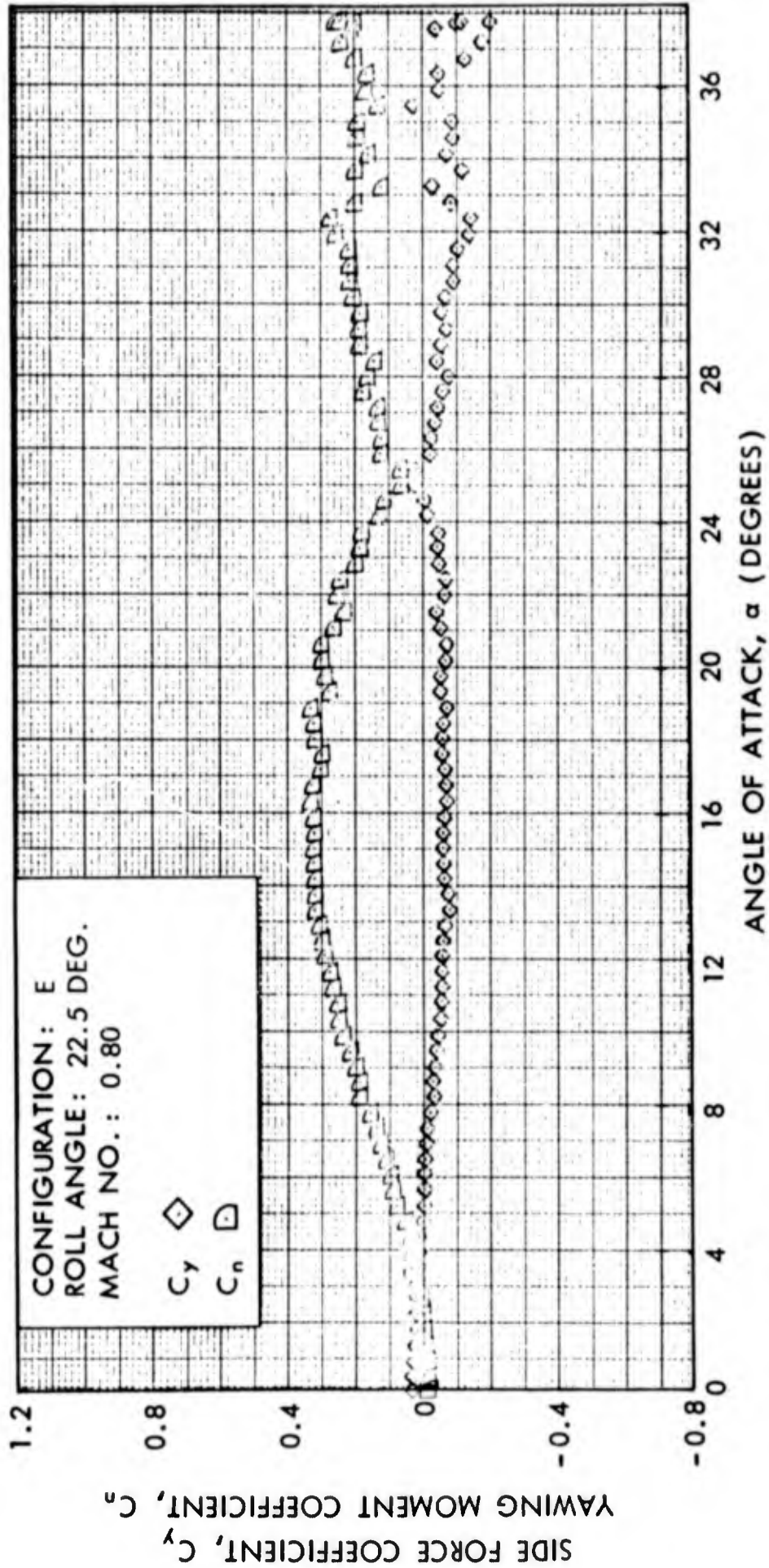


FIG. 93 SIDE FORCE COEFFICIENT AND YAWING MOMENT COEFFICIENT VERSUS ANGLE OF ATTACK

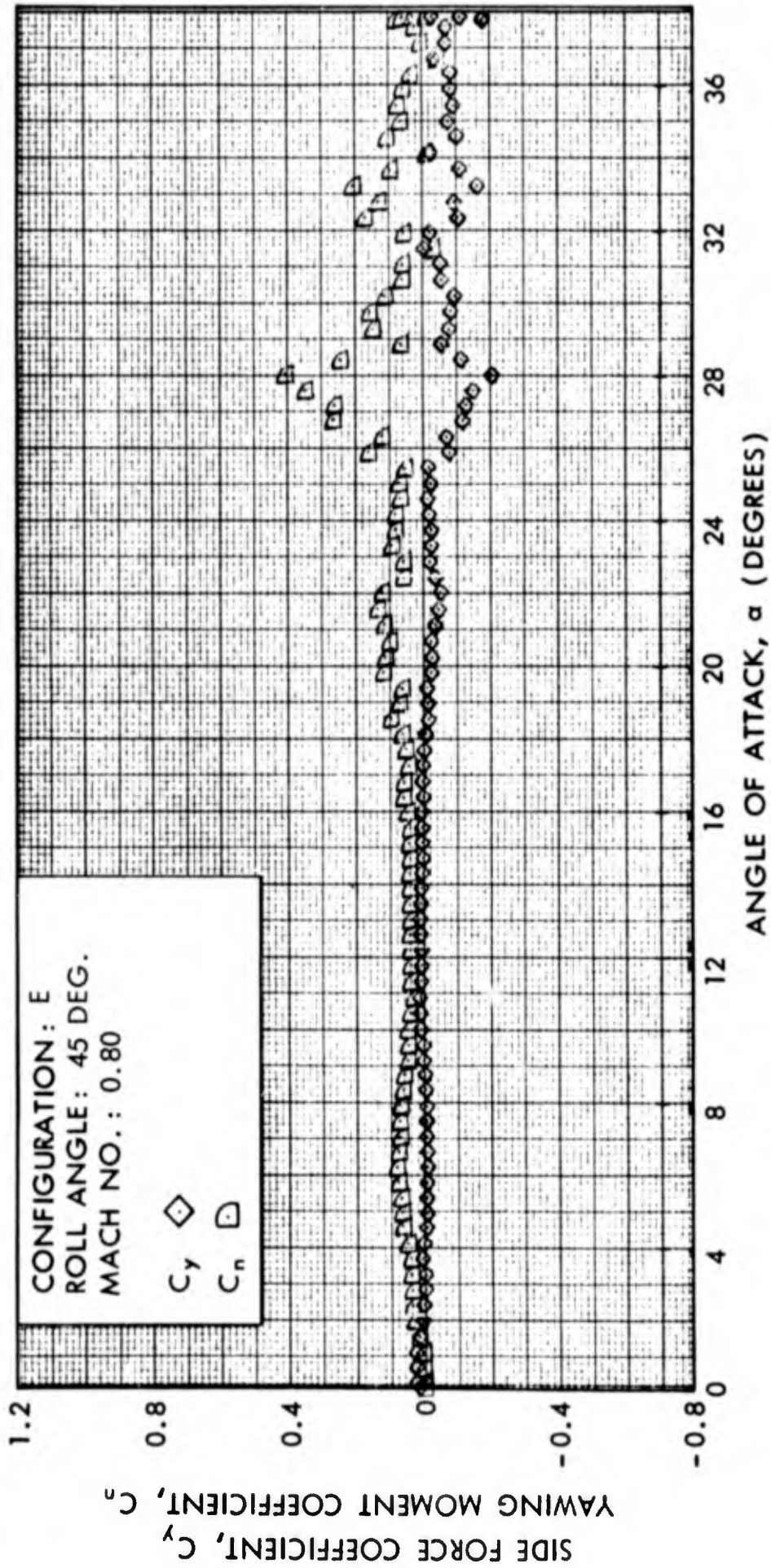


FIG. 94 SIDE FORCE COEFFICIENT AND YAWING MOMENT COEFFICIENT VERSUS ANGLE OF ATTACK

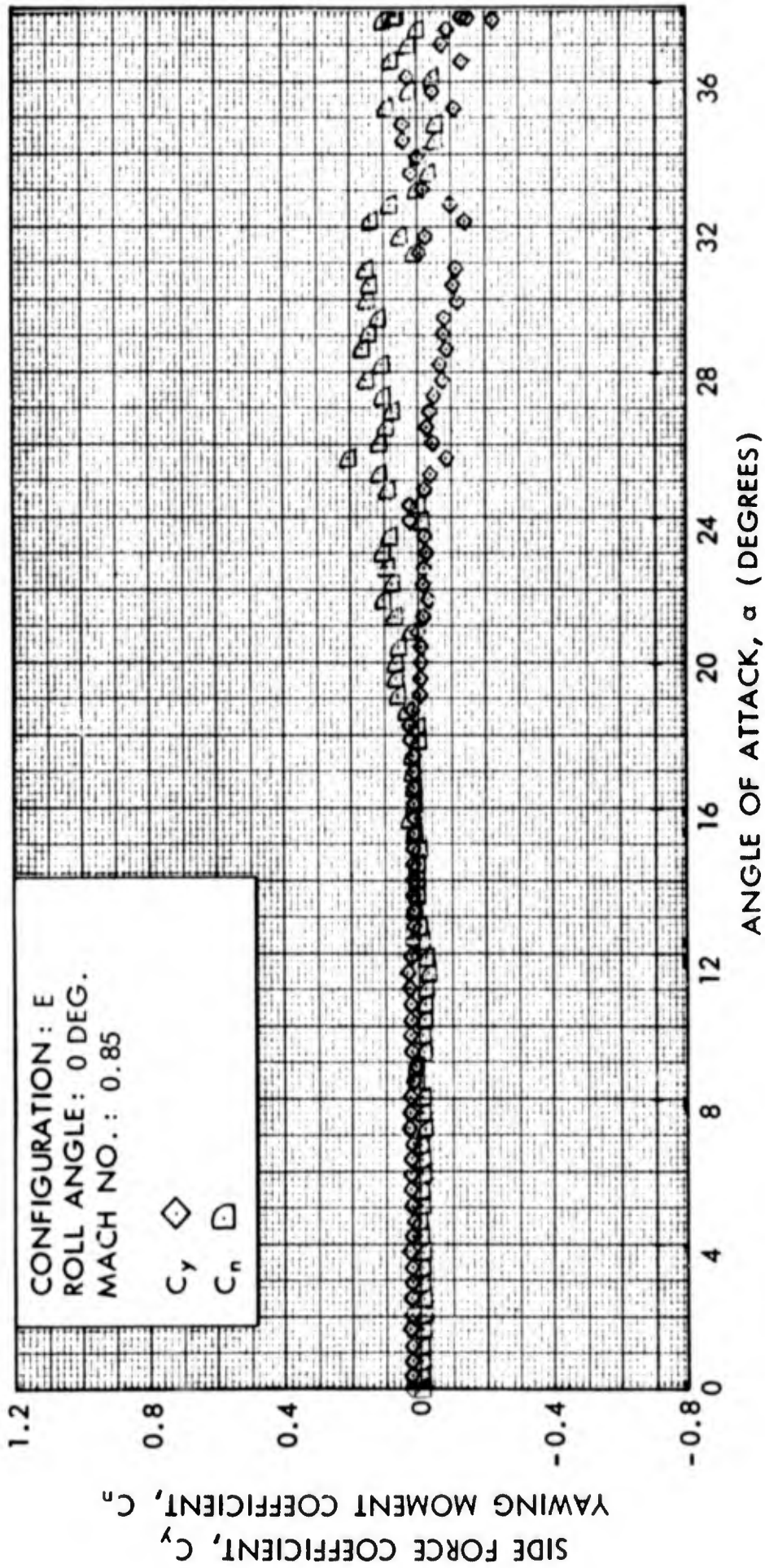


FIG. 95 SIDE FORCE COEFFICIENT AND YAWING MOMENT COEFFICIENT VERSUS ANGLE OF ATTACK

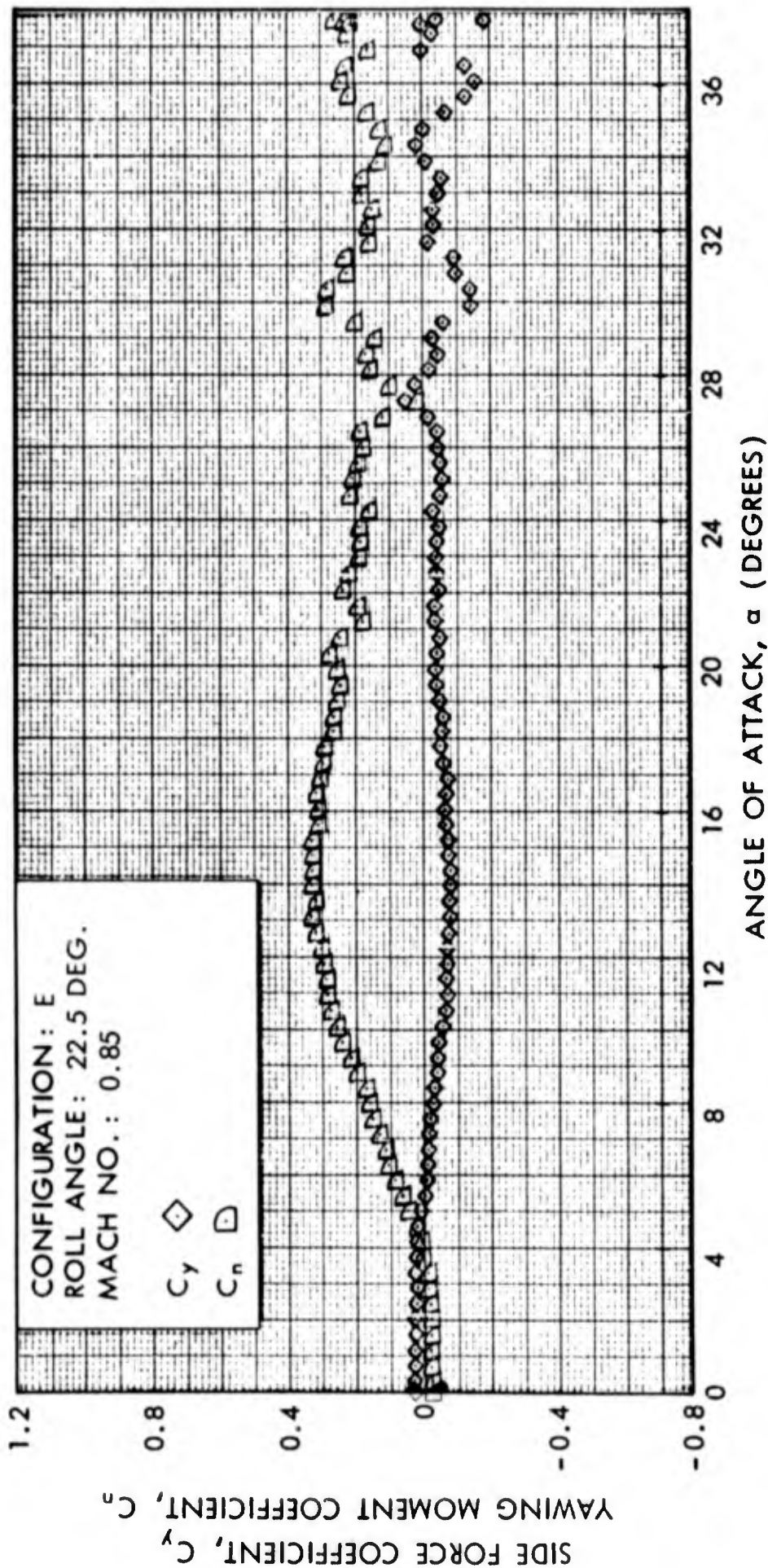


FIG. 96 SIDE FORCE COEFFICIENT AND YAWING MOMENT COEFFICIENT VERSUS ANGLE OF ATTACK

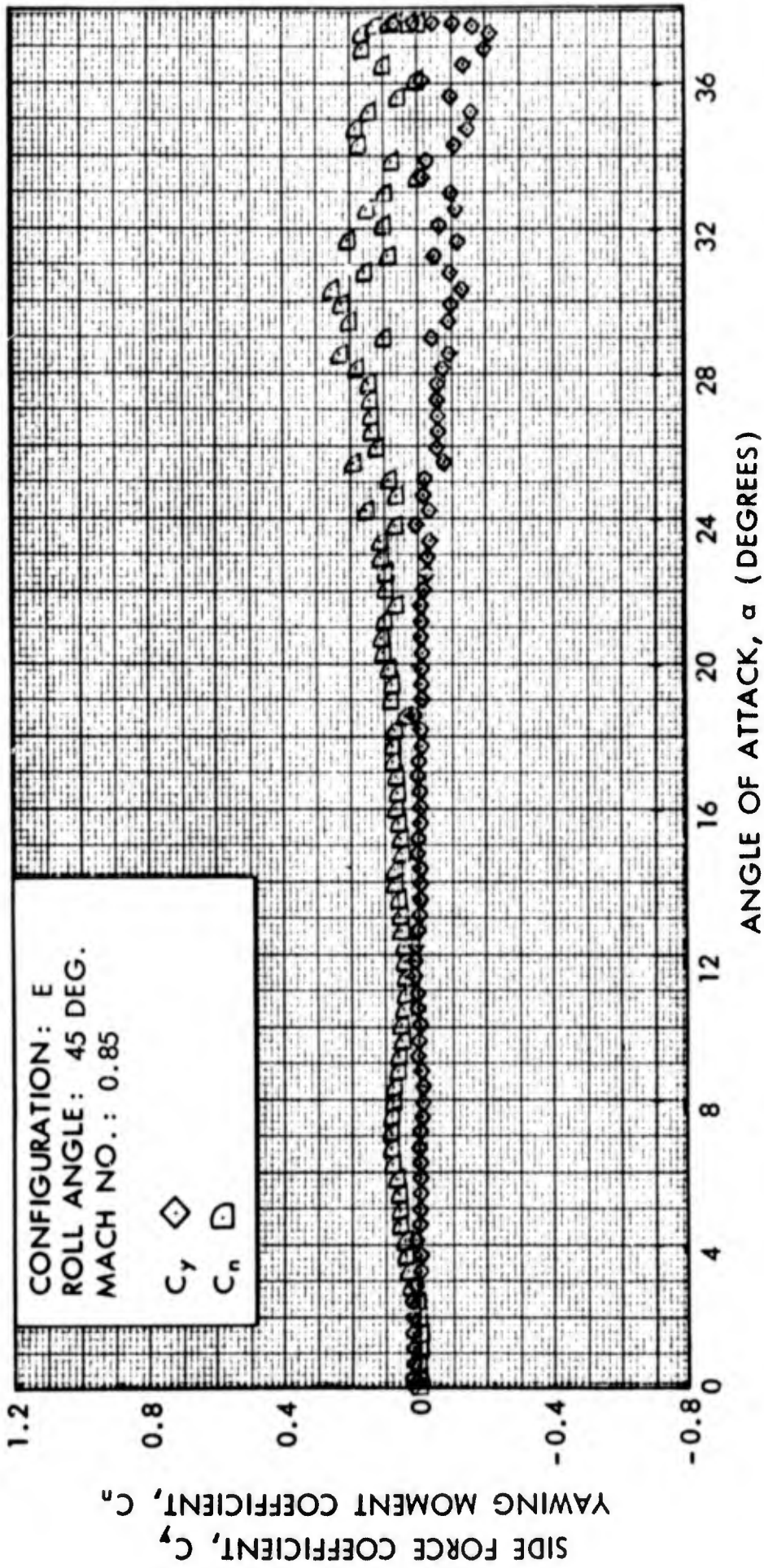


FIG. 97 SIDE FORCE COEFFICIENT AND YAWING MOMENT COEFFICIENT VERSUS ANGLE OF ATTACK

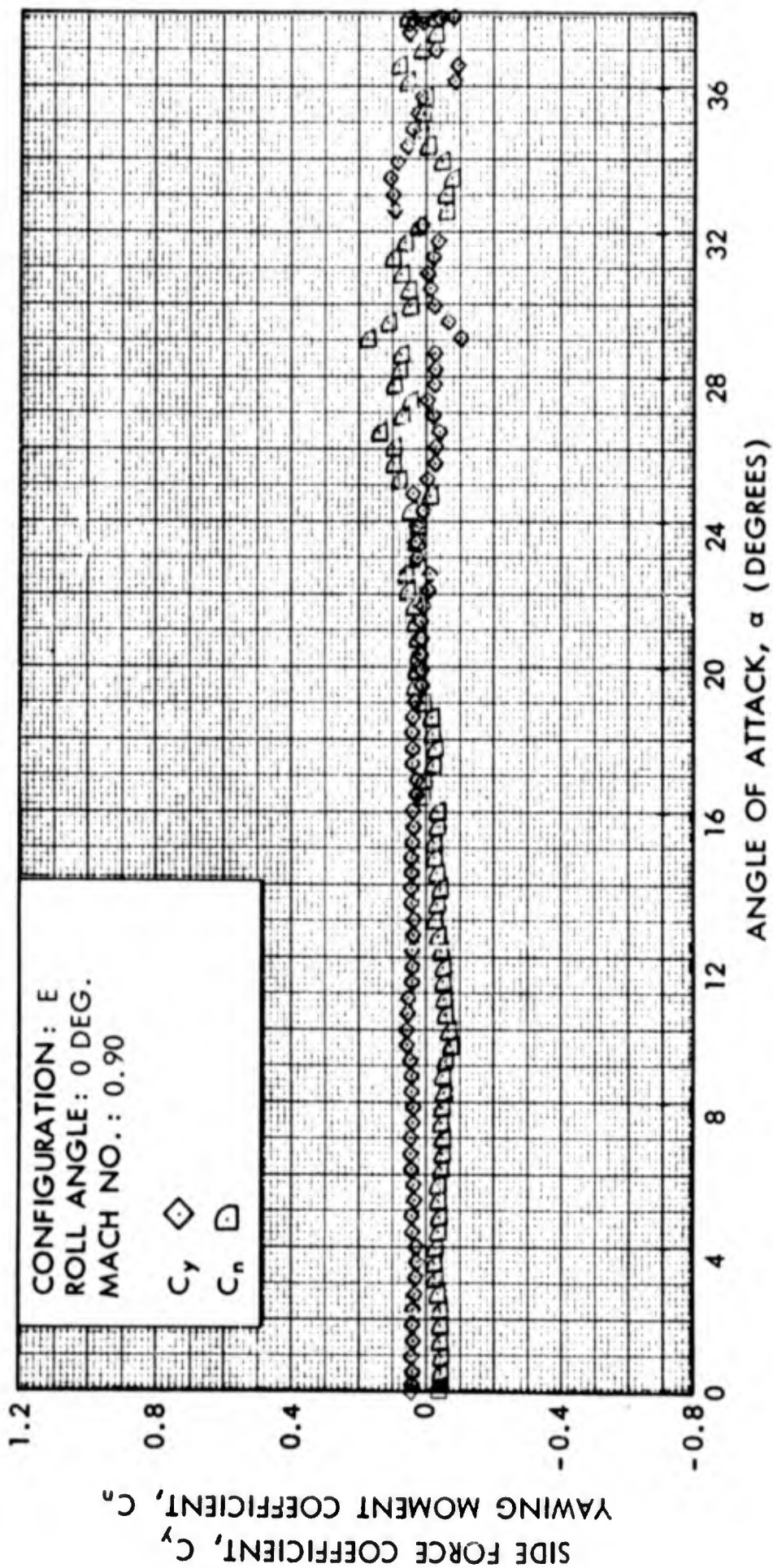


FIG. 98 SIDE FORCE COEFFICIENT AND YAWING MOMENT COEFFICIENT VERSUS ANGLE OF ATTACK

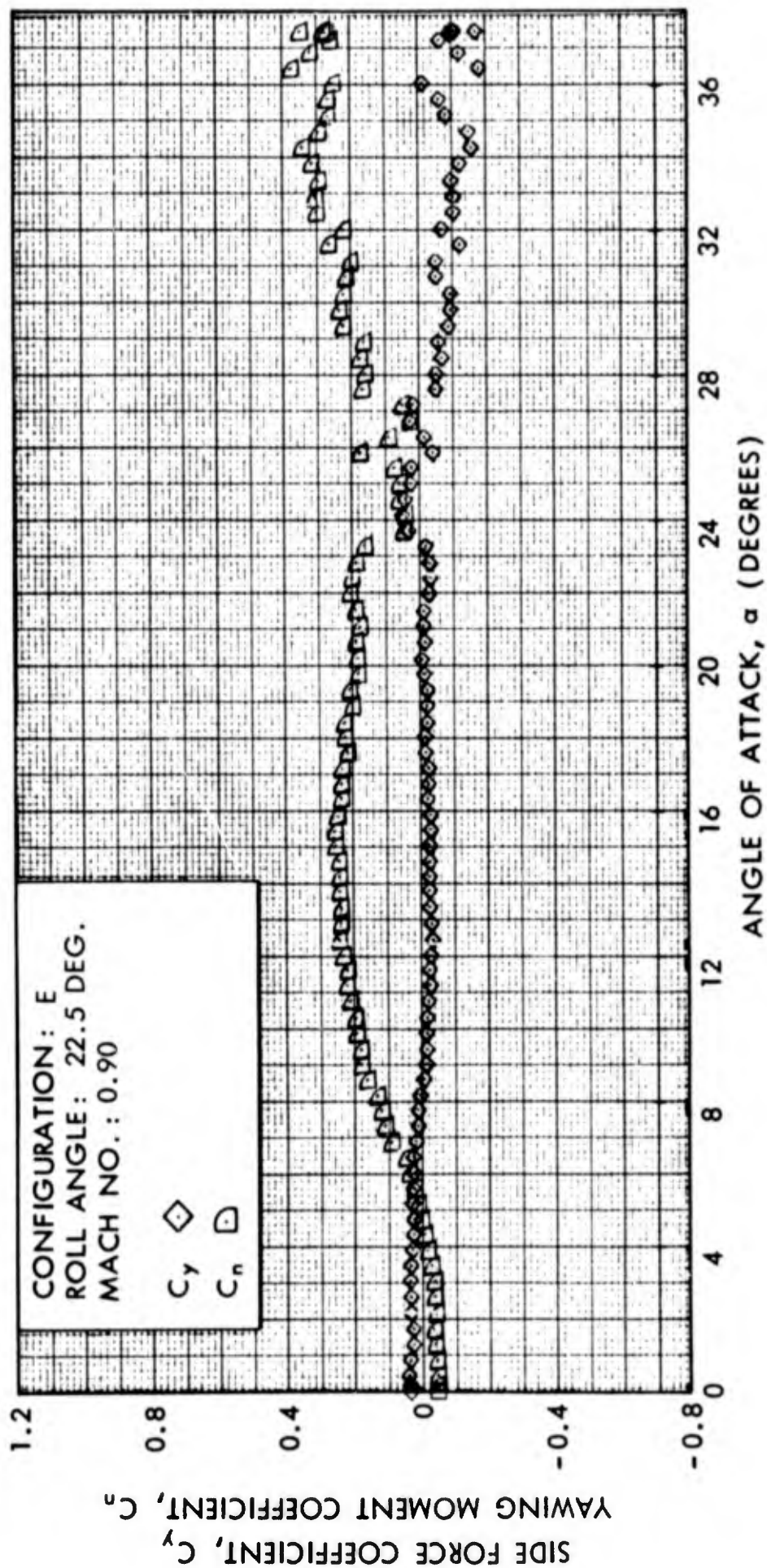


FIG. 99 SIDE FORCE COEFFICIENT AND YAWING MOMENT COEFFICIENT VERSUS ANGLE OF ATTACK

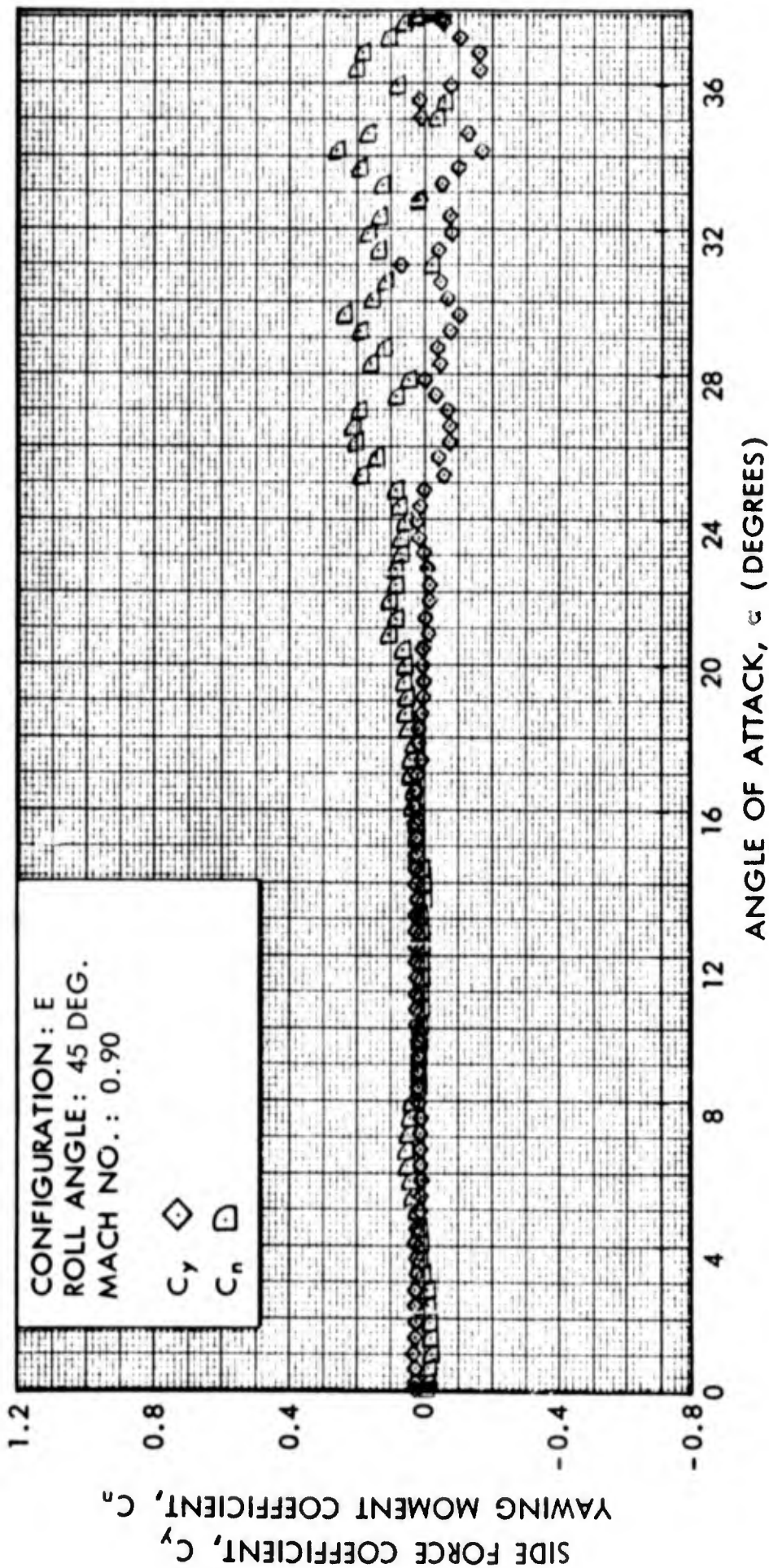


FIG. 100 SIDE FORCE COEFFICIENT AND YAWING MOMENT COEFFICIENT VERSUS ANGLE OF ATTACK

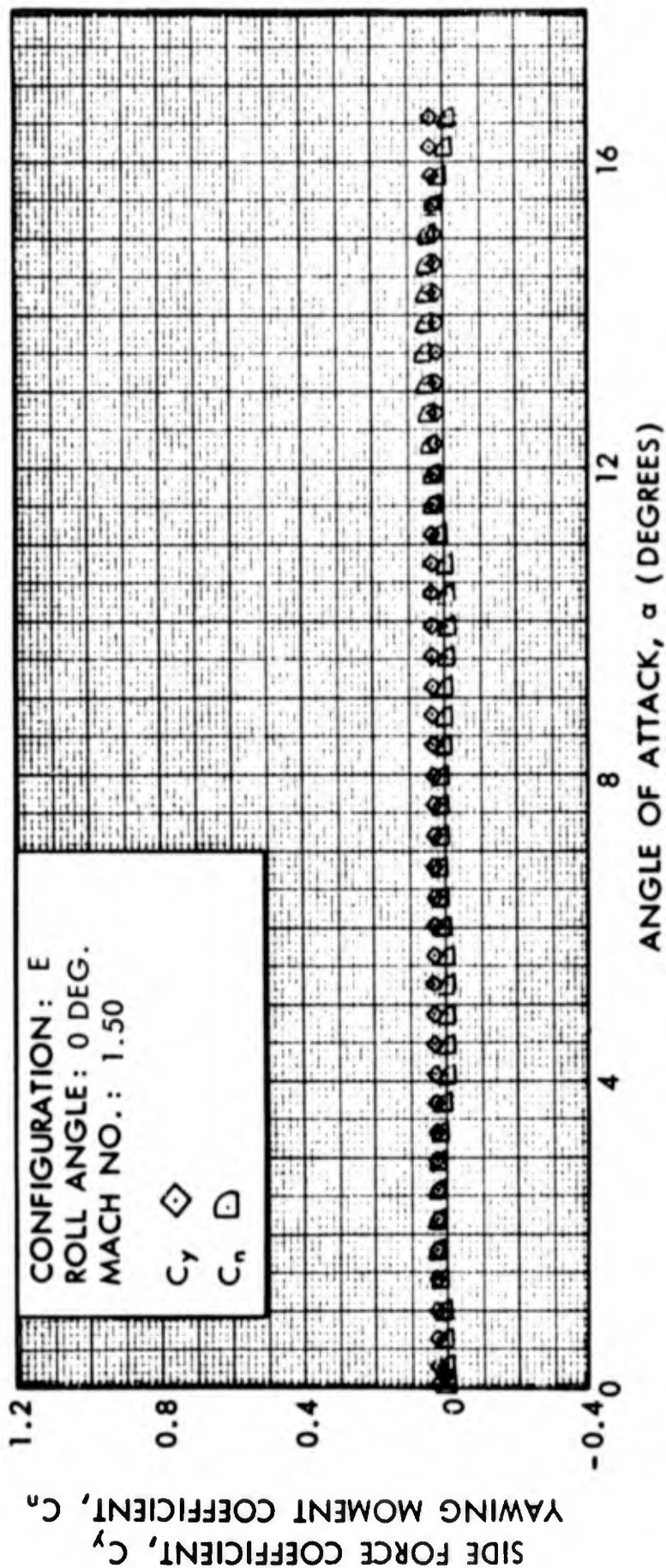


FIG. 101 SIDE FORCE COEFFICIENT AND YAWING MOMENT COEFFICIENT VERSUS ANGLE OF ATTACK

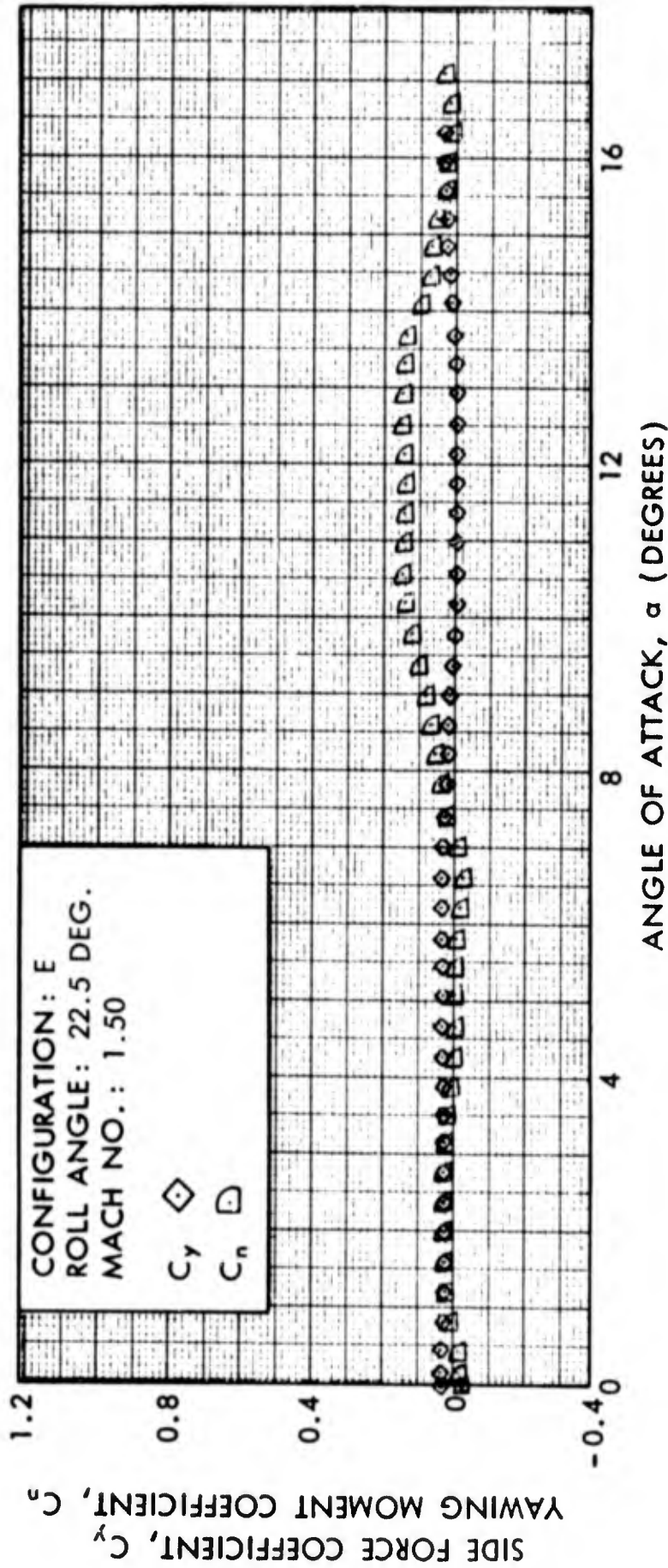


FIG. 102 SIDE FORCE COEFFICIENT AND YAWING MOMENT COEFFICIENT VERSUS ANGLE OF ATTACK

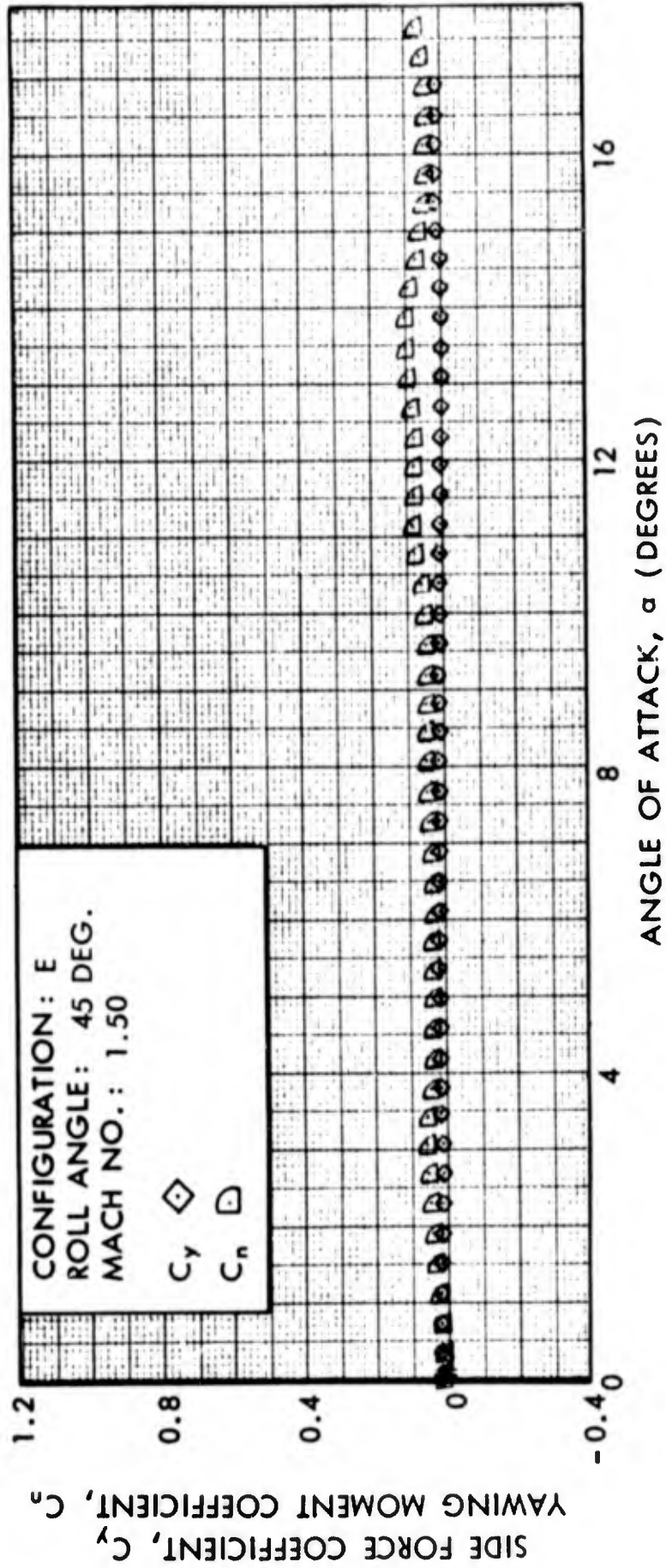


FIG. 103 SIDE FORCE COEFFICIENT AND YAWING MOMENT COEFFICIENT VERSUS ANGLE OF ATTACK

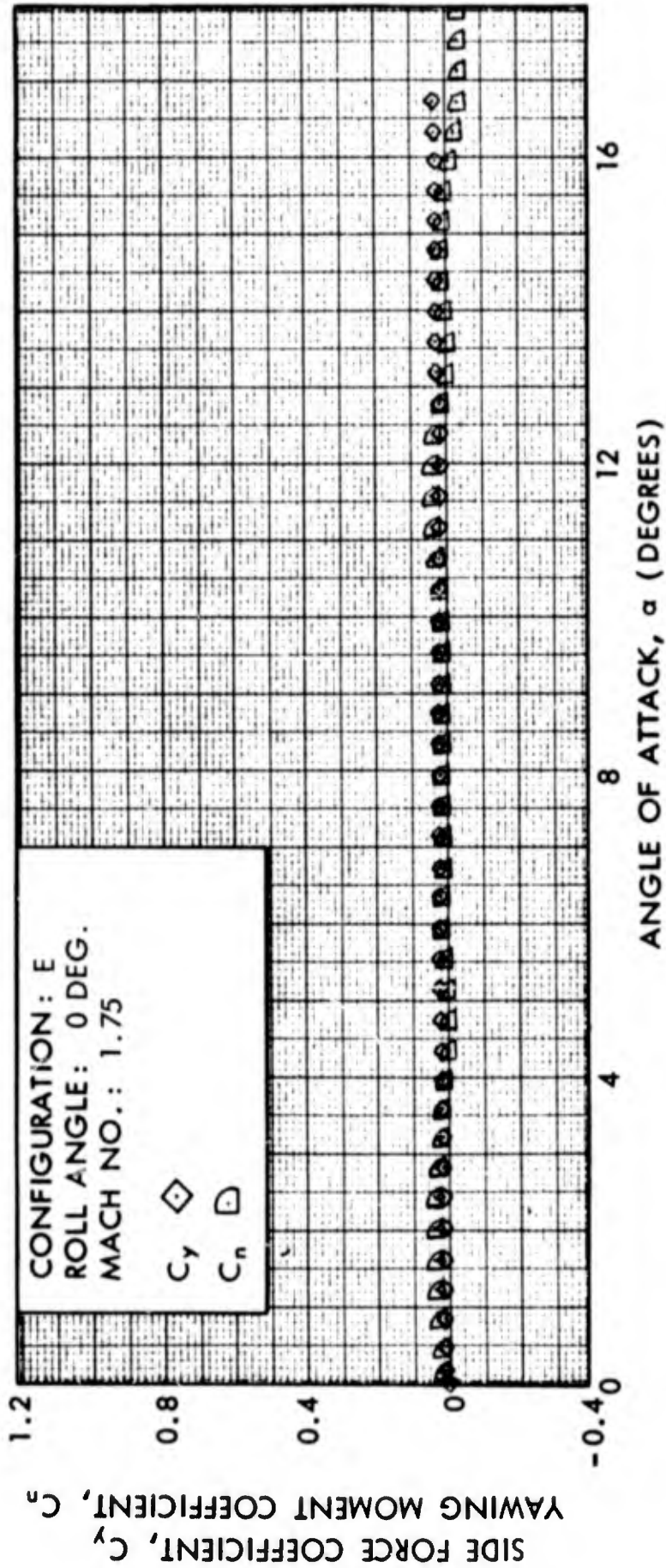


FIG. 104 SIDE FORCE COEFFICIENT AND YAWING MOMENT COEFFICIENT VERSUS ANGLE OF ATTACK

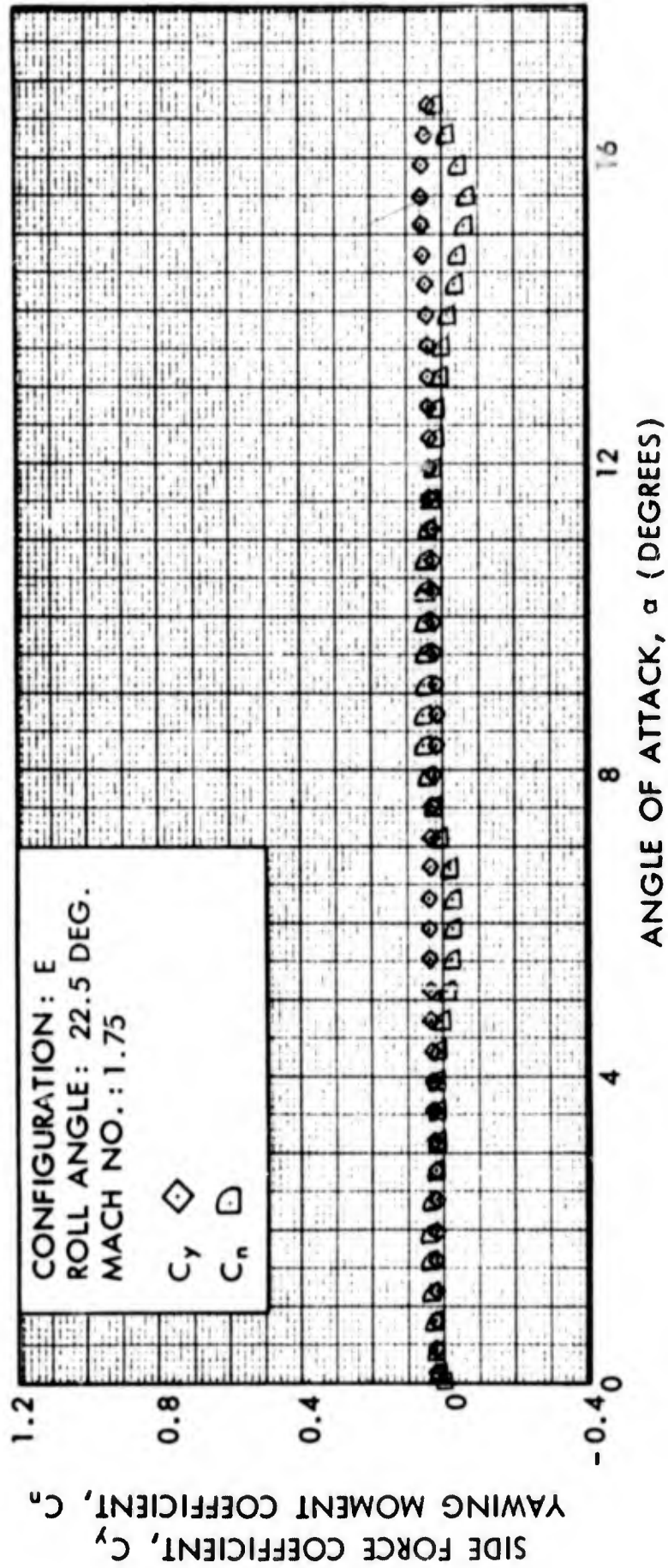


FIG. 105 SIDE FORCE COEFFICIENT AND YAWING MOMENT COEFFICIENT VERSUS ANGLE OF ATTACK

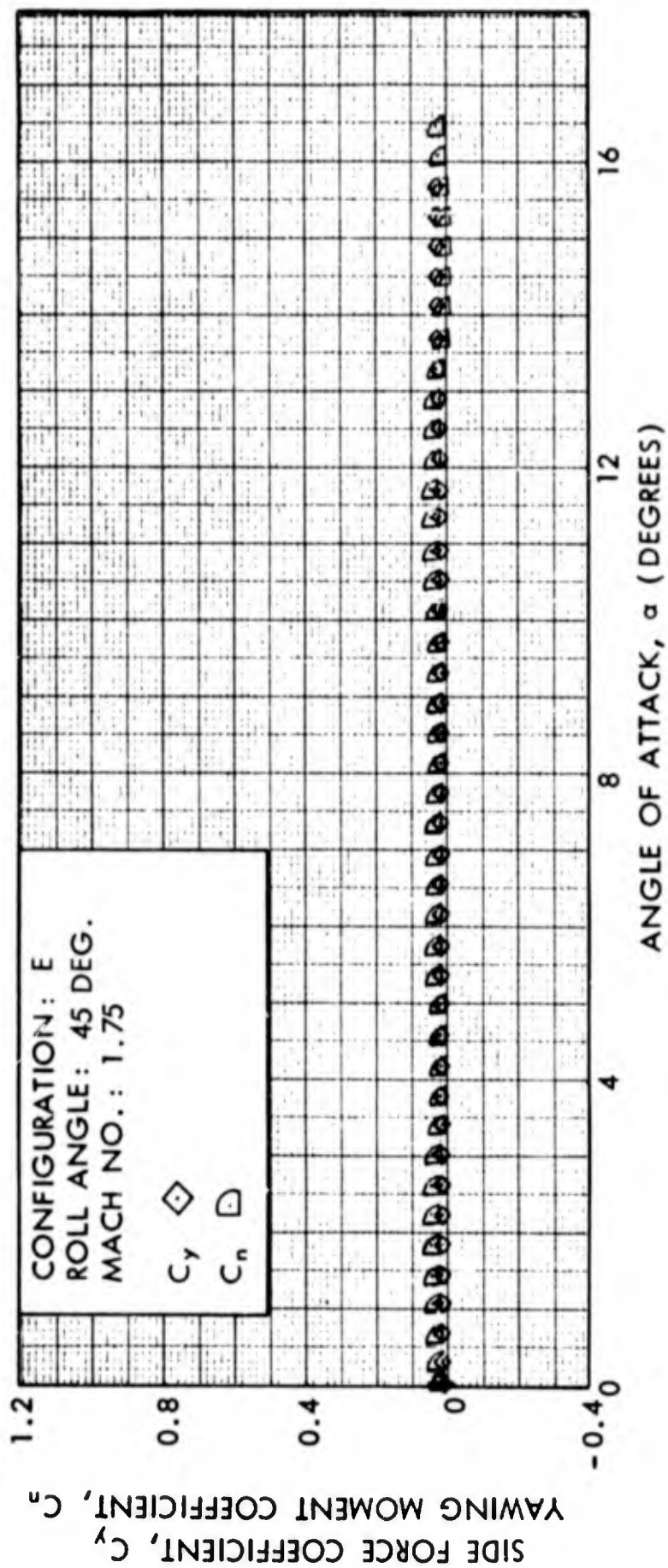


FIG. 106 SIDE FORCE COEFFICIENT AND YAWING MOMENT COEFFICIENT VERSUS ANGLE OF ATTACK

TABLE 1

CONFIGURATIONS

- A. Fixed Cruciform Tail,  $\delta = 0, 2, 4$  Degrees
- B. Free-Spinning Cruciform Tail,  $\delta = 2, 4$  Degrees
- C. Fixed Split-Skirt Tail, Skirt Angle 10 Degrees
- D. Free-Spinning Split-Skirt Tail, Skirt Angle 10 Degrees
- E. Fixed Split-Skirt Tail, Skirt Angle 15 Degrees
- F. Free-Spinning Split-Skirt Tail, Skirt Angle 15 Degrees
- G. Free-Spinning Monoplane Tail,  $\delta = 2, 4$  Degrees

TABLE 2  
TUNNEL TEST CONDITIONS

<u>MACH NUMBER</u>	<u>DYNAMIC PRESSURE (LBS/IN<sup>2</sup>)</u>	<u>REYNOLDS NO./FT x 10<sup>-6</sup></u>
0.50	2.10	3.00
0.60	2.80	3.40
0.70	3.48	3.75
0.80	4.13	4.00
0.85	4.42	4.15
0.90	4.70	4.25
0.95	4.90	4.35
1.50	6.13	4.40
1.75	5.80	4.12

UNCLASSIFIED

Security Classification

DOCUMENT CONTROL DATA - R&D		
<i>(Security classification of title, body of abstract and indexing annotation must be entered when the overall report is classified)</i>		
1 ORIGINATING ACTIVITY (Corporate author) <b>Naval Ordnance Laboratory, White Oak, Maryland</b>		2a REPORT SECURITY CLASSIFICATION <b>UNCLASSIFIED</b>
		2b GROUP
3 REPORT TITLE <b>Static Wind Tunnel Tests of the M823 Research Store with Split-Skirt Stabilizers</b>		
4 DESCRIPTIVE NOTES (Type of report and Inclusive dates)		
5 AUTHOR(S) (Last name, first name, initial) <b>Regan, Frank J., Falusi, Mary E., Holmes, John E.</b>		
6. REPORT DATE <b>12 January 1966</b>	7a TOTAL NO OF PAGES <b>12</b>	7b NO OF REFS <b>4</b>
8a. CONTRACT OR GRANT NO.	9a ORIGINATOR'S REPORT NUMBER(S) <b>NOLTR 61-89</b>	
b. PROJECT NO.	9b. OTHER REPORT NO(S) (Any other numbers that may be assigned this report) <b>Aerodynamics Research Report 160</b>	
c.		
d.		
10. AVAILABILITY/LIMITATION NOTICES <b>Distribution of this Document is unlimited.</b>		
11. SUPPLEMENTARY NOTES	12 SPONSORING MILITARY ACTIVITY	
13. ABSTRACT <b>The M823 Configuration is an instrumented free fall store used in bomb research programs. This report presents the results of static wind tunnel tests for the basic forebody with split-skirt stabilizers attached.</b>		

14 KEY WORDS  1. Bomb 2. Static Stability 3. Split-Skirt Stabilizers	LINK A		LINK B		LINK C	
	ROLE	WT	ROLE	WT	ROLE	WT

**INSTRUCTIONS**

1. **ORIGINATING ACTIVITY:** Enter the name and address of the contractor, subcontractor, grantee, Department of Defense activity or other organization (*corporate author*) issuing the report.
- 2a. **REPORT SECURITY CLASSIFICATION:** Enter the overall security classification of the report. Indicate whether "Restricted Data" is included. Marking is to be in accordance with appropriate security regulations.
- 2b. **GROUP:** Automatic downgrading is specified in DoD Directive 5200.10 and Armed Forces Industrial Manual. Enter the group number. Also, when applicable, show that optional markings have been used for Group 3 and Group 4 as authorized.
3. **REPORT TITLE:** Enter the complete report title in all capital letters. Titles in all cases should be unclassified. If a meaningful title cannot be selected without classification, show title classification in all capitals in parenthesis immediately following the title.
4. **DESCRIPTIVE NOTES:** If appropriate, enter the type of report, e.g., interim, progress, summary, annual, or final. Give the inclusive dates when a specific reporting period is covered.
5. **AUTHOR(S):** Enter the name(s) of author(s) as shown on or in the report. Enter last name, first name, middle initial. If military, show rank and branch of service. The name of the principal author is an absolute minimum requirement.
6. **REPORT DATE:** Enter the date of the report as day, month, year, or month, year. If more than one date appears on the report, use date of publication.
- 7a. **TOTAL NUMBER OF PAGES:** The total page count should follow normal pagination procedures, i.e., enter the number of pages containing information.
- 7b. **NUMBER OF REFERENCES:** Enter the total number of references cited in the report.
- 8a. **CONTRACT OR GRANT NUMBER:** If appropriate, enter the applicable number of the contract or grant under which the report was written.
- 8b, 8c, & 8d. **PROJECT NUMBER:** Enter the appropriate military department identification, such as project number, subproject number, system numbers, task number, etc.
- 9a. **ORIGINATOR'S REPORT NUMBER(S):** Enter the official report number by which the document will be identified and controlled by the originating activity. This number must be unique to this report.
- 9b. **OTHER REPORT NUMBER(S):** If the report has been assigned any other report numbers (*either by the originator or by the sponsor*), also enter this number(s).
10. **AVAILABILITY/LIMITATION NOTICES:** Enter any limitations on further dissemination of the report, other than those

imposed by security classification, using standard statements such as:

- (1) "Qualified requesters may obtain copies of this report from DDC."
- (2) "Foreign announcement and dissemination of this report by DDC is not authorized."
- (3) "U. S. Government agencies may obtain copies of this report directly from DDC. Other qualified DDC users shall request through \_\_\_\_\_."
- (4) "U. S. military agencies may obtain copies of this report directly from DDC. Other qualified users shall request through \_\_\_\_\_."
- (5) "All distribution of this report is controlled. Qualified DDC users shall request through \_\_\_\_\_."

If the report has been furnished to the Office of Technical Services, Department of Commerce, for sale to the public, indicate this fact and enter the price, if known.

11. **SUPPLEMENTARY NOTES:** Use for additional explanatory notes.
12. **SPONSORING MILITARY ACTIVITY:** Enter the name of the departmental project office or laboratory sponsoring (*paying for*) the research and development. Include address.
13. **ABSTRACT:** Enter an abstract giving a brief and factual summary of the document indicative of the report, even though it may also appear elsewhere in the body of the technical report. If additional space is required, a continuation sheet shall be attached.

It is highly desirable that the abstract of classified reports be unclassified. Each paragraph of the abstract shall end with an indication of the military security classification of the information in the paragraph, represented as (TS), (S), (C), or (U).

There is no limitation on the length of the abstract. However, the suggested length is from 150 to 225 words.

14. **KEY WORDS:** Key words are technically meaningful terms or short phrases that characterize a report and may be used as index entries for cataloging the report. Key words must be selected so that no security classification is required. Identifiers, such as equipment model designation, trade name, military project code name, geographic location, may be used as key words but will be followed by an indication of technical context. The assignment of links, roles, and weights is optional.